SUPPLEMENTARY INFORMATION

High Precision Assembly Line Synthesis for Molecules with Tailored Shapes

Matthew Burns, Stephanie Essafi, Jessica R. Bame, Stephanie P. Bull, Matthew P. Webster,

Sebastien Balieu, James W. Dale, Craig P. Butts, Jeremy N. Harvey, Varinder K. Aggarwal

Contents

Synthetic procedures

General synthetic information

All air- and water-sensitive reactions were carried out in oven-dried glassware under a N_2 atmosphere using standard Schlenk techniques. Analytical TLC was performed on aluminium backed plates pre-coated (0.25 mm) with Merck Silica Gel 60 F254. Compounds were visualized by exposure to UV-light or stained using Phosphomolybdic acid (PMA) or $KMnO_4$ followed by heating. Flash column chromatography was performed using Merck Silica Gel 60 (40-63 μm). All mixed solvent eluents are reported as v/v solutions.

^1H- and ^{13}C- Nuclear Magnetic Resonance (NMR) spectra were acquired at various field strengths as indicated using JEOL ECS 300, JEOL ECS 400, Varian 400 and Varian VNMRS500 spectrometers. ^1H spectra were referenced internally to the residual protio solvent resonance ($CHCl_3$ = 7.27 ppm). ^{13}C spectra were referenced internally to the residual protio solvent resonance ($CHCl_3$ = 77.0 ppm). ^{11}B spectra were referenced externally to $BF_3{\cdot}OEt_2$. ^1H and ^{13}C NMR coupling constants are reported in Hertz (Hz). Coupling constants are reported as follows: s = singlet, br. s = broad singlet, d = doublet, t = triplet, q = quartet, qiun = quintet, sx = sextet, sept = spetet, m = multiplet, dd = doublet of doublet, etc. Assignment of signals in ^1H- and ^{13}C-spectra was performed using ^1H-^1H COSY, DEPT, HMQC and HMBC experiments where appropriate. ^{13}C signals adjacent to boron are generally not observed due to quadrupolar relaxation. Impurity at 29.7 ppm in ^{13}C spectra is due to trace amounts of Apiezon high vacuum grease.

High resolution mass spectra were recorded using Electronic Ionization (EI), Electron Spray Ionization (ESI) or Chemical Ionization (CI). For CI, methane or NH_4OAc/MeOH was used. GC-MS was perfomed on an Agilent 6890 apparatus. All IR data was obtained on a Perkin-Elmer Spectrum One FT-IR spectrometer. Optical rotations were obtained on a Perkin-Elmer 241MC polarimeter. Melting points were determined with a Boetius hot stage apparatus and were not corrected.

Chiral HPLC was performed using Daicel Chiralpak IB column (4.6 × 250 mm × 5 μm) fitted with the respective guard (4 × 10 mm) and monitored by DAD (Diode Array Detector) on a Agilent 1100 system equipped with HP Chemstation software using. Chiral SFC was performed using Diacel Chiralpak IB column (4.6 × 250 mm × 5 μm) on a Waters TharSFC system and monitored by DAD (Diode Array Detector).

GCMS was performed using an Agilent HP-5MS column (15 m × 0.250 mm) on an Agilent 6890 GC and Agilent 5973 MS system. Compounds were identified through extract ion chromatogram and molecular ion analysis. Integration of the GCMS was carried out and is shown. Ionisation potential for boronic ester homologues are assumed to be comparable, but the data has not been calibrated. Methods: **70-1**: Flow rate: 1.0 mL/min; hold at 70 °C for 3 min; ramp 25 °C/min to 200 °C; ramp 45.0 °C/min to 250 °C; hold at 250 °C for 3 min; ramp 45.0 °C/min to 300 °C; hold at 300 °C for 3 min. **110-1**: Flow rate: 1.3 mL/min; hold at 110 °C for 1 min; ramp 45 °C/min to 300 °C; hold at 300 °C for 10 min. **110-2**: Flow rate: 1.3 mL/min; hold at 110 °C for 1 min; ramp 45 °C/min to 300 °C; hold at 300 °C for 25 min.

Materials and reagents

All reagents were used as received unless otherwise stated. Anhydrous Et_2O, PhMe and CH_2Cl_2 were dried using a purification column composed of activated alumina.[1] Anhydrous Et_2O was stored over 3 Å mol sieves. Where stated solvents were degassed using the freeze-pump-thaw method.[2] TMEDA, triethylamine and *N*,*N*-diisopropylethylamine (Hunig's base) were distilled over CaH_2 and stored in a Young's tube under N_2. (−)-Sparteine was obtained from the commercially available sulfate pentahydrate salt (ABCR chemicals) and isolated according to literature procedure.[3] (+)-Sparteine was obtained as the free base (BOC sciences), distilled over CaH_2 and stored in a Young's tube under N_2. The sparteine free base readily absorbs atmospheric carbon dioxide (CO_2) and should be stored in a Young's tube under argon/N_2 at −20 °C. Organolithiums were periodically titrated using *N*-benzylbenzamide.[4] Solutions of *n*BuLi where precipitate had formed were discarded as these were found to not be effective in Sn-Li exchange reactions. NaO*t*Bu and CuCl were stored in a Schlenk tube under N_2. Carbamate **23** was prepared according to the literature procedure.[5]

General procedures

General procedure 1 (GP1): Oxidation of boronic ester to alcohol with H_2O_2/NaOH

A premixed solution of NaOH (2 M)/H_2O_2 (30% aq.) (2:1, 3 mL) was added dropwise to a solution of boronic ester (20 – 100 mg scale) in THF (2 mL) at 0 °C. The reaction mixture was warmed to room temperature and stirred at this temperature for 1-4 h (reaction was monitored by TLC). The reaction mixture was diluted with H_2O (2 mL) and Et_2O (2 mL). The phases were separated and the aqueous phase washed with Et_2O (3 × 2 mL). The combined organic phases were washed with H_2O (5 mL), dried ($MgSO_4$) and concentrated under reduced pressure.

General procedure 2 (GP2): Iterative homologation of boronic ester with stannane 5

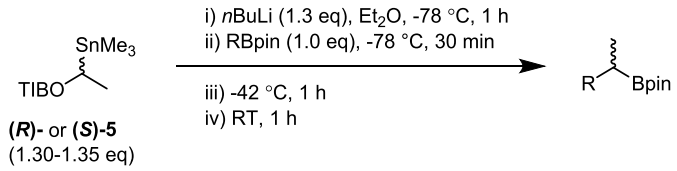

A solution of stannane **5** (1.30 – 1.35 eq) in a Schlenk reaction vessel was dissolved in anhydrous Et_2O (0.2 M) under an atmosphere of nitrogen. The reaction mixture was cooled to –78 °C (white precipitate of stannane **5** in Et_2O at –78 °C). *n*BuLi (1.5 – 1.6 M in hexanes, 1.30 eq) was added dropwise to the reaction mixture at –78 °C. The reaction mixture was stirred for 1 h at –78 °C (when the tin – lithium exchange is complete the reaction mixture will be a translucent pale yellow solution with no stannane precipitate remaining). Boronic ester (0.5 M in anhydrous Et_2O, 1.0 eq, 0.3 – 0.4 mmol) was then added dropwise to the reaction mixture at –78 °C. The reaction mixture was stirred at –78 °C for 30 min (the pale yellow solution loses its colour on the addition of the boronic ester). The reaction mixture was then transferred to a –42 °C cooling bath (MeCN/CO_2 ice bath) and stirred at this temperature for 1 h. The reaction mixture was removed from the cooling bath and stirred at room temperature for 1 h (as the 1,2-metallate rearrangement occurs a white precipitate of TIBOLi forms). The reaction mixture was filtered through silica (~10 mm depth of wetted (Et_2O) silica, using a filter frit connected directly to an oven dried receiving vessel) to give a colourless to pale yellow translucent solution. The silica was washed with Et_2O (reagent grade, 5 mL), the filter frit was removed and solvent was removed (*in situ*) under reduced pressure to give the crude boronic ester. The crude boronic ester could then be re-dissolved in anhydrous Et_2O (to make a 0.5 M solution) and used in further homologations or isolated and purified.

After every third homologation the crude reaction mixture was subjected to an aqueous workup.

Aqueous workup: After filtration the crude product was dissolved in Et_2O (5 mL) and H_2O (5 mL) and stirred for 1 min. The phases were separated and the aqueous phase extracted with Et_2O (3 × 5 mL). The combined organic phases were washed with H_2O (10 mL), dried ($MgSO_4$), filtered and the filtrate concentrated under reduced pressure to give the crude boronic ester which was then used in further homologations.

General procedure 3 (GP3): *p*-Nitro benzoate ester synthesis

Et_3N (4.0 eq) was added to a solution of alcohol (1.0 eq, approx. 0.04 mmol), DMAP (2.0 eq) and 4-nitrobenzoyl chloride (4.0 eq) in anhydrous CH_2Cl_2 (0.2 M). The reaction mixture was warmed to 40 °C and stirred at this temperature for 48 h. The reaction mixture was cooled to room temperature and diluted with water (2 mL). The phases were separated and the aqueous phase extracted with CH_2Cl_2 (3 × 5 mL). The combined organic phases were washed with brine (10 mL), dried ($MgSO_4$) and concentrated under reduced pressure. The crude product was purified by flash column chromatography.

Preparation of compounds

Ethyl 2,4,6-triisopropylbenzoate, 3

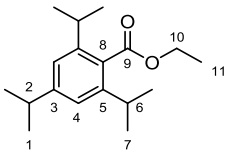

A biphasic mixture of 2,4,6-triisopropylbenzoic acid (20.2 g, 81.3 mmol, 1.0 eq), $NBu_4(HSO_4)$ (2.21 g, 6.5 mmol, 0.08 eq), NaOH (10.1 g, 252.0 mmol, 3.1 eq) and bromoethane (30.0 mL, 407 mmol, 5.0 eq) in $CHCl_3$ (400 mL) and H_2O (320 mL) in a 1 L rbf was vigorously stirred overnight at room temperature. The phases were separated and the aqueous phase extracted with CH_2Cl_2 (3 × 100 mL). The combined organic phases were washed with brine (300 mL), dried ($MgSO_4$) and concentrated under reduced pressure. The crude product was dissolved in pentane (60 mL) and the insoluble salts filtered off. The solvent was removed from the filtrate under reduced pressure to give benzoate ester **3** (20.1 g, 90%) as a colourless oil.

Spectral data were in accordance with the published values.[6]

R_f: 0.32 (97 : 3 pentane : EtOAc)

^{1}H NMR (400 MHz, $CDCl_3$): 1.25 (6H, d, *J* = 6.9 Hz, H1), 1.26 (12H, d, *J* = 6.9 Hz, H7), 1.38 (3H, t, *J* = 7.2 Hz, H11), 2.88 (3H, sept, *J* = 6.9 Hz, H2 and H6), 4.38 (2H, q, *J* = 7.2 Hz, H10), 7.02 (2H, s, H4)

^{13}C NMR (101 MHz, $CDCl_3$): 14.3 (C11), 24.0 (C1), 24.1 (C7), 31.4 (C6), 34.4 (C2), 60.8 (C10), 120.8 (C4), 130.6 (C_{Ar}-C), 144.7 (C_{Ar}-C), 150.1 (C_{Ar}-C), 170.8 (C9)

1-(Trimethylstannyl)ethyl 2,4,6-triisopropylbenzoate, (*S*)-5

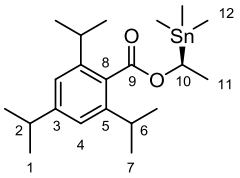

An oven-dried 1 L, two necked flask equipped with a 40 mm magnetic stirring bar, an oven-dried 100 mL pressure equalising dropping funnel and a gas inlet adaptor was attached to a vacuum manifold. The reaction flask was evacuated and refilled with nitrogen (× 3). 2,4,6-Triisopropyl ethyl benzoate **3** (11.6 g, 41.9 mmol, 1.0 eq) and (–)-sparteine (12.5 mL, 54.5 mmol, 1.3 eq) were added to the reaction vessel *via* syringe followed by the addition of anhydrous Et_2O (200 mL) *via* cannula. The solution was cooled to –78 °C and allowed to equilibrate for 10 min. *s*BuLi (1.3 M in hexanes, 41.9 mL, 54.5 mmol, 1.3 eq) was added dropwise *via* a pressure equalised dropping funnel (approx 1-2 mL/min) to the reaction mixture at –78 °C (colour change: colourless → dark brown). The reaction mixture was stirred at –78 °C for 4 h. Me_3SnCl (1.0 M in hexanes, 54.5 mL, 54.5 mmol, 1.3 eq,) in an oven dried, 100 mL Schlenk reaction vessel was added dropwise to the reaction mixture *via* cannula (colour change: dark brown → yellow). The reaction vessel containing the original solution of Me_3SnCl was washed with anhydrous Et_2O (20 mL) and this was transferred to the reaction mixture *via* cannula to wash the cannula of any Me_3SnCl. The reaction mixture was stirred at –78 ˚C for 20 min before being warmed to room temperature and stirred at this temperature for 1 h. The reaction mixture was diluted with H_3PO_4 (aq. 5%, 100 mL) and stirred for a further 20 min. The layers were separated and the organic layer washed with H_3PO_4 (aq. 5%, 3 × 100 mL). The combined aq layers were extracted with Et_2O (3 × 100 mL). The combined organic layers were dried ($MgSO_4$) and concentrated under reduced pressure to give crude stannane **(*S*)-5** (20 g, e.r. = 91 : 9).

The opposite enantiomer (**(*R*)-5**) was synthesised in identical yields and e.r. by substituting (–)-sparteine for (+)-sparteine. Alternatively **(*R*)-5** can also be synthesised by substituting (–)-sparteine for O'Brien's (+)-sparteine surrogate.[7] Racemic **5** was made by substituting (–)-sparteine for TMEDA.

Sparteine recovery[3]

The combined aqueous layers were made basic (brought to about pH 11) with NaOH ($20\%_{aq}$). The aqueous phase was extracted with Et_2O (3 × 100 mL). The combined aqueous layers were dried (K_2CO_3), filtered and concentrated under reduced pressure to give crude sparteine. Distillation over CaH_2 of the residual oil gave (–)-sparteine (11.0 mL, 88%) as a colourless oil.

Distillation conditions: bulb to bulb; 10 cm Vigreux column; pressure: 2 mbar; oil bath: 150 °C; CaH_2 (100 mg/mL); (-)-sparteine bp: 137-138 °C (1.33 mbar)

Recrystallisation of enantioenriched stannane

MeOH (3 mL/g) was added to the crude stannane in a one neck rbf. A condenser was fitted to the round bottom flask and the solution was brought to reflux (heat gun) so that all the solids had dissolved. The solution was then allowed to cool to room temperature. Crystals appeared after 10 min to 5 h depending on purity of crude stannane. The crystals were then filtered and dried under reduced pressure. Three crops of stannane were obtained. Crop 1 = 10.1 g, e.r. 98.9 : 1.1; Crop 2 = 3.89 g, e.r. 98.4 : 1.6; Crop 3 = 1.94 g, 98.4 : 1.6. The three crops were combine and recrystallised from MeOH (3 mL/g) to afford, after two crops, stannane **(*S*)-5** (10.1 g, 55%, e.r. 99.9 : 0.1) as a colourless solid.

R_f: 0.42 (97:3 pentane:Et_2O)

$[\alpha]^{20}_D$: +38.3 (*c* 1.1, $CHCl_3$)

MP: 65 – 66 ˚C (MeOH)

^{1}H NMR (400 MHz, $CDCl_3$): 0.19 (9H, s and d, *J* = 54.1 Hz and d, *J* = 51.8 Hz, H12), 1.25 (18H, d, *J* = 7.0 Hz, H1 and H7), 1.60 (3H, d, *J* = 7.6 Hz and dd, *J* = 57.8, 7.6 Hz and dd, *J* = 55.3, 7.6 Hz, H11), 2.78 – 2.98 (3H, m, H2 and H6), 5.05 (1H, q, *J* = 7.6 Hz and quin, *J* = 7.6 Hz, H10), 7.00 (2H, s, H4)

^{13}C NMR (101 MHz, $CDCl_3$): –9.9 (d, *J* = 334.2 Hz (^{13}C-^{119}Sn) and d, *J* = 319.2 Hz (^{13}C-^{117}Sn) and s, C12), 19.2 (C11), 24.0 (C1 or C7 or C7'), 24.1 (C1 or C7 or C7'), 24.3 (C1 or C7 or C7'), 31.3 (C6), 34.4 (C2), 67.0 (C10), 120.8 (C4), 130.8 (C_{Ar}-C), 144.8 (C_{Ar}-C), 149.9 (C_{Ar}-C), 171.3 (C9)

IR (ν_{max}/cm^{-1}, neat): 2957, 1693, 1256, 1071, 763

HRMS: (ESI$^+$) calcd. for $C_{21}H_{36}O_2SnNa$ (M+Na$^+$): 463.1629; Found: 463.1633

Chiral HPLC: (Daicel Chiralpak-IB column (25 cm) with guard, hexane, 0.9 mL/min, room temperature, 210.8 nm): t_R = 5.1 min (*S*), 6.8 min (*R*), e. r. = 99.9 : 0.1

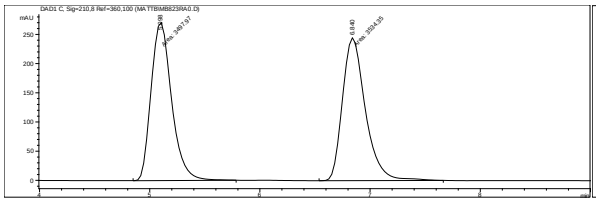

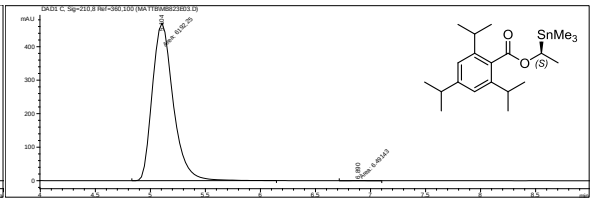

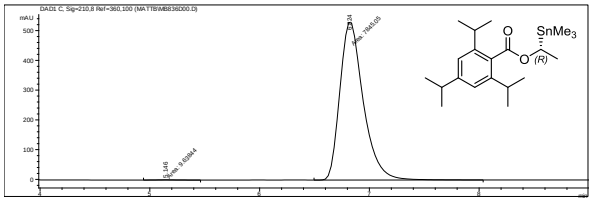

(*R*)-(1-([1,1'-Biphenyl]-4-yl)ethyl)boronic acid pinacol ester, (*R*)-10

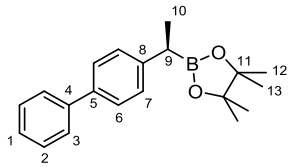

Prepared according to the procedure from Noh *et al.*[8] A solution of CuCl (34 mg, 0.33 mmol, 0.03 eq), NaO*t*Bu (64 mg, 0.66 mmol, 0.06 eq) and (*S*)-DTBM-segphos (400 mg, 0.33 mmol, 0.03 eq) in anhydrous, degassed toluene (8.0 mL) under an atmosphere of nitrogen was stirred at room temperature for 10 min. Pinacolborane (2.1 mL, 14.4 mmol, 1.3 eq) was added dropwise to the reaction mixture which was then stirred at room temperature for 10 min. 4-Vinylbiphenyl (2.0 g, 11.1 mmol, 1.0 eq) was added to the reaction mixture in one portion and the reaction mixture was stirred at room temperature for 24 h. The reaction mixture was filtered through a plug of Celite (~ 2 cm) and the filtrate was concentrated under reduce pressure. The crude product was purified by flash column chromatography (95 : 5 petroleum ether 40-60 : Et_2O) to give boronic ester **(*R*)-10** (3.02 g, 88%, e.r. = 98.0 : 2.0) as a colourless solid. The purified product was recrystallised from a minimal amount of refluxing pentane to give from 3 crops boronic ester **(*R*)-10** (2.77 g, 81%, e.r. = 99.3 : 0.7)

R_f: (95 : 5 pentane : EtOAc)
$[\alpha]^{20}_D$: –13.0 (*c* 1.0, $CHCl_3$)
MP: 67 – 69 ˚C (pentane)
^{1}H NMR (400 MHz, $CDCl_3$): 1.24 (6H, s, H12 or H13), 1.25 (6H, s, H12 or H13), 1.39 (3H, d, *J* = 7.5 Hz, H10), 2.51 (1H, q, *J* = 7.5 Hz, H9), 7.28 – 7.35 (3H, m, H_{Ar}), 7.40 – 7.47 (2H, m, H_{Ar}), 7.50 – 7.55 (2H, m, H_{Ar}), 7.28 – 7.35 (2H, m, H_{Ar})
^{13}C NMR (101 MHz, $CDCl_3$): 17.1 (C10), 24.60 (C12 or C13), 24.64 (C12 or C13), 83.3 (C11), 126.8 (C_{Ar}-H), 126.9 (C_{Ar}-H), 127.0 (C_{Ar}-H), 128.2 (C_{Ar}-H), 128.6 (C_{Ar}-H), 137.9 (C_{Ar}-C), 141.2 (C_{Ar}-C), 144.2 (C_{Ar}-C)

Boronic ester **(*R*)-10** (about 50 mg) was oxidised to the corresponding alcohol according to **GP1** for chiral HPLC analysis and to confirm the relative stereochemistry.

$[\alpha]^{22}_D$: +45.9 (*c* 1.0, $CHCl_3$)
Lit $[\alpha]^{22}_D$: +40.6 (*c* 1.0, $CHCl_3$, 94% ee, (*R*))[9]
Chiral SFC: (Daicel Chiralpak IB column (25 cm), 10.0% co-solvent (MeOH), 4.0 mL/min, 40 °C, 125 mbar, 210 nm): t_R = 3.23 min (minor), 3.51 min (major), e. r. = 99.3 : 0.7

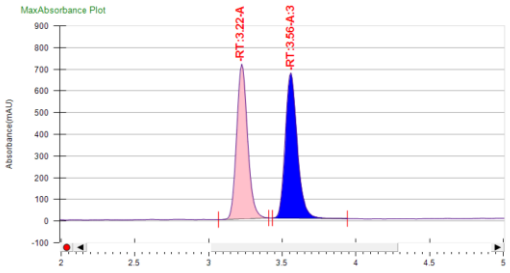

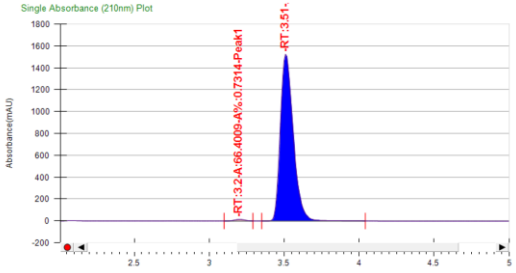

Peak Information

Peak No	% Area	Area	Ret. Time	Height	Cap. Factor
1	0.7314	66.4009	3.2 min	14.3614	3198.95
2	99.2686	9011.6746	3.51 min	1525.3675	3507.2833

(*R*)-(1-Phenylethyl)boronic acid pinacol ester, (*R*)-16

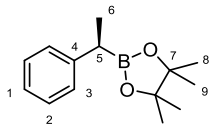

Prepared according to the procedure by Roesner *et al.*[10] *s*BuLi (1.3 M in hexanes, 3.2 mL, 4.10 mmol, 1.3 eq) was added dropwise to a solution of carbamate **(*R*)-23** (786 mg, 3.16 mmol, 1.0 eq, e.r. = 99.5 : 0.5) in anhydrous Et_2O (10.5 mL) at –78 °C under an atmosphere of nitrogen. The reaction mixture was stirred for 20 min at –78 °C before the dropwise addition of a solution of HBpin (0.92 mL, 6.31 mmol, 2.0 eq) in anhydrous Et_2O (5 mL). The reaction mixture was stirred at –78 °C for 1 h before being warmed to room temperature. The reaction mixture was stirred at room temperature for 12 h and then diluted with NH_4Cl (5 mL, sat. aq.) and H_2O (5 mL). The phases were separated and the aqueous phase extracted with Et_2O (3 × 10 mL). The combined organic phases were dried ($MgSO_4$) and concentrated under reduced pressure. The crude product was purified by flash column chromatography (95 : 5 pentane : Et_2O) to give boronic ester **(*R*)-16** (387 mg, 55%, e.r. = 98.6 : 1.4) as a colourless oil.

Spectral data were in accordance with the published values.[10]

R_f: 0.28 (95 : 5 pentane : Et_2O)

$[\alpha]^{20}_D$: –13.9 (*c* 1.0, $CHCl_3$)

Lit $[\alpha]^{20}_D$: +10.0 (*c* = 1.0, $CHCl_3$, 98% ee, (*S*))[10]

^{1}H NMR (400 MHz, $CDCl_3$): 1.21 (6H, s, H8 or H9), 1.22 (6H, s, H8 or H9), 1.34 (3H, d, *J* = 7.5 Hz, H6), 2.44 (1H, q, *J* = 7.5 Hz, H5), 7.11 – 7.17 (1H, m, H_{Ar}), 7.21 – 7.30 (4H, m, H_{Ar})

^{13}C NMR (101 MHz, $CDCl_3$): 17.0 (C6), 24.57 (C8 or C9), 24.62 (C8 or C9), 83.3 (C7), 125.1 (C1), 127.8 (C_{Ar}-H), 128.3 (C_{Ar}-H), 145.0 (C4)

Boronic ester **(*R*)-16** (about 20 mg) was oxidised to the corresponding alcohol according to **GP1** for chiral HPLC analysis.

Chiral HPLC: (Daicel Chiralpak-IB column (25 cm) with guard, 2.0% isopropanol in hexane, 1.0 mL/min, room temperature, 210.8 nm): t_R = 21.1 minutes (major), 24.1 minutes (minor), e. r. = 98.6 : 1.4

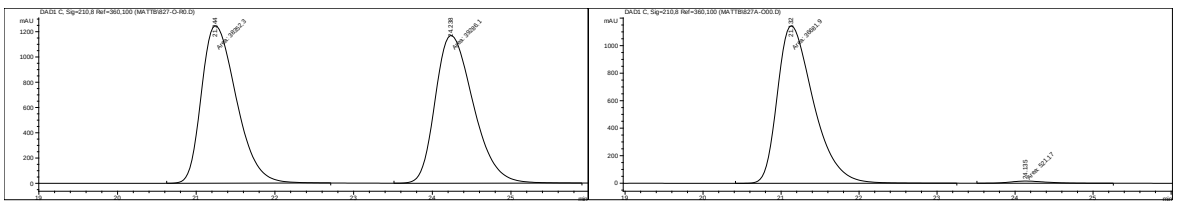

2-((2*R*,3*S*,4*S*,5*S*,6*S*,7*S*,8*S*,9*S*,10*S*,11*S*)-11-([1,1'-biphenyl]-4-yl)-3,4,5,6,7,8,9,10-octamethyldodecan-2-yl)-4,4,5,5-tetramethyl-1,3,2-dioxaborolane, 11

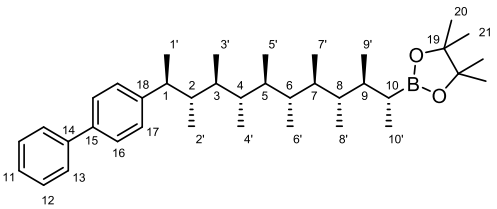

Synthesised according to **GP2**. Stannane **(*S*)-5** (237 mg, 0.54 mmol, 1.35 eq), *n*BuLi (1.57 M in hexanes, 0.33 mL, 0.52 mmol, 1.30 eq) and boronic ester **(*R*)-10** (123 mg, 0.40 mmol, 1.00 eq). Aqueous workup was performed after homologations 3 and 6 and flash column chromatography after homologation 9 (pentane : PhMe 70 : 30 → 60 : 40) to give boronic ester **11** (130 mg, 58%) as a colourless oil.

R_f: 0.33 (pentane : PhMe 60 : 40)

$[\alpha]^{20}_D$: +6.2 (*c* 1.1, $CHCl_3$)

^{1}H NMR (500 MHz, $CDCl_3$): 0.82 (3H, d, *J* = 7.0 Hz, H2'), 0.89 (3H, d, *J* = 7.0 Hz, CH_3), 0.91 (3H, d, *J* = 6.4 Hz, CH_3), 0.92 (3H, d, *J* = 7.0 Hz, CH_3), 0.94 – 1.01 (12H, m, 4 × CH_3), 1.02 (3H, d, *J* = 7.0 Hz, CH_3), 1.33 (3H, d, *J* = 7.1 Hz, H1'), 1.15 – 1.27 (1H, m, CH), 1.24 (12H, s, H20 and H21), 1.46 – 1.53 (1H, m, CH), 1.53 – 1.69 (5H, m, 5 × CH), 1.69 – 1.78 (1H, m, CH), 1.79 – 1.88 (1H, m, H2), 2.94 (1H, quin, *J* = 6.9 Hz, H1), 7.24 – 7.27 (2H, m, H_{Ar}), 7.30 – 7.35 (1H, m, H_{Ar}), 7.41 – 7.46 (2H, m, H_{Ar}), 7.50 – 7.54 (2H, m, H_{Ar}), 7.59 – 7.63 (2H, m, H_{Ar})

^{13}C NMR (125 MHz, $CDCl_3$): 15.55 (CH_3), 15.78 (CH_3), 16.08 (CH_3), 16.18 (CH_3), 16.19 (CH_3), 17.22 (CH_3), 17.40 (CH_3), 17.47 (CH_3), 17.73 (CH_3), 21.70 (CH_3), 24.72 (C20 or C21), 24.76 (C20 or C21), 39.19 (CH), 39.99 (CH), 40.07 (CH), 40.23 (CH), 40.34 (CH), 40.65 (CH), 41.11 (CH), 41.47 (CH), 42.53 (CH), 82.4 (C19), 126.5 (C_{Ar}-H), 126.88 (C_{Ar}-H), 126.92 (C_{Ar}-H), 128.65 (C_{Ar}-H), 128.70 (C_{Ar}-H), 138.4 (C_{Ar}-C), 141.1 (C_{Ar}-C), 145.9 (C_{Ar}-C)

IR (ν_{max}/cm^{-1}, neat): 5960, 2928, 2874, 1459, 1312, 1143

HRMS: (EI) calcd. for $C_{38}H_{61}BO_2$ (M^+): 560.4765; Found 560.4745

GCMS: Chromatogram for boronic ester **11** before purification. GCMS method: 110-2.

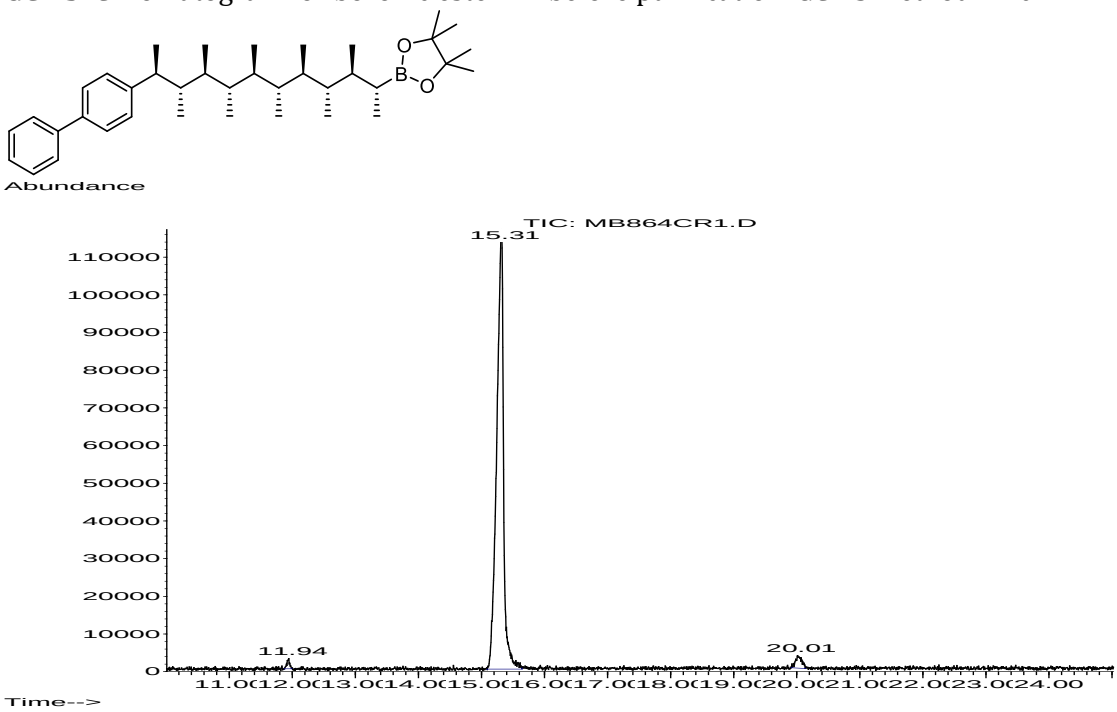

Area Percent Report

Signal : TIC

peak #	R.T. min	first scan	max scan	last scan	PK TY	peak height	corr. area	corr. % max.	% of total
1	11.944	1189	1201	1209	M3	2834	68356	0.78%	0.760%
2	15.316	1752	1791	1847	M4	116789	8727707	100.00%	97.037%
3	20.014	2597	2613	2635	M5	3406	198101	2.27%	2.203%

2-((2*S*,3*S*,4*R*,5*S*,6*R*,7*S*,8*R*,9*S*,10*R*,11*S*)-11-([1,1'-biphenyl]-4-yl)-3,4,5,6,7,8,9,10-octamethyldodecan-2-yl)-4,4,5,5-tetramethyl-1,3,2-dioxaborolane, 13

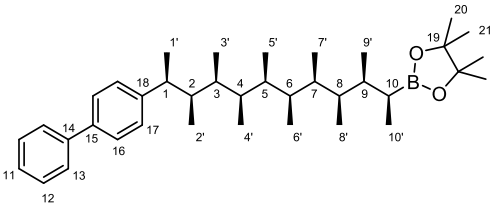

Synthesised according to **GP2**. Stannane **(*S*)-** and **(*R*)-5** (229 mg, 0.52 mmol, 1.30 eq), *n*BuLi (1.54 M in hexanes, 0.34 mL, 0.52 mmol, 1.30 eq) and boronic ester **(*R*)-10** (123 mg, 0.40 mmol, 1.00 eq). Aqueous workup was performed after homologations 3 and 6 and after homologation 9 the crude boronic ester was purified by prep HPLC (Kromacil 60-5-SIL 250 mm × 21.2 mm; hexane : EtOAc: 99 : 1; 20 mL/min) to give boronic ester **13** (98 mg, 44%) as a colourless oil.

R_f: 0.24 (pentane : Et_2O 97 : 3)

$[\alpha]^{20}_D$: –14.2 (*c* 1.3, $CHCl_3$)

^{1}H NMR (500 MHz, $CDCl_3$): 0.45 (3H, d, *J* = 6.2 Hz, CH_3), 0.62 (3H, d, *J* = 6.6 Hz, CH_3), 0.73 (6H, d, *J* = 6.7 Hz, 2×CH_3), 0.74 (3H, d, *J* = 6.2 Hz, CH_3), 0.75 (3H, d, *J* = 6.8 Hz, CH_3), 0.76 (3H, d, *J* = 6.8 Hz, CH_3), 0.88 (3H, d, *J* = 6.7 Hz, CH_3), 0.93 (3H, d, *J* = 7.2 Hz, CH_3), 1.00 – 1.08 (1H, m, H10), 1.11 – 1.21 (1H, m, CH), 1.24 (6H, s, H20 or H21), 1.25 (6H, s, H20 or H21), 1.26 (3H, d, *J* = 6.9 Hz, CH_3), 1.29 – 1.39 (1H, m, CH), 1.41 – 1.53 (4H, m, 4 × CH), 1.70(1H, dqd, *J* = 9.2, 6.7, 4.0, CH), 1.85 (dqd, *J* = 9.9, 6.7, 3.2 Hz, CH), 2.67 (1H, dq, *J* = 9.4, 6.9 Hz, H1), 7.21 – 7.25 (2H, m, H_{Ar}), 7.31 – 7.35 (1H, m, H_{Ar}), 7.41 – 7.47 (2H, m, H_{Ar}), 7.50 – 7.55 (2H, m, H_{Ar}), 7.59 – 7.64 (2H, m, H_{Ar})

^{13}C NMR (125 MHz, $CDCl_3$): 11.41 (CH_3), 11.55 (CH_3), 11.73 (CH_3), 11.78 (CH_3), 11.80 (CH_3), 11.87 (CH_3), 11.94 (CH_3), 12.47 (CH_3), 13.02 (CH_3), 19.95 (CH_3), 24.6 (C20 or C21), 24.9 (C20 or C21), 35.10 (CH), 35.35 (CH), 35.52 (2 × CH), 35.61 (CH), 35.93 (CH), 39.78 (2 × CH), 43.04 (H1), 82.7 (C19), 126.82 (C_{Ar}-H), 126.86 (C_{Ar}-H), 126.93 (C_{Ar}-H), 127.8 (C_{Ar}-H), 128.7 (C_{Ar}-H), 138.4 (C_{Ar}-C), 141.2 (C_{Ar}-C), 146.9 (C_{Ar}-C)

IR (ν_{max}/cm^{-1}, neat): 2967, 2923, 1380, 1312, 763, 696

HRMS: (EI) calcd. for $C_{38}H_{61}BO_2$ (M^+): 560.4765; Found 560.4742

GCMS: Chromatogram for boronic ester **13** before purification. GCMS method: 110-1.

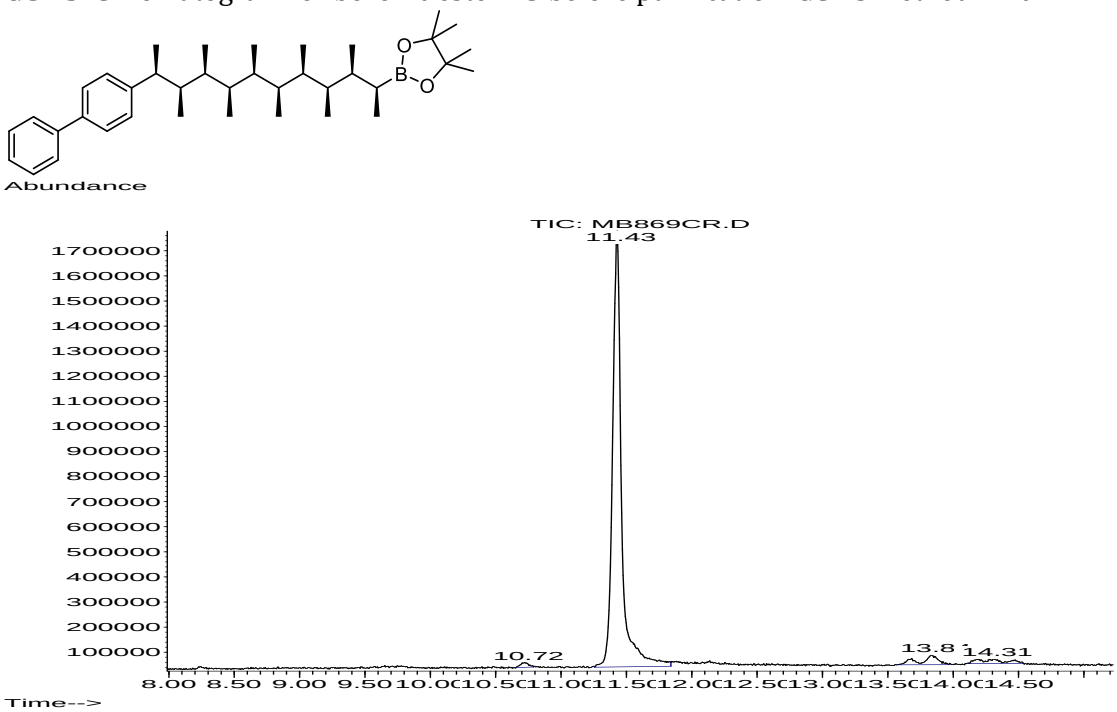

Area Percent Report

Signal : TIC

peak #	R.T. min	first scan	max scan	last scan	PK TY	peak height	corr. area	% max.	% of total
1	10.720	976	987	999	M	18334	685511	0.80%	0.754%
2	11.429	1081	1111	1217	M	1742835	85482678	100.00%	94.032%
3	13.841	1494	1533	1546	M	35185	2416930	2.83%	2.659%
4	14.310	1583	1615	1654	M	18228	2322553	2.72%	2.555%

4,4,5,5-tetramethyl-2-((2*S*,3*S*,4*S*,5*R*,6*R*,7*S*,8*S*,9*R*,10*R*,11*S*)-3,4,5,6,7,8,9,10-octamethyl-11-phenyldodecan-2-yl)-1,3,2-dioxaborolane, 17

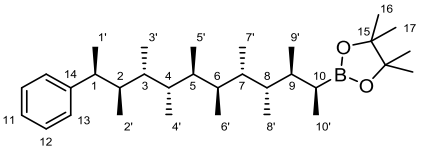

Synthesised according to **GP2**. Stannane **(*S*)-** and **(*R*)-5** (171 mg, 0.39 mmol, 1.30 eq), *n*BuLi (1.60 M in hexanes, 0.24 mL, 0.39 mmol, 1.30 eq) and boronic ester **(*R*)-16** (69 mg, 0.30 mmol, 1.00 eq). Aqueous workup was performed after homologations 3 and 6 and flash column chromatography after homologation 9 (pentane : PhMe 60 : 40 → 50 : 50) to give boronic ester **17** (65 mg, 45%) as a colourless solid.

R_f: 0.34 (pentane : PhMe 60 : 40)

$[\alpha]^{20}_D$: +2.8 (*c* 0.7, $CHCl_3$)

MP: 155 – 158 °C (pentane)

^{1}H NMR (500 MHz, $CDCl_3$): 0.65 (3H, d, *J* = 6.3 Hz, CH_3), 0.67 (3H, d, *J* = 5.9 Hz, CH_3), 0.68 (3H, d, *J* = 6.1 Hz, CH_3), 0.69 (3H, d, *J* = 6.1 Hz, CH_3), 0.717 (3H, d, *J* = 6.2 Hz, CH_3), 0.719 (3H, d, *J* = 6.7 Hz, CH_3), 0.83 (3H, d, *J* = 7.1 Hz, CH_3), 0.84 (3H, d, *J* = 7.8 Hz, CH_3), 0.90 (3H, d, *J* = 6.3 Hz, CH_3), 1.14 (3H, d, *J* = 7.2 Hz, CH_3), 1.25 (6H, s, H16 or H17), 1.26 (6H, s, H16 or H17), 1.34 (1H, qd, *J* = 7.7, 3.3 Hz, H10), 1.46 – 1.70 (8H, m, 8 × CH), 3.14 (1H, qd, *J* = 7.1, 2.7 Hz, H1), 7.15 – 7.20 (1H, m, H_{Ar}), 7.21 – 7.26 (2H, m, H_{Ar}), 7.28 – 7.33 (2H, m, H_{Ar})

^{13}C NMR (125 MHz, $CDCl_3$): 7.96 (CH_3), 11.16 (CH_3), 11.28 (CH_3), 11.29 (CH_3), 11.36 (CH_3), 11.37 (CH_3), 11.41 (CH_3), 11.42 (CH_3), 11.80 (CH_3), 15.79 (CH_3), 24.7 (C16 or C17), 25.0 (C16 or C17), 35.12 (CH), 35.20 (CH), 35.40 (CH), 35.68 (CH), 35.71 (CH), 35.80 (CH), 35.83 (CH), 39.13 (CH), 42.82 (CH), 82.8 (C15), 125.4 (C_{Ar}-H), 127.86 (C_{Ar}-H), 127.89 (C_{Ar}-H), 147.7 (C_{Ar}-C)

IR (ν_{max}/cm^{-1}, neat): 2965, 2930, 1370, 1313, 1143, 698

HRMS: (ESI^+) calcd. for $C_{32}H_{57}BO_2Na$ ($M+Na^+$): 507.4350; Found 507.4346

GCMS: Chromatogram for boronic ester **17** after flash column chromatography. GCMS method: 70-1.

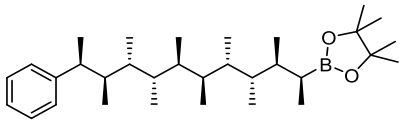

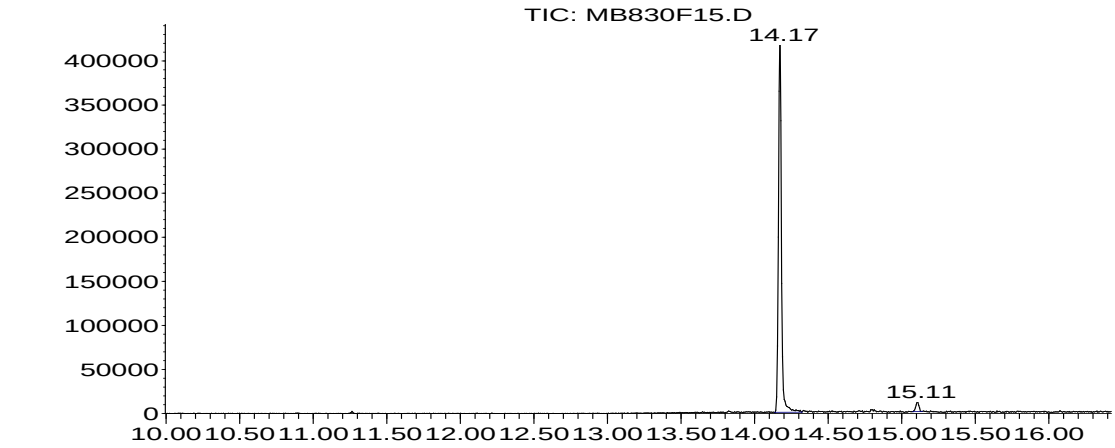

Area Percent Report

Signal : TIC

peak #	R.T. min	first scan	max scan	last scan	PK TY	peak height	corr. area	% max.	corr. % total
1	14.173	1935	1941	1967	M	440636	5984284	100.00%	97.277%
2	15.104	2099	2104	2109	M3	11776	167512	2.80%	2.723%

(2*R*,3*R*,4*R*,5*R*,6*R*,7*R*,8*S*,9*S*,10*S*,11*S*)-11-([1,1'-biphenyl]-4-yl)-3,4,5,6,7,8,9,10-octamethyldodecan-2-ol, 22

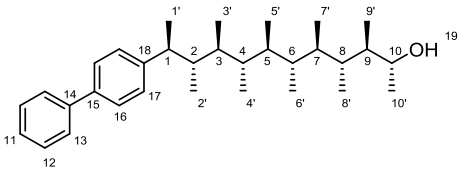

Boronic ester **11** (50 mg, 0.089 mmol) was oxidised to alcohol **22** according to **GP1**. The crude product was purified by flash column chromatography (pentane : Et_2O 80 : 20 → 65 : 35) to give alcohol **22** (33 mg, 82%) as a colourless solid.

R_f: 0.32 (pentane : Et_2O 65 : 35)

$[\alpha]^{22}_D$: +16.7 (*c* 1.8, $CHCl_3$)

^{1}H NMR (500 MHz, $CDCl_3$): 0.83 (3H, d, *J* = 7.0 Hz, CH_3), 0.92 (6H, d, *J* = 6.9 Hz, 2 × CH_3), 0.94 (3H, d, *J* = 7.0 Hz, CH_3), 0.95 (3H, d, *J* = 6.2 Hz, CH_3), 0.98 (3H, d, *J* = 7.0 Hz, CH_3), 1.02 (3H, d, *J* = 6.8 Hz, CH_3), 1.03 (3H, d, *J* = 7.0 Hz, CH_3), 1.06 (1H, br. s, H19), 1.19 (3H, d, *J* = 6.5 Hz, CH_3), 1.34 (3H, d, *J* = 7.1 Hz, CH_3), 1.51 – 1.69 (6H, m, 6 × CH), 1.69 – 1.78 (1H, m, CH), 1.79 – 1.88 (1H, m, CH), 2.95 (1H, apart. quin, *J* = 6.8 Hz, H1), 4.04 (1H, br. q, *J* = 6.4 Hz, H10), 7.24 – 7.27 (2H, m, H_{Ar}), 7.30 – 7.35 (1H, m, H_{Ar}), 7.41 – 7.46 (2H, m, H_{Ar}), 7.50 – 7.54 (2H, m, H_{Ar}), 7.59 – 7.63 (2H, m, H_{Ar})

^{13}C NMR (125 MHz, $CDCl_3$): 12.31 (CH_3), 15.37 (CH_3), 16.05 (CH_3), 16.22 (CH_3), 16.39 (CH_3), 17.01 (CH_3), 17.18 (CH_3), 17.36 (CH_3), 21.63 (CH_3), 23.09 (CH_3), 39.46 (CH), 39.82 (CH), 39.93 (CH), 40.15 (CH), 40.29 (CH), 40.35 (CH), 40.36 (CH), 41.37 (CH), 42.57 (CH), 67.27 (H10), 126.5 (C_{Ar}-H), 126.90 (C_{Ar}-H), 126.92 (C_{Ar}-H), 128.66 (C_{Ar}-H), 128.73 (C_{Ar}-H), 138.5 (C_{Ar}-C), 141.1 (C_{Ar}-C), 145.7 (C_{Ar}-C)

IR (ν_{max}/cm^{-1}, neat): 3443, 2964, 2876, 1456, 1374, 757, 691

HRMS: (EI) calcd. for $C_{32}H_{50}O$ (M^+): 450.3862; Found: 450.3855

(2*S*,3*R*,4*S*,5*R*,6*S*,7*R*,8*R*,9*S*,10*R*,11*S*)-11-([1,1'-biphenyl]-4-yl)-3,4,5,6,7,8,9,10-octamethyldodecan-2-ol, 14

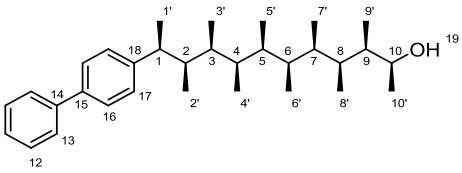

Boronic ester **13** (53 mg, 0.095 mmol) was oxidised to alcohol **14** according to **GP1**. The crude product was purified by flash column chromatography (pentane : Et_2O 75 : 25 → 65 : 35) to give alcohol **14** (40 mg, 94%) as a colourless oil.

R_f: 0.30 (pentane : Et_2O 65 : 35)

$[\alpha]^{21}_D$: +6.9 (*c* 1.2, $CHCl_3$)

^{1}H NMR (500 MHz, $CDCl_3$): 0.44 (3H, d, *J* = 6.3 Hz, H5'), 0.61 (3H, d, *J* = 6.7 Hz, H4'), 0.71 (3H, d, *J* = 6.9 Hz, H9'), 0.74 (3H, d, *J* = 6.4 Hz, H6'), 0.75 (3H, d, *J* = 6.6 Hz, H3'), 0.80 (6H, d, *J* = 6.4 Hz, H7' and H8'), 0.90 (3H, d, *J* = 6.4 Hz, H2'), 1.15 (1H, dqd, *J* = 8.8, 6.6, 2.5 Hz, H3), 1.20 (3H, d, *J* = 5.7 Hz, H10'), 1.27 (3H, d, *J* = 6.7 Hz, H1'), 1.39 – 1.52 (4H, m, 4 × CH(H4, H5, H6 and H7)), 1.56 (1H, dqd, *J* = 7.3, 6.9, 3.1 Hz, H9), 1.76 (1H, dqd, *J* = 9.9, 6.4, 3.1 Hz, H8), 1.87 (1H, dqd, *J* = 9.4, 6.4, 2.5 Hz, H2), 2.65 (1H, dq, *J* = 9.4, 6.7 Hz, H1), 3.65 (1H, dq, *J* = 7.3, 5.7 Hz, H10), 7.21 – 7.26 (2H, m, H_{Ar}), 7.31 – 7.36 (1H, m, H_{Ar}), 7.41 – 7.47 (2H, m, H_{Ar}), 7.51 – 7.56 (2H, m, H_{Ar}), 7.59 – 7.64 (2H, m, H_{Ar})

^{13}C NMR (125 MHz, $CDCl_3$): 10.25 (C9'), 11.43 (C3'), 11.58 (C5'), 11.68 (C4' and C6'), 11.73 (C2'), 11.79 (C7'), 11.89 (C8'), 20.29 (C1'), 21.53 (C10'), 34.51 (C8), 35.01 (C4), 35.10 (C7), 35.25 (C6), 35.36 (C5), 35.90 (C3), 35.98 (C2), 40.88 (C9), 43.22 (C1), 69.83 (C10), 126.8 (C_{Ar}-H), 126.88 (C_{Ar}-H), 126.91 (C_{Ar}-H), 127.8 (C_{Ar}-H), 128.7 (C_{Ar}-H), 138.5 (C_{Ar}-C), 141.1 (C_{Ar}-C), 146.9 (C_{Ar}-C)

IR (ν_{max}/cm^{-1}, neat): 3375, 2967, 2924, 2877, 1653, 1559, 1457, 1380

HRMS: (ESI$^+$) calcd. for $C_{32}H_{50}ONa$ (M+Na$^+$): 473.3754; Found 473.3743

((2*S*,3*R*,4*R*,5*S*,6*R*,7*S*,8*S*,9*R*,10*R*,11*S*)-11-(methoxymethoxy)-3,4,5,6,7,8,9,10-octamethyldodecan-2-yl)benzene, 18

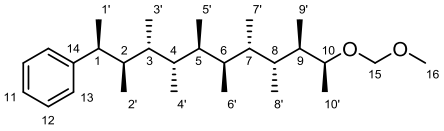

Boronic ester **17** (28 mg, 58 µmol) was oxidised to the corresponding alcohol according to **GP1**. The crude product then dissolved in anhydrous CH_2Cl_2 (2 mL). To the reaction mixture was added chloromethyl methyl ether (30 µL, 0.39 mmol, 6.7 eq) and Hünig's base (70 µL, 0.40 mmol, 6.9 eq). The reaction mixture was stirred at room temperature for 5 h before being diluted with water (3 mL). The phases were separated and the aqueous phase extracted with CH_2Cl_2 (3 × 2 mL). The combined organic phases were washed with brine (5 mL), dried ($MgSO_4$) and concentrated under reduced pressure. The crude product was purified by flash column chromatography (pentane : Et_2O 95 : 5) to give methyl ether **18** (9 mg, 37%) as a colourless solid.

R_f: 0.22 (95 : 5 pentane : Et_2O)

$[\alpha]^{20}_D$: -13.3 (*c* 0.3, $CHCl_3$)

MP: 138 – 141 °C

^{1}H NMR (500 MHz, $CDCl_3$): 0.65 (3H, d, *J* = 6.3 Hz, H2'), 0.67 (3H, d, *J* = 6.4 Hz, CH_3), 0.69 (3H, d, *J* = 6.2 Hz, CH_3), 0.70 (3H, d, *J* = 6.1 Hz, CH_3), 0.72 (3H, d, *J* = 6.3 Hz, CH_3), 0.74 (3H, d, *J* = 6.8 Hz, H8'), 0.88 (3H, d, *J* = 6.7 Hz, H9'), 0.91 (3H, d, *J* = 6.3 Hz, H3'), 1.06 (3H, d, *J* = 6.4 Hz, H10'), 1.15 (3H, d, *J* = 7.1 Hz, H1'), 1.38 (1H, dqd, *J* = 9.2, 6.8, 1.9 Hz, H8), 1.48 – 1.65 (6H, m, 6 × CH), 1.71 (1H, dqd, *J* = 9.2, 6.7, 3.5 Hz, H9), 3.14 (1H, qd, *J* = 7.1, 3.4 Hz, H1), 3.39 (3H, s, H16), 3.92 (1H, qd, *J* = 6.4, 3.5 Hz, H10), 4.66 (1H, d, *J* = 6.7 Hz, H15), 4.68 (1H, d, *J* = 6.7 Hz, H15'), 7.16 – 7.21 (1H, m, H_{Ar}), 7.21 – 7.26 (2H, m, H_{Ar}), 7.28 – 7.34 (1H, m, H_{Ar})

^{13}C NMR (125 MHz, $CDCl_3$): 11.03 (C9'), 11.14 (C2'), 11.17 (CH_3), 11.30 (CH_3), 11.37 (CH_3), 11.38 (CH_3), 11.40 (C1'), 11.41 (C8'), 11.79 (C3'), 13.61 (C10'), 35.17 (C8), 35.29 (CH), 35.32 (CH), 35.41 (CH), 35.67 (C3), 35.73 (CH), 39.13 (C1), 39.86 (C9), 42.8 (C2), 55.2 (C16), 73.9 (C10), 94.7 (C15), 125.4 ($C_{Ar\text{-}H}$), 127.86 ($C_{Ar\text{-}H}$), 127.90 ($C_{Ar\text{-}H}$), 147.7 ($C_{Ar\text{-}C}$)

IR (ν_{max}/cm^{-1}, neat): 2969, 2929, 2881, 1470, 1375, 1035

HRMS: (ESI$^+$) calcd. for $C_{28}H_{50}O_2Na$ (M+Na$^+$): 441.3703; Found: 441.3697

(2*R*,3*R*,4*R*,5*R*,6*R*,7*R*,8*S*,9*S*,10*S*,11*S*)-11-([1,1'-biphenyl]-4-yl)-3,4,5,6,7,8,9,10-octamethyldodecan-2-yl 4-nitrobenzoate, 12

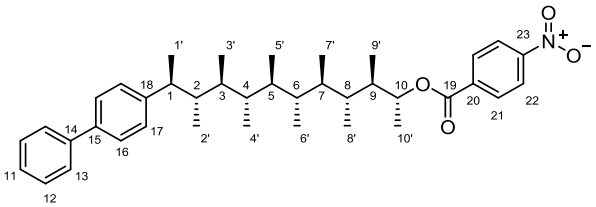

Synthesised according to general procedure **GP3** from alcohol **22** (21 mg, 47 µmol). Flash column chromatography (pentane : Et_2O 93 : 7) gave benzoate ester **12** (24 mg, 85%) as a colourless solid. Crystals suitable for X-ray diffraction were obtained by recrystallisation from IPA/Et_2O using a slow evaporation technique.

R_f: 0.39 (pentane : Et_2O 90 : 10)

[α]$^{22}_D$: –13.8 (*c* 0.65, $CHCl_3$)

MP: 155 – 158 °C (Et_2O/IPA)

^{1}H NMR (500 MHz, $CDCl_3$): 0.81 (3H, d, *J* = 7.1 Hz, H2'), 0.86 (3H, d, *J* = 6.9 Hz, CH_3), 0.90 (3H, d, *J* = 6.4 Hz, CH_3), 0.94 – 0.98 (9H, m, 3 × CH_3), 1.01 (3H, d, *J* = 7.0 Hz, CH_3), 1.19 (3H, d, *J* = 7.1 Hz, H9'), 1.33 (3H, d, *J* = 7.0 Hz, H1'), 1.36 (3H, d, *J* = 6.4 Hz, H10'), 1.54 – 1.68 (5H, m, 5 × CH), 1.68 – 1.76 (1H, m, CH), 1.79 – 1.86 (1H, m, H2), 1.86 – 1.92 (1H, m, H9), 2.92 (1H, app. quin, *J* = 7.0 Hz, H1), 5.40 (1H, qd, *J* = 6.4, 1.4 Hz, H10), 7.22 – 7.26 (2H, m, H_{Ar}), 7.30 – 7.35 (1H, m, H_{Ar}), 7.40 – 7.46 (2H, m, H_{Ar}), 7.49 – 7.53 (2H, m, H_{Ar}), 7.58 – 7.62 (2H, m, H_{Ar}), 8.18 – 8.22 (2H, m, H_{Ar}), 8.28 – 8.32 (2H, m, H_{Ar})

^{13}C NMR (125 MHz, $CDCl_3$): 13.78 (C9'), 14.81 (CH_3), 16.13 (C2'), 16.19 (CH_3), 16.20 (CH_3), 16.92 (CH_3), 17.16 (CH_3), 17.29 (CH_3), 19.60 (C10'), 21.67 (C1'), 38.43 (C9), 39.54 (CH), 39.99 (CH), 40.13 (CH), 40.28 (CH), 40.30 (CH), 40.31 (CH), 41.40 (C1), 42.50 (C2), 72.27 (C10), 123.5 (C_{Ar}-H), 126.5 (C_{Ar}-H), 126.9 (2 × C_{Ar}-H), 128.66 (C_{Ar}-H), 128.69 (C_{Ar}-H), 130.5 (C_{Ar}-H), 136.5 (C_{Ar}-C), 138.5 (C_{Ar}-C), 141.1 (C_{Ar}-C), 145.8 (C_{Ar}-C), 150.4 (C23), 164.0 (C19)

IR (ν_{max}/cm^{-1}, neat): 2967, 1695, 1278, 1100, 762

HRMS: (EI$^+$) calcd. for $C_{39}H_{53}NO_4$ (M): 599.3975; Found: 599.3968

(2*S*,3*R*,4*S*,5*R*,6*S*,7*R*,8*R*,9*S*,10*R*,11*S*)-11-([1,1'-biphenyl]-4-yl)-3,4,5,6,7,8,9,10-octamethyldodecan-2-yl 4-nitrobenzoate, 15

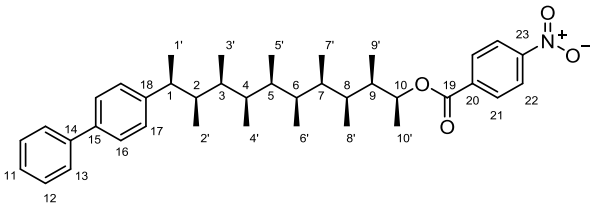

Synthesised according to general procedure **GP3** from alcohol **14** (15 mg, 33 µmol). Flash column chromatography (pentane : Et_2O 95 : 5 → 90 : 10) gave benzoate ester **15** (20 mg, 100%) as a colourless solid. Crystals suitable for X-ray diffraction were obtained by recrystallisation from IPA/Et_2O using a slow evaporation technique.

R_f: 0.35 (pentane : Et_2O 90 : 10)

[α]$^{22}_D$: -50.9 (*c* 0.55, $CHCl_3$)

MP: 147-149 °C (Et_2O/IPA)

^{1}H NMR (500 MHz, $CDCl_3$): 0.47 (3H, d, *J* = 5.8 Hz, CH_3), 0.64 (3H, d, *J* = 6.6 Hz, CH_3), 0.73 (3H, d, *J* = 5.9 Hz, CH_3), 0.74 (3H, d, *J* = 6.7 Hz, H3'), 0.76 (3H, d, *J* = 6.4 Hz, CH_3), 0.78 (3H, d, *J* = 6.6 Hz, CH_3), 0.84 (3H, d, *J* = 7.0 Hz, H9'), 0.88 (3H, d, *J* = 6.7 Hz, H2'), 1.18 (1H, dqd, *J* = 9.8, 6.7, 3.0 Hz, H3), 1.26 (3H, d, *J* = 6.9 Hz, H1'), 1.34 (3H, d, *J* = 6.3 Hz, H10'), 1.42 – 1.62 (5H, m, 5 × CH), 1.85 (1H, dqd, *J* = 9.7, 6.7, 3.0 Hz, H2), 1.99 (1H, dqd, *J* = 8.6, 7.0, 3.3 Hz, H9), 2.66 (1H, dq, *J* = 9.7, 6.9 Hz, H1), 5.16 (1H, dq, *J* = 8.6, 6.3 Hz, H10), 7.22 – 7.26 (2H, m, H_{Ar}), 7.31 – 7.36 (1H, m, H_{Ar}), 7.41 – 7.47 (2H, m, H_{Ar}), 7.51 – 7.56 (2H, m, H_{Ar}), 7.60 – 7.65 (2H, m, H_{Ar}), 8.18 – 8.23 (2H, m, H_{Ar}), 8.27 – 8.32 (2H, m, H_{Ar})

^{13}C NMR (125 MHz, $CDCl_3$): 10.24 (C9'), 11.43 (C3'), 11.63 (CH_3), 11.71 (CH_3), 11.73 (CH_3), 11.75 (CH_3), 11.79 (CH_3), 11.91 (CH_3), 18.02 (C10'), 20.09 (C1'), 34.77 (CH), 34.82 (CH), 35.03 (CH), 35.28 (CH), 35.49 (CH), 35.83 (C3), 38.25 (C9), 39.65 (C2), 43.08 (C1), 74.70 (C10), 123.5 (C_{Ar}-H), 126.84 (C_{Ar}-H), 126.90 (C_{Ar}-H), 126.92 (C_{Ar}-H), 127.8 (C_{Ar}-H), 128.7 (C_{Ar}-H), 130.57 (C_{Ar}-H), 136.16 (C20), 138.46 (C_{Ar}-C), 141.09 (C_{Ar}-C), 146.8 (C_{Ar}-C), 150.4 (C23), 164.1 (C19)

IR (ν_{max}/cm^{-1}, neat): 2972, 1715, 1526, 1282, 839

HRMS: (ESI$^+$) calcd. for $C_{39}H_{53}NO_4Na$ (M+Na$^+$): 622.3867; Found: 622.3860

Decomposition of lithiated benzoate 6

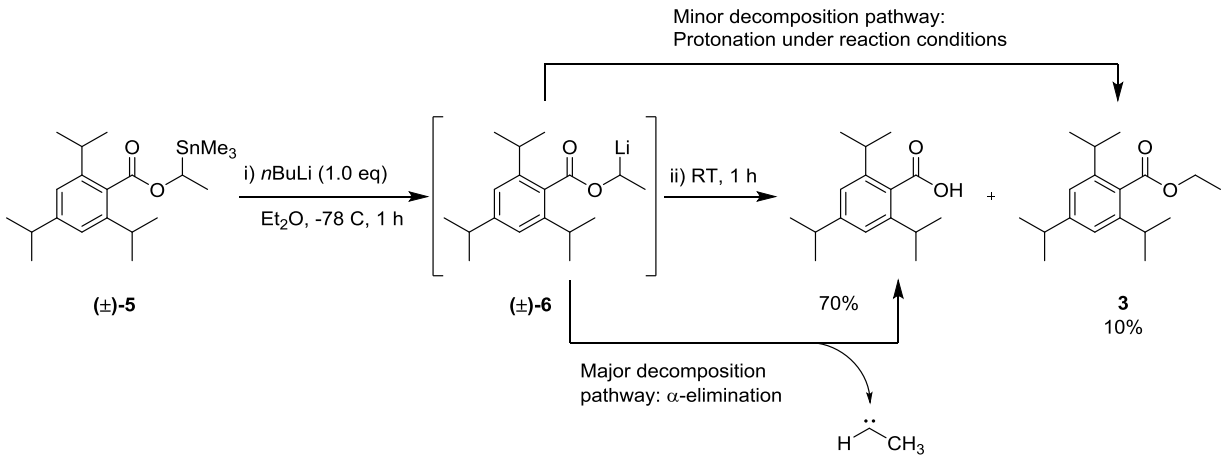

*n*BuLi (1.6 M in hexanes, 0.38 mL, 0.6 mmol, 1.0 eq) was added dropwise to a solution of **(±)-5** (263 mg, 0.6 mmol, 1.0 eq) in anhydrous Et_2O (3.0 mL) at -78 °C. The reaction mixture was stirred at -78 °C for 1 h before being warmed to room temperature. The reaction mixture was stirred at room temperature for 1 h before being diluted with H_2O (5 mL) and Et_2O (5 mL). The phases were separated and the aqueous phase extracted with Et_2O (3 × 10 mL). The combined organic phases were dried ($MgSO_4$) and concentrated under reduced pressure. The crude product was purified by flash column chromatography (95 : 5 → 50 : 50pentane : Et_2O) to give benzoate ester **3** (17 mg, 10%) as a colourless oil and 2,4,6-triisopropylbenzoic acid (104 mg, 70%) as a colourless solid.

Spectral data for benzoate ester **3** matched that previously described in this report.

Spectral data for 2,4,6-triisopropylbenzoic acid matched that of the commercially available material.

The proposed major decomposition pathway (α-elimination) was investigated. Attempts were made to trap the carbene generated with styrene and 1-methyl-1-cyclohexene, however, these experiments yielded none of the expected cyclopropanes.

Computational procedures

General computational information

Preliminary calculations were performed using the TINKER 6.0 package[11] along with the MM3 force field.[12,13,14] The SCAN routine was used to search the potential energy surface for conformers with energies up to 30 kcal.mol^{-1} above the global minimum. This program uses a method called "basin hopping search". Briefly, trial structures are generated by activation of various normal modes from the initial minimum (automatic selection of torsional angles to rotate, argument 0) and optimized to an rms gradient of 0.0001 kcal.mol^{-1}.Å^{-1}. Whenever an unknown minimum is localized, the structure is stored and the procedure is repeated. Due to the specificity of the molecules under study two keywords were added to the keyfile, namely enforce-chirality (causes the chirality to be maintained during calculations) and pisystem (sets the atoms that are part of the π-system; the MM3 force field uses this information to adjust the corresponding parameters). Conformers with very similar backbone dihedral angles were checked manually for redundancy. In each case, a small difference could be found, typically in the conformation of the alcohol (rotation around the C-O bond), which confirmed that each structure corresponds to a unique conformer.

Selected conformers were reoptimized using the GAUSSIAN 09 suite of programs.[15]Density Functional Theory (DFT) was applied by the means of the B3LYP hybrid functional[16,17] corrected for dispersion as proposed by Grimme (D2 correction).[18] The 6-311+G(d) basis set was used for all atoms. Geometry optimizations were performed without any symmetry constraints. Electronic energies were refined in two different ways: a first set of electronic energies ($E^{gas,1}$) was obtained by replacing the D2 dispersion correction by the newest D3 correction[19] (BJ damping[20]); a second set of electronic energies ($E^{gas,2}$) was obtained by doing single point energy calculations at the DF-LMP2-F12 level of theory[21] (ansatz = 3*A(loc))[22] using the specially optimized correlation consistent VDZ-F12 basis set along with its default auxiliary basis.[23] The latter calculations were performed using the Molpro 2010.1 package.[24,25] Integral direct algorithms were used as recommended for large molecules. Density-fitted local correlation methods offer dramatic reduction of computational cost which makes them applicable to much larger systems than the corresponding canonical methods. Such improvements in computational efficiency are naturally the result of approximations and these have to be considered carefully. It has been shown that the use of explicitly correlated terms (F12) greatly eliminates both basis set incompleteness errors and errors due to the domain approximation.[22] This allows one to use smaller basis sets such as double or triple zeta basis sets. Because of the size of the molecules under study (73 atoms), calculations had to be performed using the double zeta VDZ-F12 basis set. Convergence was checked by comparing the

results obtained for a model system (*n*-hexane, 20 atoms) using VDZ-F12 and VTZ-F12 basis sets (see Table S1 and discussion below). The valence orbitals were localized using the Pipek-Mezey procedure. The orbital domains were determined automatically using the procedure of Boughton and Pulay along with the default completeness criterion of 0.980. In order to improve the localization, contributions of the most diffuse basis function of each angular momentum was removed (keyword pipek,delete=1).

The stationary points were characterized by full vibration frequencies calculations at the B3LYP-D2/6-311+G* level of theory. Gibbs free energies at 298.15 K were computed based on the rigid rotor harmonic oscillator approach to statistical mechanics. Solvent effects ($CHCl_3$) were included by means of SMD single point calculations on the gas-phase optimized structures at the same level of theory.[26] Gibbs free energies in solution were estimated as: $G^{CHCl3} = G^{gas} + E^{CHCl3} - E^{gas}$. Relative populations were estimated from a Boltzmann distribution at room temperature (298.15 K). A degeneracy factor of 1 was used all along.

Experimental data

Experimental studies were carried out using a variety of end-groups. For simplicity, all calculations were performed using a phenyl group at one end, and a hydroxyl group at the other end. This led to the model compounds **14a**, **18a** and **22a** respectively analogues of **14**, **18** and **22** (Figure S1). In addition to these three compounds, our methodology was tested against *n*-hexane. Results for *n*-hexane are included and compared to the literature.[27]

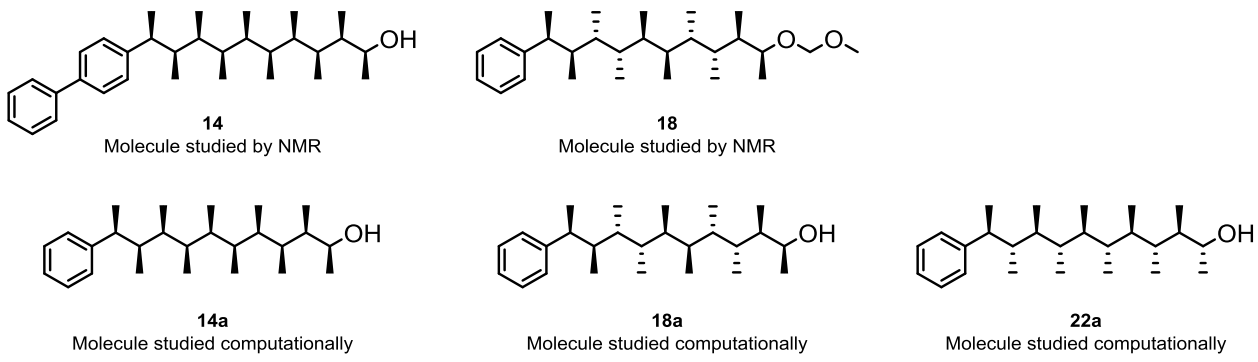

Figure S1: Compounds studied computationally and by NMR.

Calculated data for *n*-Hexane

The MM3 scan of the potential energy surface for *n*-hexane generated 12 unique conformers (Figure S2). Both the structures and the relative MM3 energies (Table S1) were found in excellent agreement with MM2 results reported previously.[27] Relative electronic energies calculated at different levels of theory are presented in Table S1. B3LYP gives the same energetic order as MM3 as well as similar relative energies ($\Delta\Delta E^{max}$ = 0.4 kcal.mol^{-1}). Inclusion of dispersion through the D2 correction strongly favors folded rotamers compared to the linear or partially linear ones ($\Delta\Delta E^{max}$ > 2.0 kcal.mol^{-1} for ***conformers 3***, ***9***, ***10*** and ***12***). This effect is significantly reduced when the D3 correction is used instead ($\Delta\Delta E^{max}$ ≈ 1 kcal.mol^{-1} for the same conformers), in agreement with the previously noted tendancy of the D2 correction to slightly overestimate dispersion interactions.[19] LMP2-F12 energies are found almost identical to the B3LYP-D3 ones ($\Delta\Delta E^{max}$ = 0.3 kcal.mol^{-1}). Comparison between VDZ-F12 and VTZ-F12 results suggests that convergence toward the basis set limit is reached already with the double-zeta basis set. Interestingly, addition of thermal, entropic and solvent corrections yields an overall distribution which is very similar to the distribution predicted by the MM3 energies (Table S2). This suggests that these effects are partially accounted for by the force field.

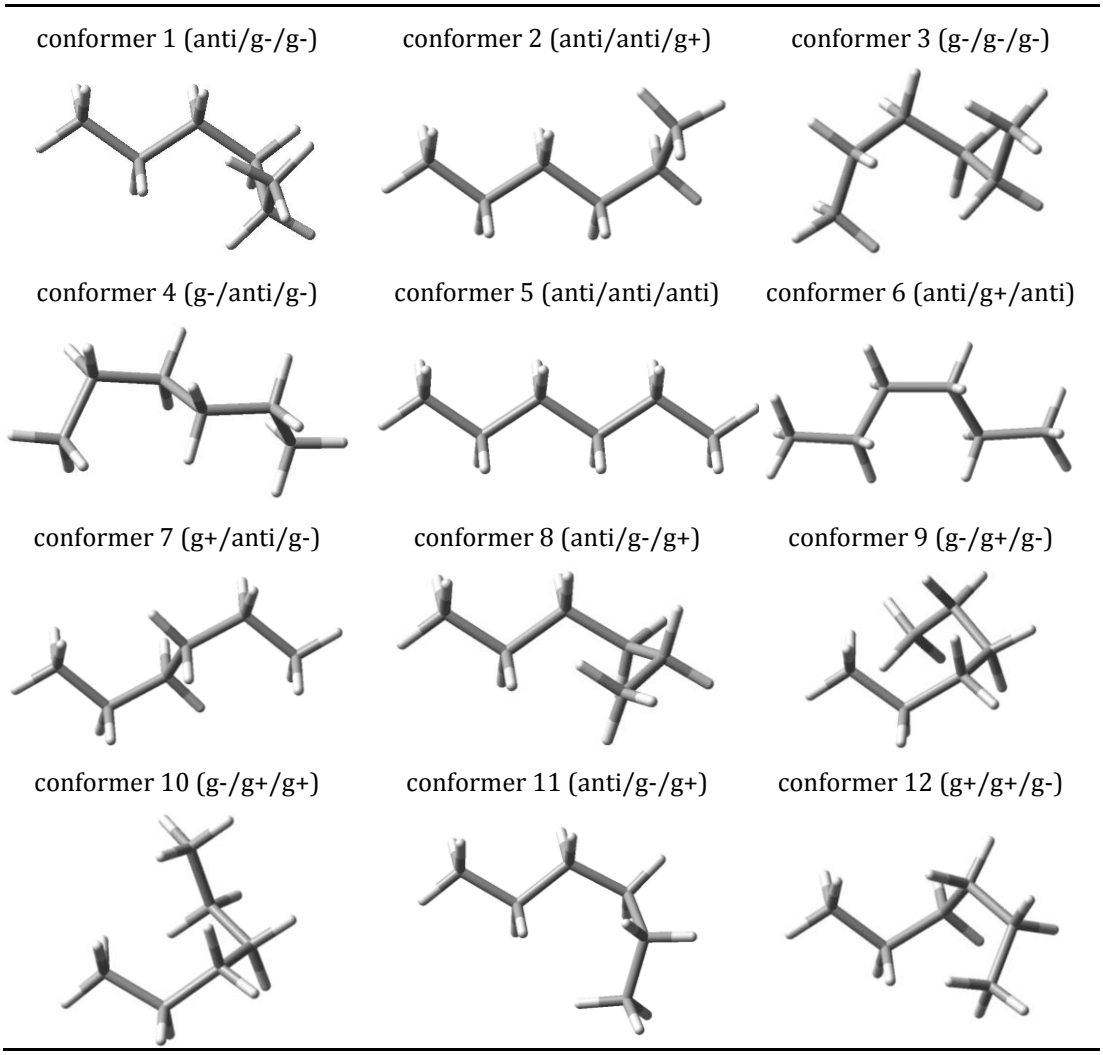

Figure S2: Conformers of *n*-hexane.

geometry optimization	MM3	B3LYP-D2/6-311+G*				
electronic energies	MM3	B3LYP/ 6-311+G*	B3LYP-D2/ 6-311+G*	B3LYP-D3/ 6-311+G*	LMP2-F12/ VDZ-F12	LMP2-F12/ VTZ-F12
conformer 1	1.6	2.0	0.2	0.9	0.7	0.8
conformer 2	0.8	1.0	0.3	0.6	0.5	0.6
conformer 3	2.4	3.1	0.2	1.3	0.9	1.0
conformer 4	1.6	1.9	0.6	1.1	1.0	1.1
conformer 5	0.0	0.0	0.0	0.0	0.0	0.0
conformer 6	0.9	1.0	0.3	0.6	0.5	0.6
conformer 7	1.8	1.9	0.7	1.2	1.2	1.2
conformer 8	3.3	3.6	1.9	2.6	2.6	2.7
conformer 9	6.0	6.7	3.5	4.8	4.8	5.0
conformer 10	4.2	4.8	1.8	3.0	2.9	3.0
conformer 11	3.4	3.6	2.0	2.6	2.7	2.8
conformer 12	4.3	4.6	2.3	3.2	3.2	3.3

Table S1: Calculated relative energies (kcal.mol^{-1}) for the conformers of *n*-hexane.

	population (%) $/E^{gas,MM3}$	population (%) $/E^{gas,1}$	population (%) $/G^{CHCl3,1}$	population (%) $/E^{gas,2}$	population (%) $/G^{CHCl3,2}$
conformer 1	3.8	9.3	3.7	11.1	4.7
conformer 2	14.5	15.6	17.5	15.4	18.2
conformer 3	1.1	4.7	0.8	8.1	1.5
conformer 4	3.7	6.5	4.3	6.6	4.6
conformer 5	60.2	40.5	56.8	37.2	54.3
conformer 6	13.1	16.1	12.9	15.1	12.7
conformer 7	3.1	5.6	3.7	5.2	3.6
conformer 8	0.2	0.6	0.2	0.5	0.2
conformer 9	0.0	0.0	0.0	0.0	0.0
conformer 10	0.1	0.3	0.0	0.3	0.0
conformer 11	0.2	0.5	0.1	0.4	0.1
conformer 12	0.0	0.2	0.0	0.2	0.0

Table S2: Calculated Boltzmann populations for the conformers of *n*-hexane. [1] and [2] refer respectively to B3LYP-D3/6-311+G* and LMP2-F12/VDZ-F12 calculations.

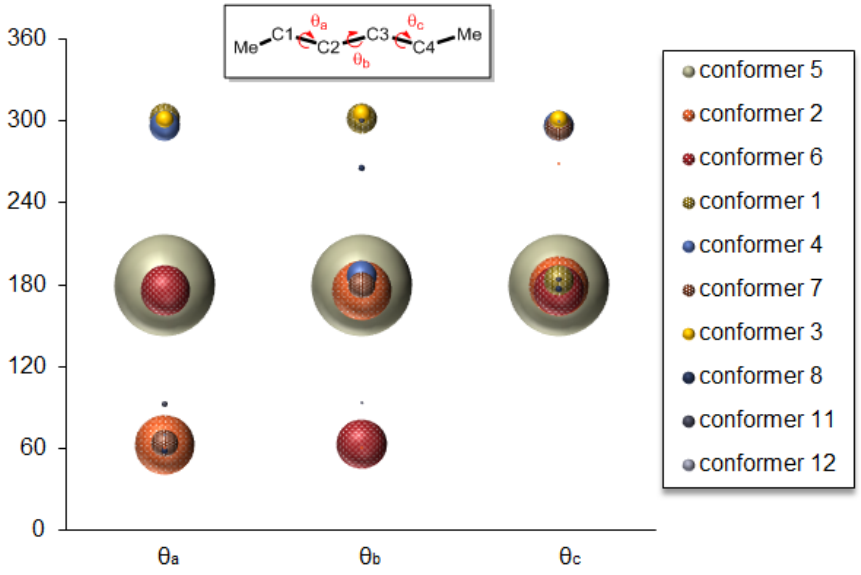

Figure S3: Solution rotamer distribution of *n*-hexane as predicted at the LMP2-F12/VDZ-F12 level of theory (last column in Table S2). Each populated rotamer is shown as 3 dots, of size proportional to the calculated relative abundance of that rotamer, and with a position defined by the calculated value of the corresponding backbone dihedral angle.

Calculated data for 14a

The initial scan of the potential energy surface using MM3 generated 9710 conformers. Only 18 of these conformers are associated with a Boltzmann population greater than 1%. The major conformer (***conformer 1***, 65%) corresponds to a tight C6-helix similar to the X-Ray structure but shifted along the chain, with a backbone arrangement displaying a regular alternating gauche/anti pattern (45°/180°). Conformers with a predicted population greater than 0.05% were then reoptimized at the B3LYP-D2 level of theory (66 conformers; Figure S5a). This spans conformers with MM3 energies up to 4.2 kcal.mol^{-1} above the global minimum. Although this threshold is somewhat arbitrary, we estimated that the major conformers in solution should be in this pool of conformers as it greatly exceeds the average error MM3 typically makes on conformational energies (< 0.5 kcal.mol^{-1} for various hydrocarbon derivatives).[28] The reoptimized geometries were found to be very similar to the MM3 ones, with an average change in the backbone dihedral angles of 4.3°. No significant conformational change was observed during this process. The distribution of populations however was found to be deeply altered by going from MM to DFT or LMP2-F12 calculations (Table S3 and Figure S5c and S5d). The tight helix conformation is strongly disfavoured compared to various other conformations, including a looser C9-helix presenting the same alternating gauche/anti pattern but with wider dihedral angles (75°/210°). Inclusion of thermal, entropic and solvent corrections made the preference for the looser helix even stronger. The major conformer predicted by this initial search is ***conformer 10*** (Table S3 and Figure S4). Despite a very good agreement between predicted and measured NOEs along the backbone, large errors were found for H-H distances at the OH end. This led us to look for new conformations manually. Starting from ***conformer 10***, rotation of the alcohol group generated two new conformers, one of which could not be found in the structures initially generated by the MM3 scan of the PES. This new conformer, ***conformer 39*** (Table S3 and Figure S4), was optimized and found to lie very low in energy. Interestingly, optimization of this conformer with MM3 yielded the tight C6-helix described previously (***conformer 1***). This may be due to the fact that for this molecule, the structure of each conformation, and the nature of the preferred conformation, appears to result from a delicate balance. On the one hand, 1,4 interactions favour traditional gauche or *anti* arrangements with C-C-C-C dihedral angles of +/- 60 degrees or 180 degrees. On the other hand, *syn*-pentane interactions, where present, favour distortion away from these ideal dihedral angles. This leads to a significant number of optimized structures in which dihedral angles are observed to differ significantly from the ideal values of +/- 60 degrees. It appears that MM3 does not always provide a balanced description of this region of the potential energy surface, leading to incorrect structures for some conformers. This seems to be particularly true for functional groups, suggesting that some special care has to be taken when considering the conformation of the end groups. A manual check of the major

conformers by rotation of the end groups did not yield any new conformation. The overall predicted population for the loose C9-helix (***conformers 10***, ***27***, ***28***, ***32***, and ***39***, Figure S5b) ranges between 80% and 74% respectively at the B3LYP-D3 and LMP2-F12 level of theory. The new distribution fits almost perfectly with the NMR data. Although we do not claim that our procedure is exhaustive space, the very good agreement between predicted and measured coupling constants and NOEs gives confidence that we have located the major conformers.

	population (%) $/E^{gas,MM3}$	population (%) $/E^{gas,1}$	population (%) $/G^{CHCl3,1}$	population (%) $/E^{gas,2}$	population (%) $/G^{CHCl3,2}$
conformer 1	66.5	2.3	1.7	7.6	4.4
conformer 2	3.7	4.0	0.4	5.2	0.4
conformer 3	3.4	3.4	0.3	5.4	0.4
conformer 4	3.3	0.2	0.1	0.3	0.1
conformer 5	2.7	4.5	0.1	5.1	0.1
conformer 6	2.7	3.3	0.1	4.9	0.2
conformer 7	2.0	0.3	0.5	0.5	0.8
conformer 8	1.5	2.8	0.6	4.0	0.7
conformer 9	1.4	2.1	0.1	3.6	0.1
conformer 10	1.0	4.6	18.5	4.1	13.5
conformer 11	0.6	1.3	0.7	2.0	0.9
conformer 12	0.6	0.6	0.0	0.6	0.0
conformer 13	0.6	0.9	1.0	1.7	1.4
conformer 14	0.6	0.4	0.0	0.5	0.0
conformer 15	0.6	0.3	1.2	0.3	1.1
conformer 16	0.5	0.0	0.0	0.0	0.0
conformer 17	0.4	0.1	0.5	0.4	2.4
conformer 18	0.4	0.1	0.4	0.2	1.0
conformer 19	0.3	1.7	1.8	2.5	2.2
conformer 20	0.3	7.5	0.0	4.4	0.0
conformer 21	0.3	1.8	2.1	1.6	1.6
conformer 22	0.3	1.7	0.0	0.4	0.0
conformer 23	0.3	0.5	0.0	0.6	0.0
conformer 24	0.3	0.1	0.5	0.1	0.9
conformer 25	0.2	1.3	0.1	1.8	0.1
conformer 26	0.2	0.4	0.4	0.2	0.2
conformer 27	0.2	1.8	4.5	1.7	3.5
conformer 28	0.2	1.4	2.4	1.7	2.5
conformer 29	0.2	0.1	0.3	0.1	0.5
conformer 30	0.1	2.1	0.1	1.9	0.1
conformer 31	0.1	1.0	0.1	1.6	0.1
conformer 32	0.1	2.0	8.6	2.3	7.8
conformer 33	0.1	2.0	0.8	1.0	0.3
conformer 34	0.1	1.6	0.8	1.1	0.5
conformer 35	0.1	0.6	0.1	0.6	0.1
conformer 36	0.1	0.5	0.1	0.8	0.2
conformer 37	0.1	0.2	4.1	0.2	3.5
conformer 38	0.1	1.3	0.1	1.4	0.1
conformer 39	not a minima	20.8	45.7	26.0	46.6

Table S3:. Calculated Boltzmann populations for the major conformers of **14a**. [1] and [2] refer respectively to B3LYP-D3/6-311+G* and LMP2-F12/VDZ-F12 calculations.

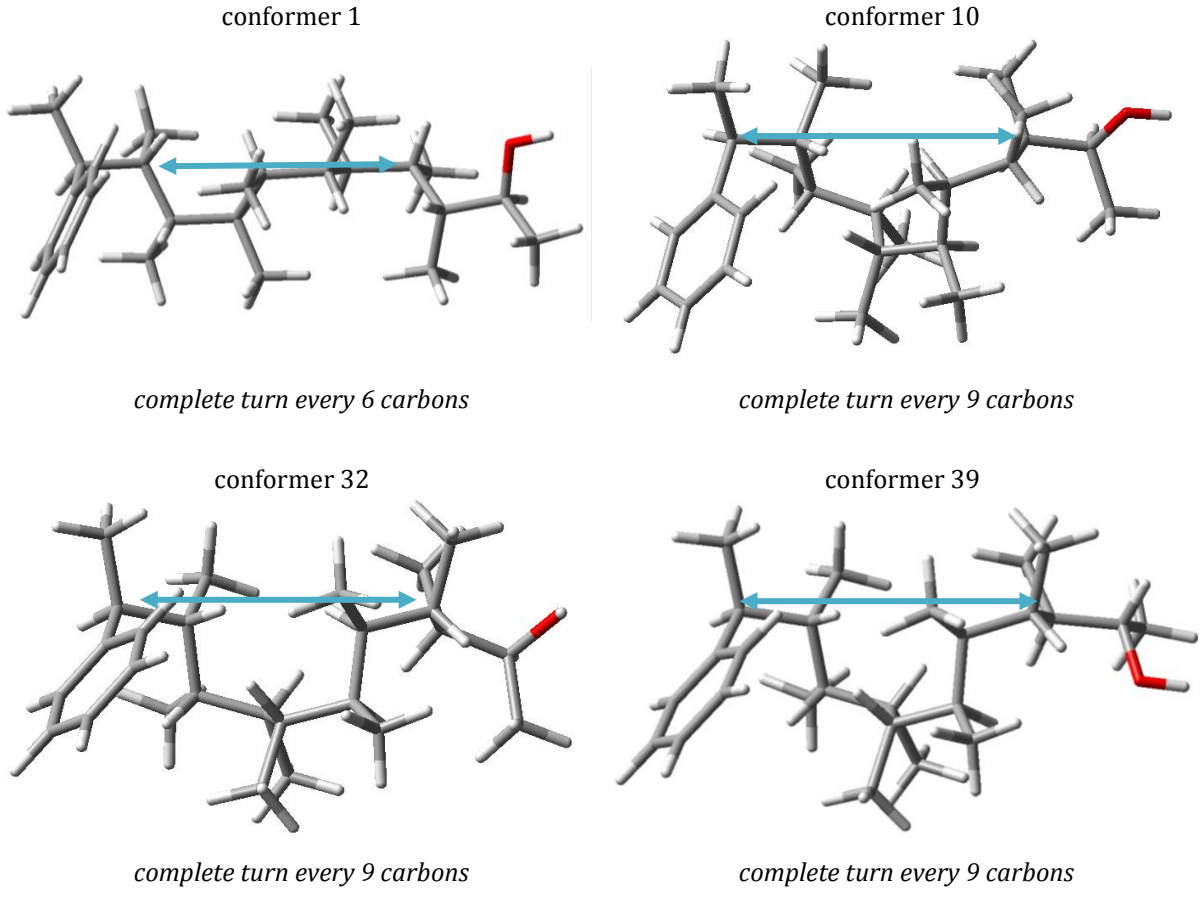

Figure S4:. Selected conformers of **14a**.

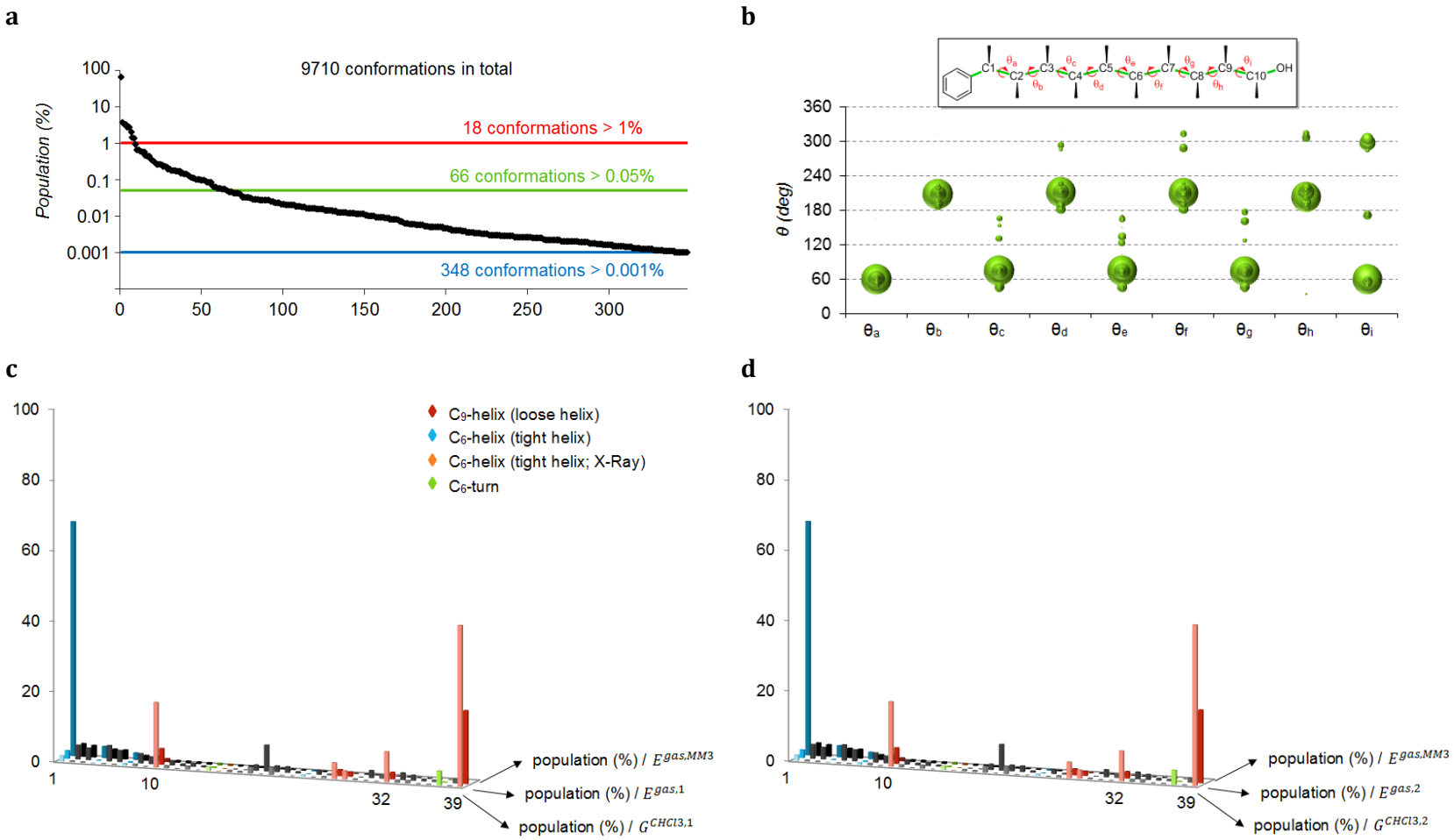

Figure S5: Results for compound 14a. **a** MM3 predicted Boltzmann populations for the major conformers. **b** Solution conformer distribution of **14a** as predicted at the LMP2-F12 level of theory. Each populated rotamer is shown as 9 dots, of size proportional to the calculated relative abundance of that rotamer, and with a position defined by the calculated value of the corresponding backbone dihedral angle. **c** and **d** Solution conformer distribution of **14a** as predicted at the B3LYP-D3 and LMP2-F12 levels of theory respectively. Distributions derived from gas phase energies are given for comparison.

Calculated data for 18a

The initial scan of the potential energy surface using MM3 generated 3970 conformers. The vast majority of these conformers were predicted to be unpopulated at room temperature, with only 17 conformers having a Boltzmann population greater than 1%. The most populated conformers display a linear or partially linear arrangement, in agreement both with NMR data and X-Ray analysis (around 80% of the total population show a linear arrangement between C2 and C9, *i.e.* $\theta_b \approx \theta_c \approx \theta_d \approx \theta_e \approx \theta_f \approx \theta_g \approx \theta_h \approx 180°$). Following the same strategy as adopted for **18a**, conformers with an MM3 predicted population greater than 0.05% were then reoptimized at the B3LYP-D2 level of theory (50 conformers; Figure S7a). This led to a radically different picture, with folded conformers presenting a CH-π or OH-π interaction (displayed in Figure S6) becoming more populated than the linear ones (Table S4, Figure S7c and S7d). As observed in the *n*-hexane case, inclusion of thermal, entropic and solvent corrections restored the preference for the linear arrangement. The overall predicted population for the linear conformation (***conformers 1***, ***2***, ***3***, ***4***, ***7***, ***8***, ***9***, ***10***, ***12***, ***13***, ***14***, ***17***, ***23*** and ***29***, Figure S7b) ranges between 92% and 95% respectively at the B3LYP-D3 and LMP2-F12 level of theory. The final distribution is in excellent agreement with NOE data.

	population (%) $/E^{gas,MM3}$	population (%) $/E^{gas,1}$	population (%) $/G^{CHCl3,1}$	population (%) $/E^{gas,2}$	population (%) $/G^{CHCl3,2}$
conformer 1	18.4	0.1	82.5	0.8	85.6
conformer 2	17.6	0.1	3.9	0.7	3.3
conformer 3	17.4	0.4	1.2	1.9	1.0
conformer 4	16.1	0.2	1.4	1.4	1.8
conformer 5	3.2	0.2	0.1	0.8	0.0
conformer 6	3.0	0.2	0.1	0.8	0.1
conformer 7	1.9	0.0	0.0	0.0	0.0
conformer 8	1.8	0.1	0.9	0.3	0.7
conformer 9	1.7	0.0	0.0	0.0	0.0
conformer 10	1.7	0.1	0.2	0.6	0.1
conformer 11	1.6	1.7	4.7	7.8	3.5
conformer 12	1.6	0.2	1.8	0.7	1.4
conformer 13	1.5	0.0	0.2	0.1	0.3
conformer 14	1.5	0.0	0.0	0.0	0.0
conformer 15	1.5	18.2	0.3	35.1	0.1
conformer 16	1.5	1.3	1.4	6.5	1.2
conformer 17	1.4	0.0	0.0	0.1	0.1
conformer 18	0.0	4.0	0.0	0.8	0.0
conformer 19	0.7	54.6	0.2	12.6	0.0
conformer 20	0.1	1.1	0.0	0.8	0.0
conformer 21	0.3	2.9	0.0	3.7	0.0
conformer 22	0.1	2.0	0.0	3.6	0.0
conformer 23	0.6	0.0	0.0	0.1	0.0
conformer 24	0.3	5.2	0.1	4.3	0.0
conformer 25	0.2	1.7	0.0	4.4	0.0
conformer 26	0.2	0.3	0.1	0.5	0.0
conformer 27	0.1	4.2	0.1	8.3	0.0
conformer 28	0.1	0.2	0.0	0.6	0.0
conformer 29	0.5	0.0	0.1	0.1	0.1
conformer 30	0.2	0.2	0.0	0.4	0.0

Table S4:. Calculated Boltzmann populations for the major conformers of **18a**. [1] and [2] refer respectively to B3LYP-D3/6-311+G* and LMP2-F12/VDZ-F12 calculations.

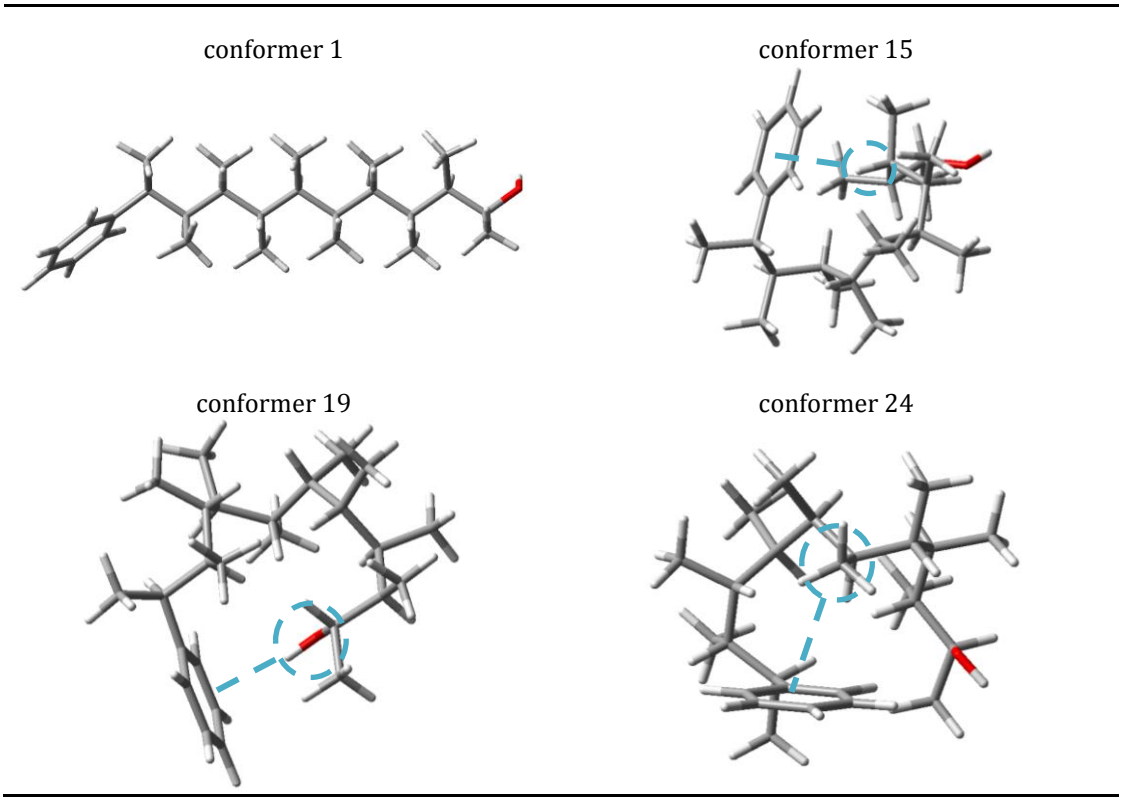

Figure S6: Selected conformers of **18a**. In blue: CH or OH-π interactions.

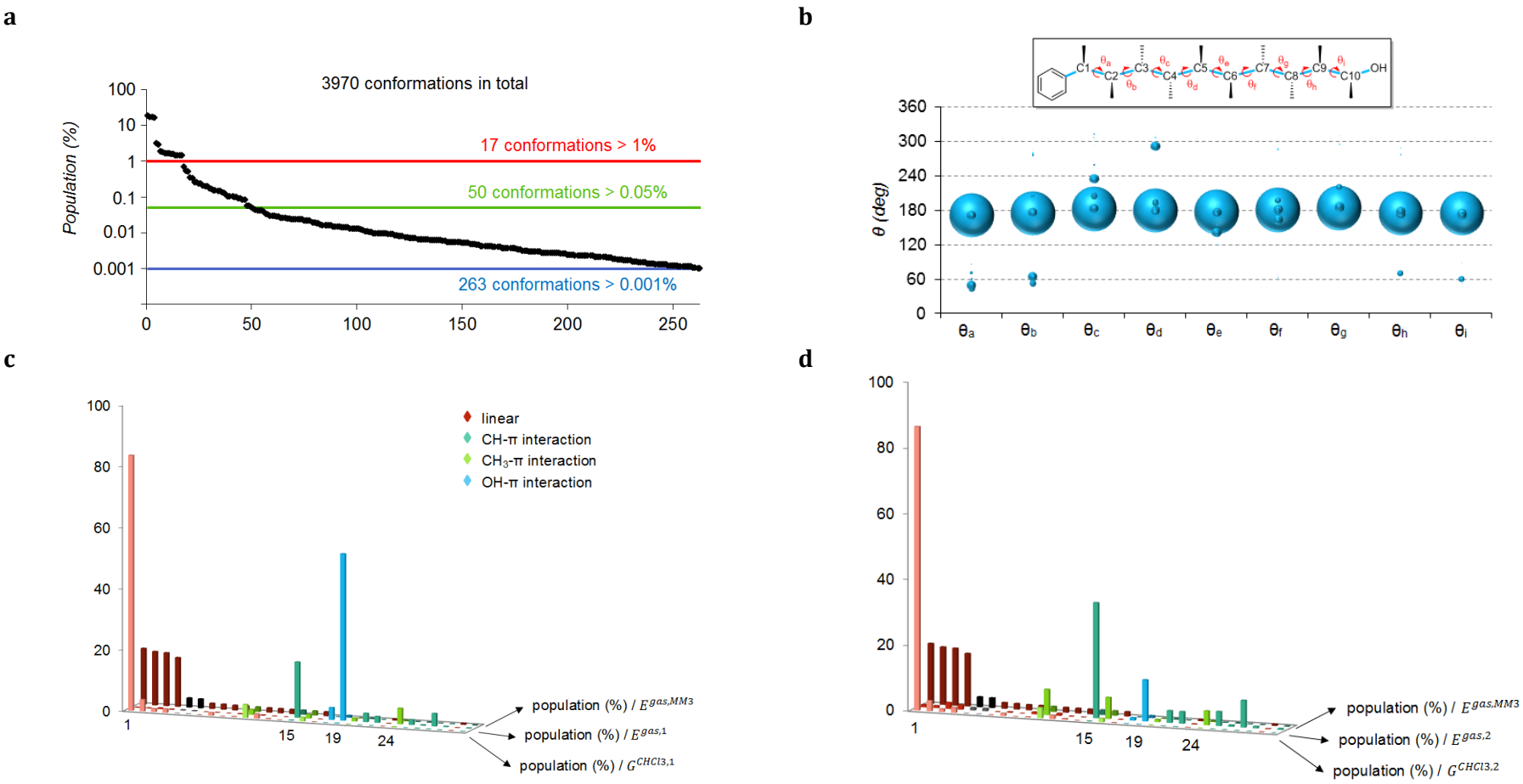

Figure S7: Results for compound 18a. **a** MM3 predicted Boltzmann populations for the major conformers. **b** Solution conformer distribution of **18a** as predicted at the LMP2-F12 level of theory. Each populated rotamer is shown as 9 dots, of size proportional to the calculated relative abundance of that rotamer, and with a position defined by the calculated value of the corresponding backbone dihedral angle. **c** and **d** Solution conformer distribution of **18a** as predicted at the B3LYP-D3 and LMP2-F12 levels of theory respectively. Distributions derived from gas phase energies are given for comparison. Conformations shown in red are predominantly linear (*i.e.* at least 7 *anti* dihedral angles).

Calculated data for 22a

The initial scan of the potential energy surface using MM3 generated 2173 conformers, with 19 of these conformers associated with a Boltzmann population greater than 1%. The distribution of dihedral angles is visibly more scattered than those of the two previous compounds (Figure S8), in agreement with the experimental observation that the molecule does not adopt a particular conformation in solution nor in the solid state. Even though MM3 results have to be interpreted cautiously, we know from the study of compounds **14a** and **18a** that the overall picture it gives is quite reliable. In the absence of detailed NMR results for this compound, no further computational work was undertaken.

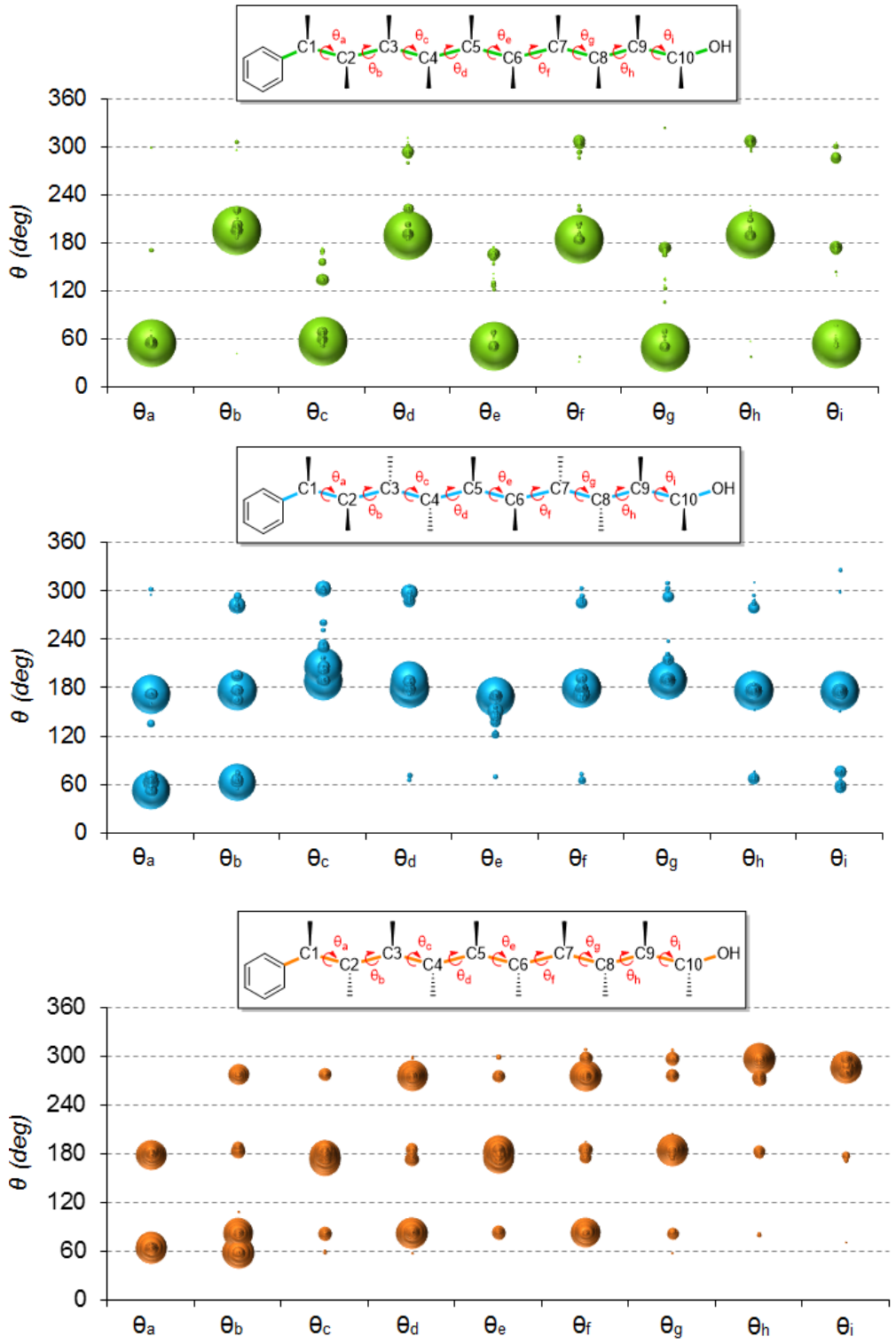

Figure S8: MM3 results for compounds 14a, 18a and 22a. Each populated rotamer is shown as 9 dots, of size proportional to the calculated relative abundance of that rotamer, and with a position defined by the calculated value of the corresponding backbone dihedral angle.

NMR procedures

General NMR information

NMR experiments were performed on a 500 MHz Varian VNMRS Direct Drive NMR spectrometer equipped with an Agilent OneNMR probe. Spectra collected were analysed and processed using MestreNova version 8.1.2-11880. All NMR experiments were run at 25°C. NMR experiments used for assignment of compound **14** and **18** were ^{1}H NMR (8 scans, spectral width 20ppm (10,000 Hz)), ^{13}C NMR (125 MHz, 2000 scans, spectral width 275 ppm (34,345 Hz)), HSQC (4 scans, 200 t1 increments , spectral widths F2 20 ppm (10,000 Hz), F1 200 ppm (25,000 Hz)), H2BC (4 scans, 200 t1 increments, spectral widths F2 20 ppm (10,000 Hz), F1 200 ppm (25,000 Hz)), HMBC (8 scans, 200 t1 increments , spectral widths F2 20 ppm (10,000 Hz), F1 200 ppm (25,000 Hz)), DQF-COS (8 scans, 200 t1 increments, spectral width F2 10 ppm (10,000 Hz), F1 10ppm (10,000 Hz)).

Determination of *J*-couplings

Measurement of ^{1}H-^{1}H scalar couplings were taken directly from multiplets in ^{1}H NMR spectrum. For more precise determination of couplings ≤ 3Hz, simulations of the ^{1}H NMR multiplet shapes were created via the MestreNova Spin Simulation module from values of ^{1}H chemical shifts, estimated *J*-couplings and line widths of peaks. Modification of the *J*-coupling constants allowed fitting of simulated with experimental spectra. Where ^{1}H-^{1}H coupling constants could be measured twice (once from each ^{1}H multiplet) the experimental value reported is the average of the two measured values.

Measurement of ^{1}H-^{13}C scalar couplings were obtained from EXSIDE[29] spectra (2 scans, 1675 t1 increments, spectral width F2 -20 ppm (10,000 Hz), F1 200ppm (25,000 Hz)) for each resolved ^{1}H resonance. ^{1}H-^{13}C scalar couplings are measured directly from F1-doublets in the spectra as illustrated for H1-C1' shown below in Figure S9, a *J*-scaling factor of 15 was used in the EXSIDE experiment to increase the doublet splitting in F1 and thus allow more accurate assessment of *J*.

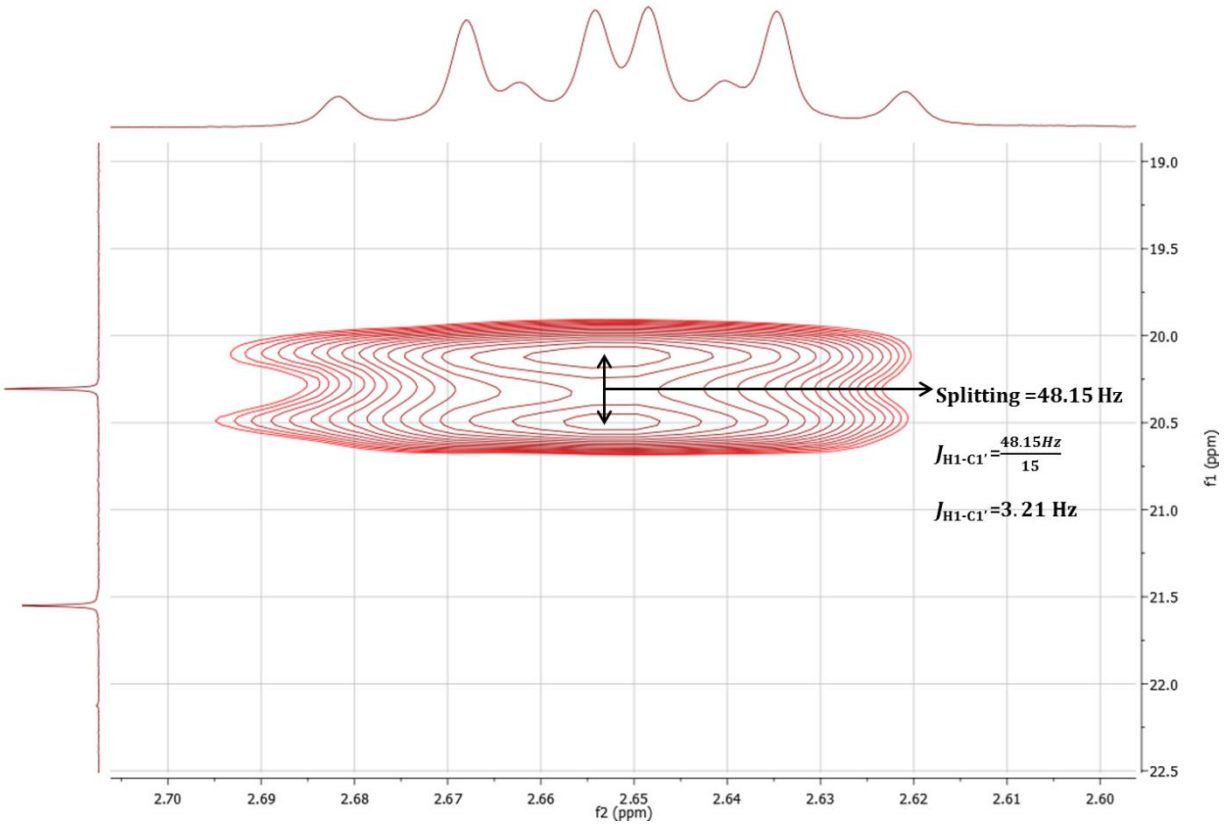

Figure S9: EXSIDE spectrum measurement between H1 and C1' in compound **14**.

Determination of interatomic distances

To determine interatomic distances between protons in the molecule, DPFGSE 1D NOE spectra[30] were collected (128 scans, mixing time 500 ms, spectral width 20 ppm (10,000 Hz)) and using Equation 1.[31]

$$r_{NOE} = r_{ref}[\frac{\eta_{NOE}}{\eta_{ref}}]^{-\frac{1}{6}}$$

Equation 1: *r* is interproton atomic distance and η is NOE signal intensity.

We have previously reported[32,33,34] that by assuming a single reference distance between two protons in the same molecule, r_{ref} , and measuring its associated NOE intensity, η_{ref} , one can determine unknown distances between a second proton pair, r_{NOE} , via measurement of the corresponding pairs' NOE intensity, η_{NOE}. In order to compare NOE intensities across all 1D NOESY spectra and correct for differing rates of external relaxation for each nucleus, the PANIC method[35] was employed whereby the intensity (integral) of the irradiated peak in each NOE

spectrum was set to a single value (arbitrarily 1000 intensity units in this analysis), as seen in Figure S10. For each compound, the reference distance (r_{ref}) was between a CH and its adjacent CH_3 group (Compound **18** H1-H1' 2.69 Å, Compound **14** H10-H10' 2.80 Å), as these are insensitive to molecular conformation *NB* the difference between these two calibration distances arises from post-analysis scaling of the distance data to optimise the fit between experiment and calculation by varying the calibration distances.

1D NOE spectra were obtained for all resolved resonances in the ^1H NMR spectrum of each compound. Figure S10 shows the result from irradiation of H10 of **14/14a**, giving rise to NOE signals for protons within ~4 Å of H10. Taking H10-H10' as the reference distance (2.80 Å) , the corresponding H10-H10' NOE intensity (25.38), and the NOE intensity for H10-H8 (7.84), one can apply Equation 1 to determine the H10-H8 distance (*NB:* The H10-H10' NOE reference intensity must first be divided by 3 (25.38 = 8.46) to correct for the three equivalent protons in the CH_3 group which gives rise to this signal – this process is used for all NOEs to CH_3 groups in this analysis):

$$R_{H10\text{-}H8} = 2.80\ Å*(7.84/8.46)^{-(1/6)} = 2.84\ Å$$

This H10-H8 distance for **14/14a** was subsequently averaged against the H8-H10 distance (2.76 Å) determined from the independent 1D-NOE spectrum for H8, to give the final experimental value of 2.80 Å (Table S7).

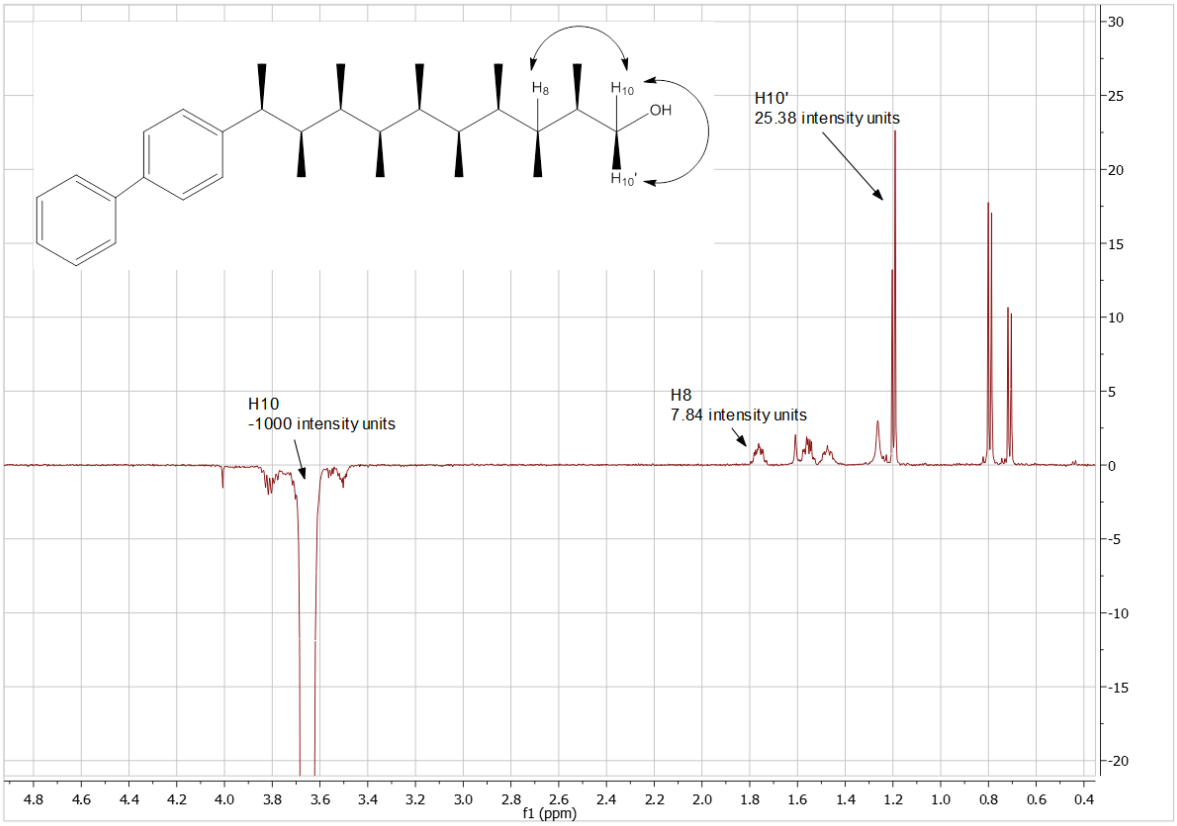

Figure S10: 1D NOE spectrum of H10 for **14**, with annotated intensities for NOE signals of H10-H10' and H10-H8.

Computational comparison to experimental NMR results and measurements

The NMR data determined (NOE-distances and *J*- values) were compared to computed values derived from the most populated conformers determined for compounds **14/14a** and compound **18/18a** [See above] (8 conformers for **18/18a** which account for 98.9% of the total conformer population, and 9 conformers of compound **14/14a** which account for 84.8% of the total conformer population. Bifulco *et al.*[36] have previously identified that an optimal methodology for *J*-coupling calculations (both ^{1}H-^{1}H and ^{1}H-^{13}C) as using the DFT hybrid functional mpw1pw91 and 6311-G (d,p) basis set. Consequently each conformer geometry was re-optimised using this method through the Gaussian 3.09 suite of programs as above. *J*- values and interproton distances were extracted directly from the computational output matrices. The conformational ensemble interproton distances and ^{1}H-^{1}H and ^{1}H-^{13}C *J*-couplings were then determined by population-averaging the contribution from each conformer (with r^{-6} weighting prior to averaging, then r^{-6} recalculation of distances in the former case to reflect the averaging of NOEs rather than distances, and linear weighting in the latter case).

NMR data

NMR measured *vs* calculated data for 14/14a

Note: Where ^{1}H-^{1}H coupling constants or interproton distances could be measured twice (from each ^{1}H multiplet/irradiation) the experimental value reported is the average of the two measured values.

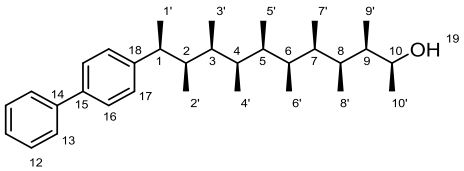

H_A	H_X	Exp *J* (Hz)	Cal *J* (Hz)	Error (Hz)
1	2	9.35	8.83	0.52
9	10	7.32	5.57	1.74
9	9'	6.93	6.25	0.67
3	3'	6.56	6.34	0.22
8	8'	6.39	6.25	0.14
2	2'	6.41	6.11	0.30
1'	1	6.68	5.99	0.69
10'	10	5.74	5.30	0.44
2	3	2.50	2.41	0.09
3	4	8.77	8.34	0.43
9	8	3.07	1.62	1.45
8	7	9.89	8.16	1.73
16	17	7.39	6.69	0.69

Table S5: ^{1}H-^{1}H *J*-Couplings (Hz) for **14/14a**

H_A	C_X	Exp *J* (Hz)	Cal *J* (Hz)	Error (Hz)
10	9'	1.45	2.22	-0.77
10	10'	0.95	0.09	0.86
10	8	2.61	2.53	0.08
10	9	2.18	2.36	-0.18
1	2'	2.00	1.76	0.24
1	1'	3.21	3.53	-0.32
1	3	2.01	1.85	0.16
1	2	3.62	4.03	-0.41
1	18	5.28	5.12	0.16
8	9'	5.15	4.45	0.70
8	8'	2.99	3.64	-0.65
8	6	2.66	3.58	-0.92
8	7'	1.75	1.09	0.66
8	7	4.11	4.53	-0.42
8	9	4.43	4.03	0.40
8	10	2.59	3.41	-0.82
3	3'	4.57	3.92	0.65
3	5	4.18	3.78	0.40
2	1'	2.55	2.17	0.38
2	3'	4.93	4.64	0.29
2	2'	3.01	3.81	-0.80
2	4	2.84	3.84	-1.00
2	3	2.79	3.75	-0.96
2	1	4.11	3.95	0.16
2	18	2.81	2.47	0.34
9	9'	3.70	4.17	-0.47
9	8'	4.75	4.74	0.01
9	7	3.18	3.63	-0.45
9	10'	3.44	2.86	0.58
9	8	3.12	3.57	-0.45
9	10	6.26	5.61	0.66

Table S6: ^{1}H-^{13}C *J*-Couplings (Hz) for **14/14a**

H Irradiated	H Observed	Exp distance (Å)	Cal distance (Å)	Error (Å)	% Error
1	2	2.83	3.03	-0.20	7%
1	1'	2.57	2.60	-0.03	1%
1	2'	2.80	3.00	-0.20	7%
1	3	2.69	2.80	-0.11	4%
2	1'	2.80	2.96	-0.16	5%
2	2'	2.63	2.58	0.05	2%
2	3	2.32	2.58	-0.26	10%
2	5'	3.24	3.67	-0.43	12%
8	9	2.57	2.59	-0.02	1%
8	10	2.80	2.86	-0.06	2%
8	10'	3.61	3.00	0.61	19%
9	10	2.70	2.68	0.02	1%
9	10'	2.86	2.93	-0.07	2%
10	9'	3.01	2.93	0.08	3%
10	10'	2.80	2.60	0.20	7%
1'	2'	2.98	2.90	0.08	3%
4'	3	2.90	3.18	-0.28	9%
4'	5'	3.29	2.91	0.37	12%
9'	10'	3.14	3.11	0.03	1%

Table S7: Interproton Distances (Å) for **14/14a**

NMR measured *vs* calculated data for 18/18a

Note: Where ^{1}H-^{1}H coupling constants or interproton distances could be measured twice (from each ^{1}H multiplet/irradiation) the experimental value reported is the average of the two measured values.

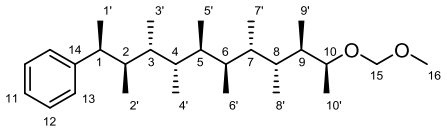

H_A	H_X	Exp *J* (Hz)	Cal *J* (Hz)	Error (Hz)
1	2	3.43	4.00	-0.57
1	1'	7.06	6.24	0.82
2	2'	6.32	5.94	0.38
8	9	9.15	8.12	1.03
9	10	3.53	3.67	-0.14
9	9'	6.65	5.85	0.80
10	10'	6.43	5.58	0.85

Table S8: ^{1}H-^{1}H *J*-Couplings (Hz) for **18/18a**

H_A	C_X	Exp *J* (Hz)	Cal *J* (Hz)	Error (Hz)
1	14	6.62	6.68	-0.07
1	13	3.53	3.74	-0.21
1	2	4.12	4.63	-0.50
1	3	1.44	1.38	0.06
9	10	6.69	5.93	0.76
9	10'	4.87	4.43	0.44
10	9	1.32	0.37	0.95
10	10'	1.69	1.71	-0.02
10	9'	4.88	4.10	0.78

Table S9: ^{1}H-^{13}C *J*-Couplings (Hz) for **18/18a**

H irradiated	H observed	Exp distance (Å)	Cal distance (Å)	Error (Å)	% Error
1	2	2.23	2.45	-0.22	2%
1	1'	2.69	2.58	0.11	1%
1	3'	2.32	2.42	-0.11	1%
8	10	2.69	3.09	-0.40	4%
8	10'	2.53	2.64	-0.11	1%
8	9'	2.85	2.92	-0.07	1%
8	8'	2.69	2.61	0.09	1%
8	6'	2.35	2.39	-0.04	0%
9	10	2.36	2.42	-0.06	1%
9	9'	2.60	2.60	0.00	0%
9	8'	2.81	2.90	-0.09	1%
10	10'	2.70	2.59	0.11	1%
10	8'	2.38	2.44	-0.06	1%
1'	3	2.37	2.58	-0.21	2%
1'	2'	3.13	3.10	0.02	0%
10'	9'	3.25	3.11	0.14	1%
3'	3	2.50	2.61	-0.11	1%
3'	4'	3.03	3.13	-0.11	1%
1	2'	3.95	3.74	0.21	1%
9	7'	2.52	2.47	0.04	0%
9	10'	3.97	3.89	0.08	1%
10'	8'	3.75	3.72	0.03	0%
10'	6'	4.65	4.71	-0.06	0%
1'	3'	3.74	3.69	0.05	0%
1'	5'	4.19	4.65	-0.46	3%
3'	5	2.41	2.53	-0.12	1%
9'	7'	3.53	3.59	-0.06	0%
9'	7	2.25	2.45	-0.20	2%

Table S10: Interproton Distances (Å) for **18/18a**

References

[1] Pangborn, A. B., Giardello, M. A., Grubbs, R. H., Rosen, R. K. & Timmers, F. J. Safe and convenient procedure for solvent purification. *Organometallics* **15**, 1518-1520 (1996)

[2] Shriver, D. F. & Drezdzon, M. A. The manipulation of air-sensitive compounds 2nd ed., (Wiley: New York, 1986)

[3] Nikolic, N. A. & Beak, P. *Org. Synth.* **74**, 23 (1997)

[4] Burchat, A. F., Chong, J. M. & Nielsen, N. Titration of alkyllithiums with a simple reagent to a blue endpoint. *J*. *Organomet*. *Chem*. **542**, 281-283 (1997)

[5] Stymiest, J. L., Bagutski, V., French, R. & Aggarwal, V. K. Enantiodivergent conversion of chiral secondary alcohols into tertiary alcohols *Nature* **456**, 778–782 (2008)

[6] Beak, P. & Carter, L. G. Dipole-stabilized carbanions from esters: α-oxo lithiations of 2,6-substituted benzoates of primary alcohols *J. Org. Chem.* **46**, 2363-2373 (1981)

[7] Dearden, M. J., Firkin, C. R., Hermet, J.-P. R. & O'Brien, P. A readily-accessible (+)-sparteine surrogate *J. Am. Chem. Soc*. **124**, 11870-11871 (2002)

[8] Noh, D., Yoon, S. K., Won, J., Lee, J. Y. & Yun, J. An efficient copper(I)-catalyst system for the asymmetric hydroboration of β-substituted vinylarenes with pinacolborane *Chem. Asian J.* ***6***, 1967-1969 (2001)

[9] Inagaki, T., Phong, L. T., Furuta, A., Ito, J. & Nishiyama, H. Iron- and cobalt-catalyzed asymmetric hydrosilylation of ketones and enones with bis(oxazolinylphenyl)amine ligands *Chem. -Eur. J.* **16**, 3090-3096 (2010)

[10] Roesner, S., Brown, C. A., Mohiti, M., Pulis, A. P., Rasappan, R., Blair, D. J., Essafi, S., Leonori, D. & Aggarwal, V. K. Stereospecific conversion of alcohols into pinacol boronic esters using lithiation–borylation methodology with pinacolborane *Chem. Commun.* **50**, 4053-4055 (2014)

[11] Ponder, J. W. TINKER: Software Tools for Molecular Design, Version 6.0 (2011)

[12] Allinger, N. L., Yuh, Y. H. & Lii, J.-H. Molecular mechanics. The MM3 force field for hydrocarbons. 1. *J. Am. Chem. Soc*. **111**, 8551-8566 (1989)

[13] Lii, J.-H. & Allinger, N. L. Molecular mechanics. The MM3 force field for hydrocarbons. 2. Vibrational frequencies and thermodynamics. *J. Am. Chem. Soc*. **111**, 8566-8575 (1989)

[14] Lii, J.-H. & Allinger, N. L. Molecular mechanics. The MM3 force field for hydrocarbons. 3. The van der Waals' potentials and crystal data for aliphatic and aromatic hydrocarbons. *J. Am. Chem. Soc*. **111**, 8576-8582 (1989)

[15] Gaussian 09, Revision B.01: M. J. Frisch, G. W. Trucks, H. B. Schlegel, G. E. Scuseria, M. A. Robb, J. R. Cheeseman, G. Scalmani, V. Barone, B. Mennucci, G. A. Petersson, H. Nakatsuji, M. Caricato, X. Li, H. P. Hratchian, A. F. Izmaylov, J. Bloino, G. Zheng, J. L. Sonnenberg, M. Hada, M. Ehara, K. Toyota, R. Fukuda, J. Hasegawa, M. Ishida, T. Nakajima, Y. Honda, O. Kitao, H. Nakai, T. Vreven, J. A. Montgomery, Jr., J. E. Peralta, F. Ogliaro, M. Bearpark, J. J. Heyd, E. Brothers, K. N. Kudin, V. N. Staroverov, T. Keith, R. Kobayashi, J. Normand, K. Raghavachari, A. Rendell, J. C. Burant, S. S. Iyengar, J. Tomasi, M. Cossi, N. Rega, J. M. Millam, M. Klene, J. E. Knox, J. B. Cross, V. Bakken, C. Adamo, J. Jaramillo, R. Gomperts, R. E. Stratmann, O. Yazyev, A. J. Austin, R. Cammi, C. Pomelli, J. W. Ochterski, R. L. Martin, K. Morokuma, V. G. Zakrzewski, G. A. Voth, P. Salvador, J. J. Dannenberg, S. Dapprich, A. D. Daniels, O. Farkas, J. B. Foresman, J. V. Ortiz, J. Cioslowski, and D. J. Fox, Gaussian, Inc., Wallingford CT, (2010)

[16] Becke, A. D. Density-functional thermochemistry. III. The role of exact exchange *J. Chem. Phys*. **98**, 5648-5652 (1993)

[17] Stephens, P. J., Devlin, F. J., Chabalowski, C. F. & Frisch, M. J. Ab initio calculation of vibrational absorption and circular dichroism spectra using density functional force fields *J. Phys. Chem*. **98**, 11623-11627 (1994)

[18] Grimme, S. Semiempirical GGA-type density functional constructed with a long-range dispersion correction. *J. Comput. Chem*. **27**, 1787-1799 (2006)

[19] Grimme, S., Antony, J., Ehrlich, S. & Krieg, H. A consistent and accurate ab initio parametrization of density functional dispersion correction (DFT-D) for the 94 elements H-Pu. *J. Chem. Phys*. **132**, 154104 (2010)

[20] Grimme, S., Ehrlich, S. & Goerigk, L. Effect of the damping function in dispersion corrected density functional theory. *J. Comput. Chem*. **32**, 1456-146 (2011).

[21] Adler, T. B., Werner, H.-J. & Manby, F. R. Local explicitly correlated second-order perturbation theory for the accurate treatment of large molecules. *J. Chem. Phys*. **130**, 054106 (2009).

[22] Werner, H.-J. Eliminating the domain error in local explicitly correlated second-order Møller–Plesset perturbation theory. *J. Chem. Phys*. **129**, 101103 (2008)

[23] For VnZ-F12 basis sets: Peterson, K. A., Adler, T. B. & Werner, H.-J. Systematically convergent basis sets for explicitly correlated wavefunctions: The atoms H, He, B–Ne, and Al–Ar. J. Chem. Phys. **128,** 084102 (2008). For auxiliary basis: Yousaf, K. E. & Peterson, K. A. Optimized auxiliary basis sets for explicitly correlated methods. *J. Chem. Phys*. **129**, 184108 (2008).

[24] MOLPRO, version 2010.1, a package of ab initio programs, H.-J. Werner, P. J. Knowles, G. Knizia, F. R. Manby, M. Schütz, P. Celani, T. Korona, R. Lindh, A. Mitrushenkov, G. Rauhut, K. R. Shamasundar, T. B. Adler, R. D. Amos, A. Bernhardsson, A. Berning, D. L. Cooper, M. J. O. Deegan, A. J. Dobbyn, F. Eckert, E. Goll, C. Hampel, A. Hesselmann, G. Hetzer, T. Hrenar, G. Jansen, C. Köppl, Y. Liu, A. W. Lloyd, R. A. Mata, A. J. May, S. J. McNicholas, W. Meyer, M. E. Mura, A. Nicklass, D. P. O'Neill, P. Palmieri, D. Peng, K. Pflüger, R. Pitzer, M. Reiher, T. Shiozaki, H. Stoll, A. J. Stone, R. Tarroni, T. Thorsteinsson, and M. Wang, , see http://www.molpro.net.

[25] Werner, H.-J., Knowles, P. J., Knizia, G., Manby, F. R., Schütz, M. Molpro: a general-purpose quantum chemistry program package. WIREs *Comput. Mol. Sci*. **2**, 242-253 (2012)

[26] Marenich, A. V., Cramer, C. J. & Truhlar, D. G. Universal solvation model based on solute electron density and a continuum model of the solvent defined by the bulk dielectric constant and atomic surface tensions. *J. Phys. Chem. B*, **113**, 6378-96 (2009).

[27] Tsuzuki, S., Schafer, L., Goto, H, Jemmis, E. D., Hosoya, H., Siam, K., Tanabe, K. & Osawa, E. Investigation of intramolecular interactions in n-alkanes. Cooperative energy

increments associated with GG and GTG' sequences. *J. Am. Chem. Soc*. **113**, 4665–4671 (1991).

[28] Gundertofte, K., Liljefors, T., Norrby, P.-O. & Pettersson, I. A Comparison of conformational energies calculated by several molecular mechanics methods. *J. Comput. Chem.* **17**, 429-449 (1996).

[29] Krishnamurthy, V. V. Excitation-sculptured indirect-detection experiment (EXSIDE) for long-range CH coupling-constant measurement *J. Magn. Reson.* **121**, 33-41 (1996)

[30] Stott, K., Keeler, J., Van, Q. N. & Shaka, A. J. One-dimensional NOE using pulsed field gradients *J. Magn. Reson.* **125**, 302-324 (1997)

[31] Neuhaus, D.; & Williamson, M. P. The nuclear Overhauser effect in structural and conformational analysis, 2nd ed. (John Wiley & Sons, Inc., New York , 2000)

[32] Butts, C. P., Jones, C. R. & Harvey J. N. Accuracy in determining interproton distances using nuclear Overhauser Effect data from a flexible molecule. Beilstein *J. Org. Chem*. **7**, 145–150 (2011)

[33] Butts, C. P., Jones, C. R., Towers, E. C., Flynn, J. L., Appleby, L. & Barron, N. J. Interproton distance determinations by NOE – surprising accuracy and precision in a rigid organic molecule. *Org. Biomol. Chem*. **9**, 177 – 184 (2011)

[34] Butts, C. P., Jones, C. R. & Harvey, J. N. High precision NOEs as a probe for low level conformers – a second conformation of strychnine. *Chem. Commun*. **47**, 1193-1195 (2011)

[35] Hu, H. & Krishnamurthy, K. Revisiting the initial rate approximation in kinetic NOE measurements *J. Magn. Reson.* **182**, 173-177 (2006)

[36] Bifulco, G., Dambruoso, P., Gomez-Paloma, L. & Riccio, R. Determination of relative configuration in organic compounds by NMR spectroscopy and computational methods *Chem. Rev.* **107**, 3744-3779 (2007)

NMR Spectra

Ethyl 2,4,6-triisopropylbenzoate, 3

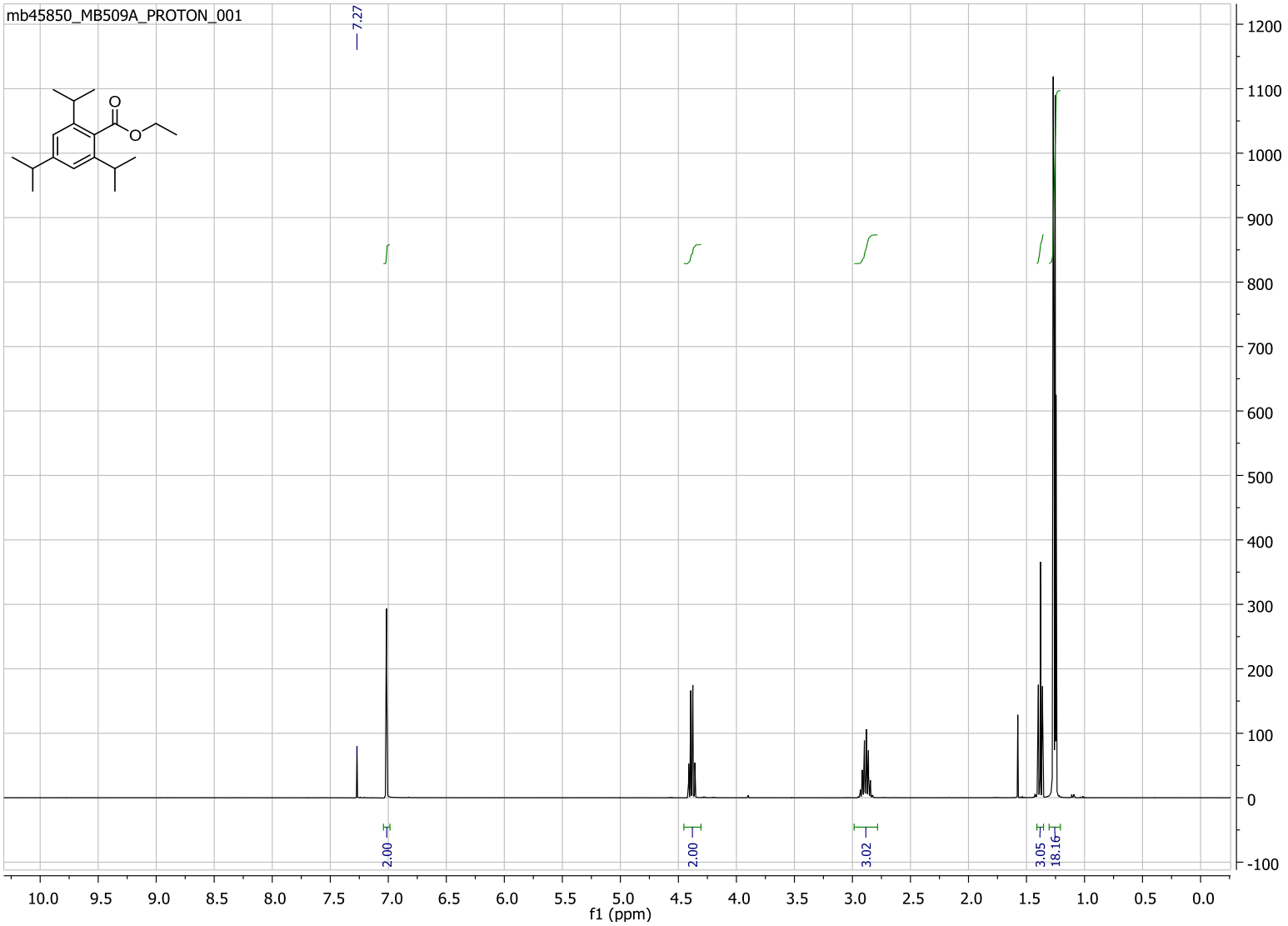

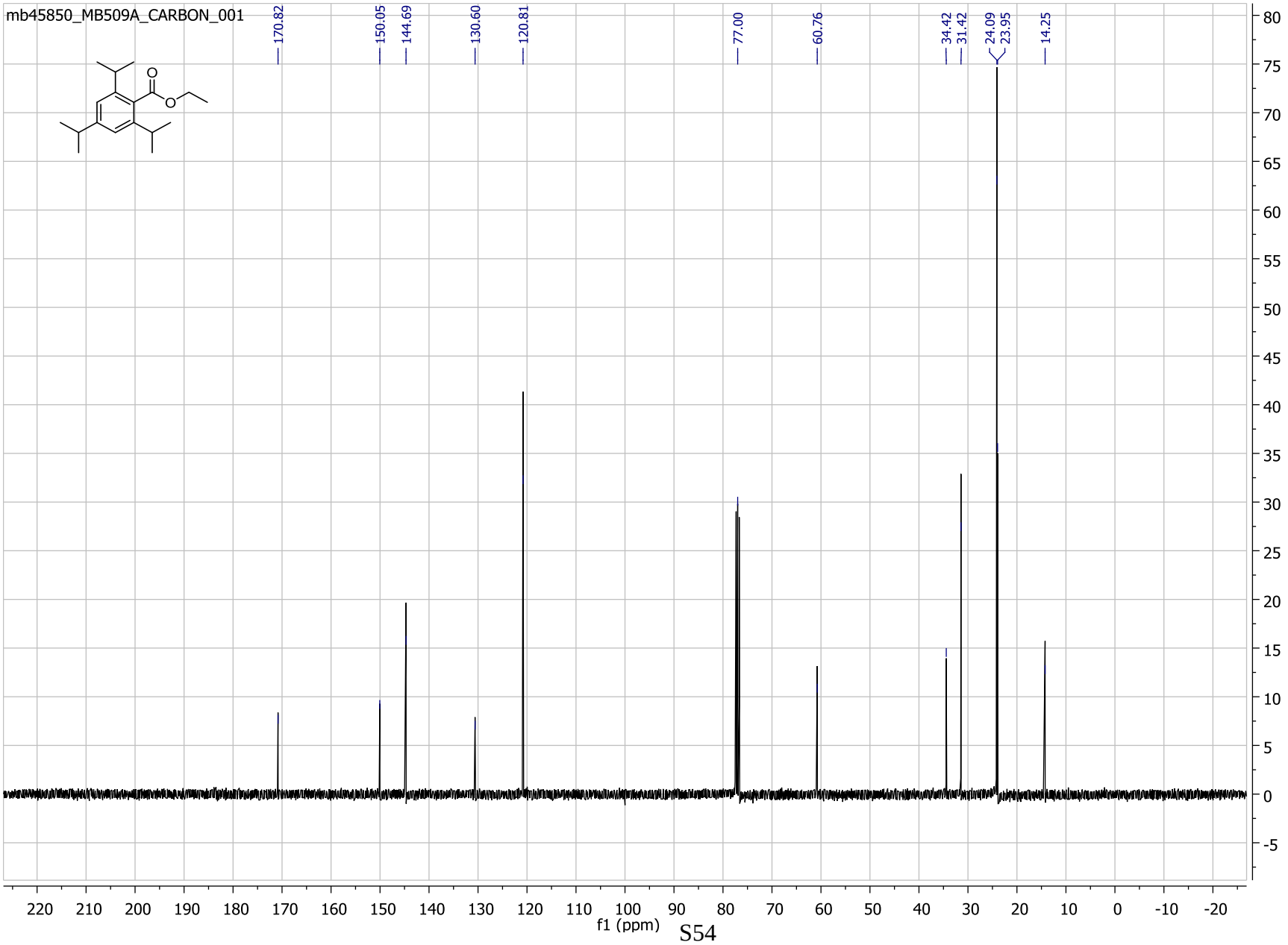
mb45850_MB509A_CARBON_001
170.82
150.05
144.69
130.60
120.81
77.00
60.76
34.42
31.42
24.09
23.95
14.25
f1 (ppm)

1-

(Trimethylstannyl)ethyl 2,4,6-triisopropylbenzoate, (*S*)-5

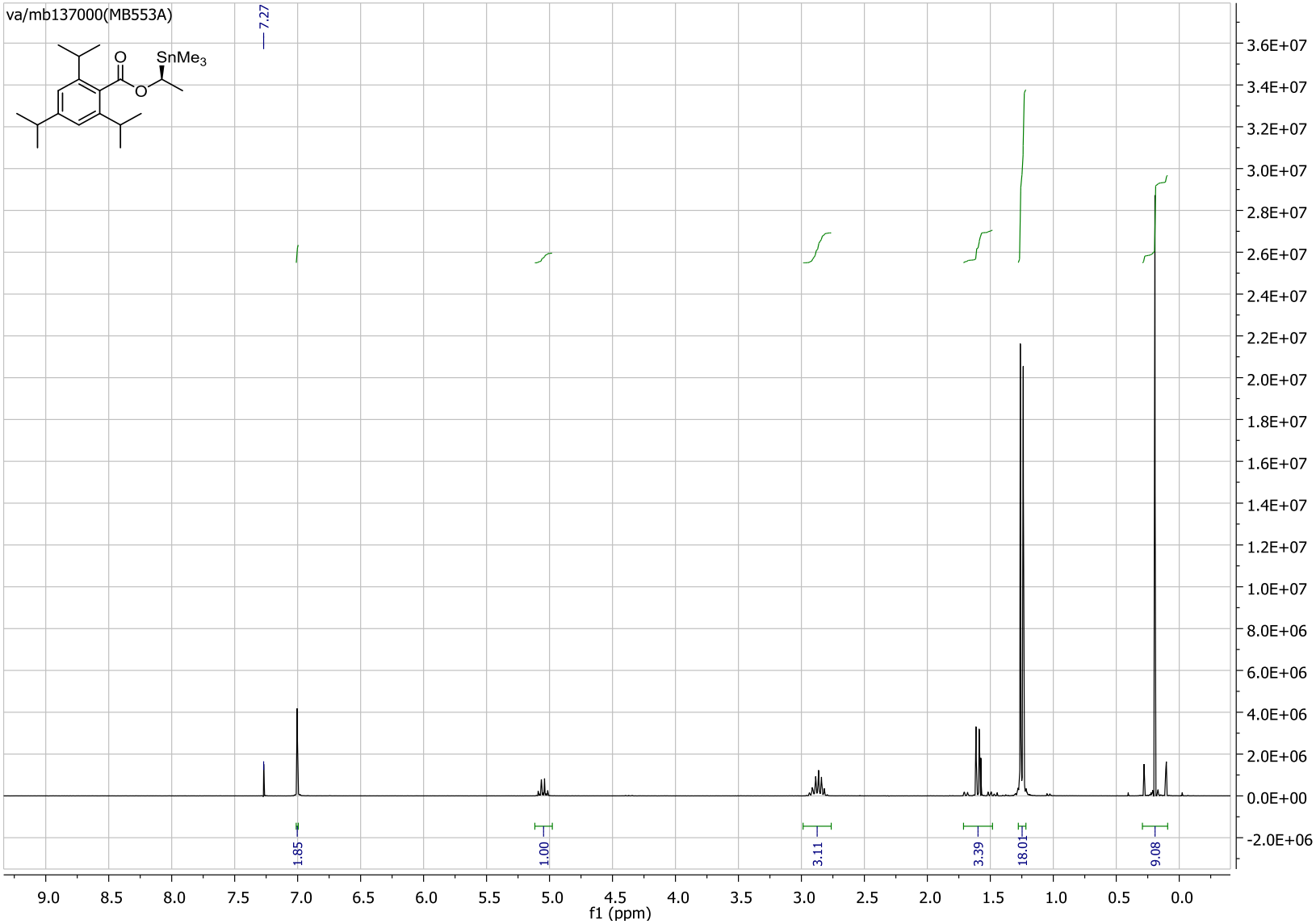

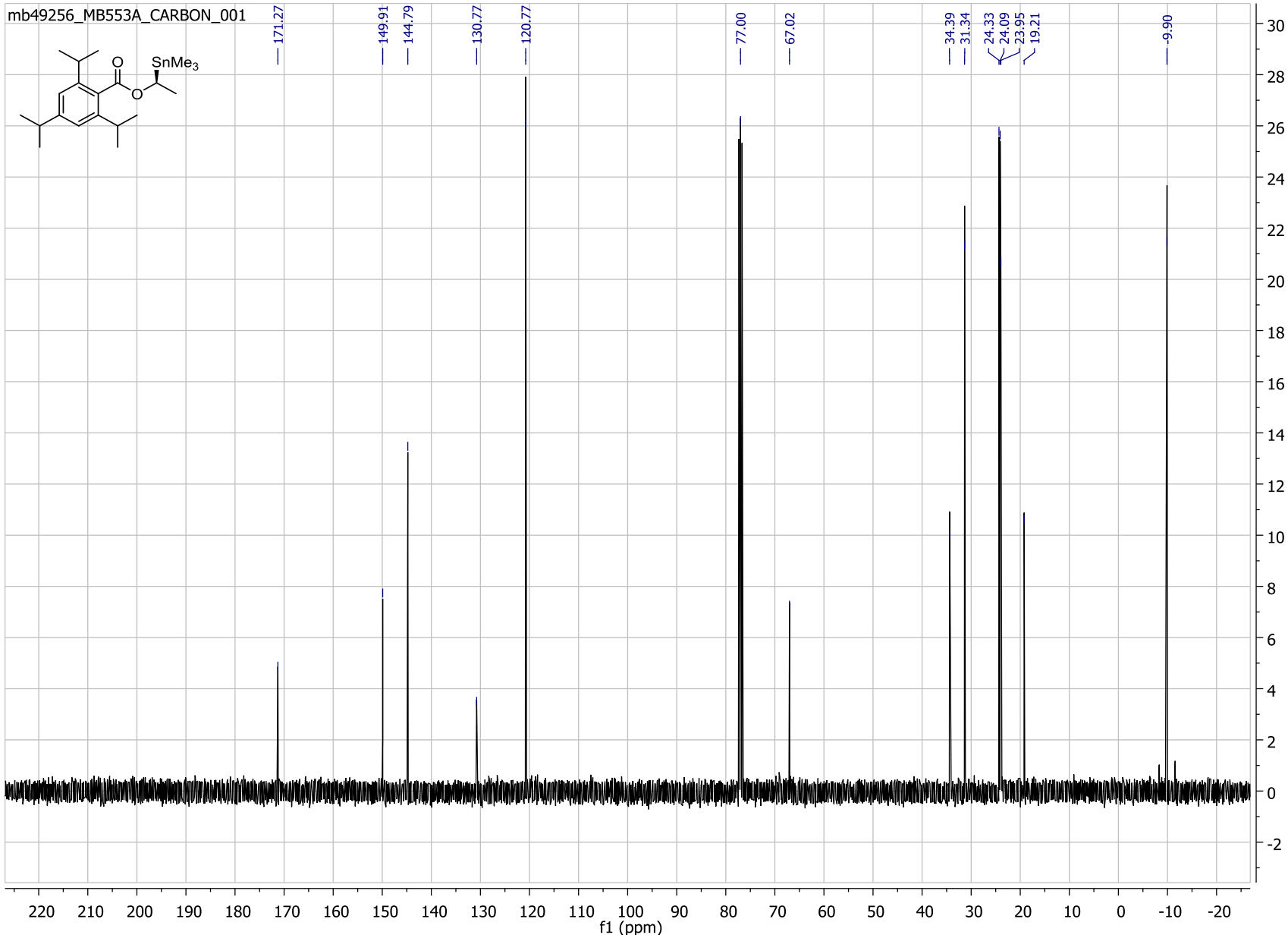
mb49256_MB553A_CARBON_001
171.27
149.91
144.79
130.77
120.77
77.00
67.02
34.39
31.34
24.33
24.09
23.95
19.21
-9.90
O
O
SnMe3
f1 (ppm)

(1-([1,1'-biphenyl]-4-yl)ethyl)boronic acid pinacol ester, (*R*)-10

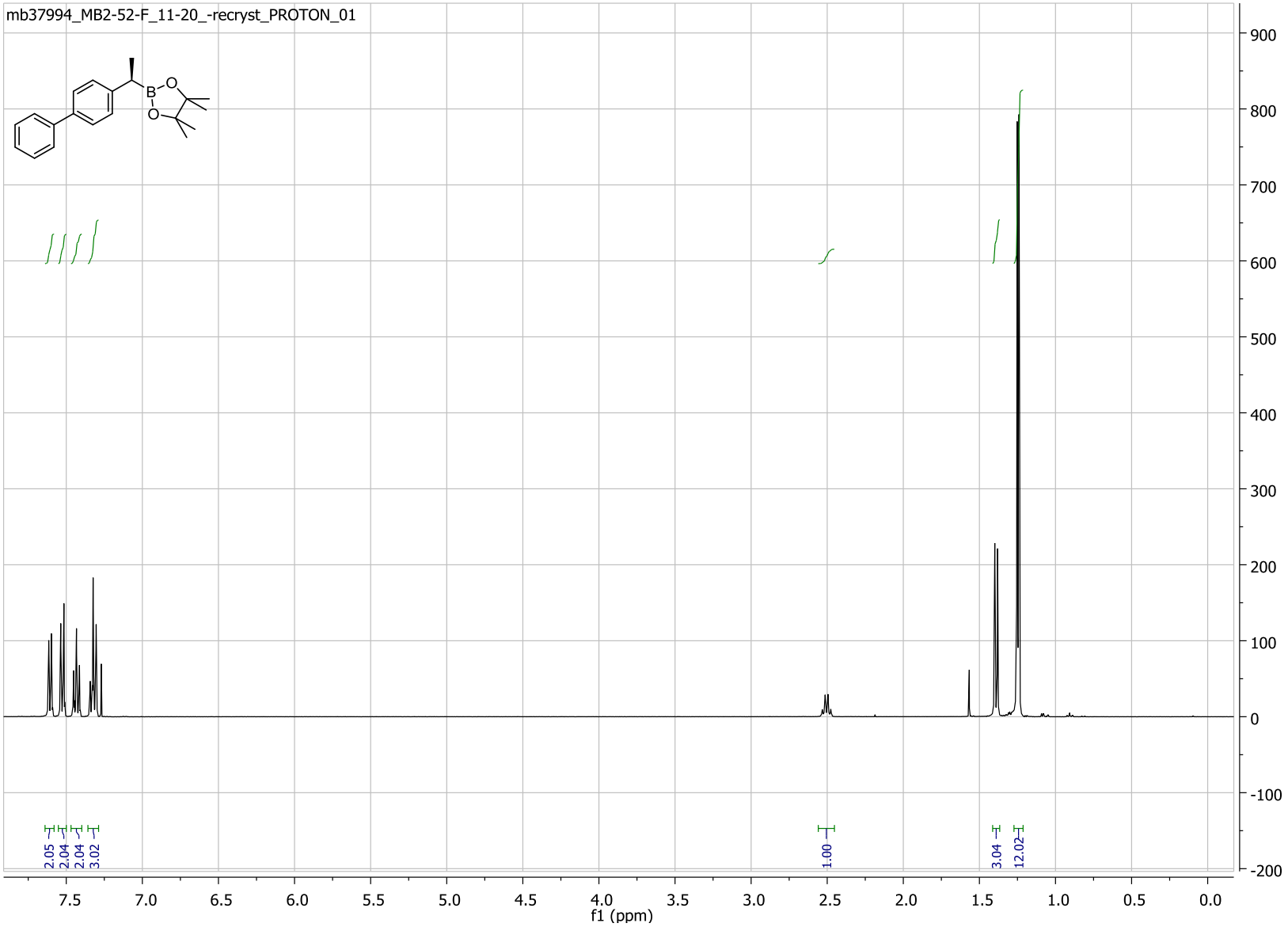

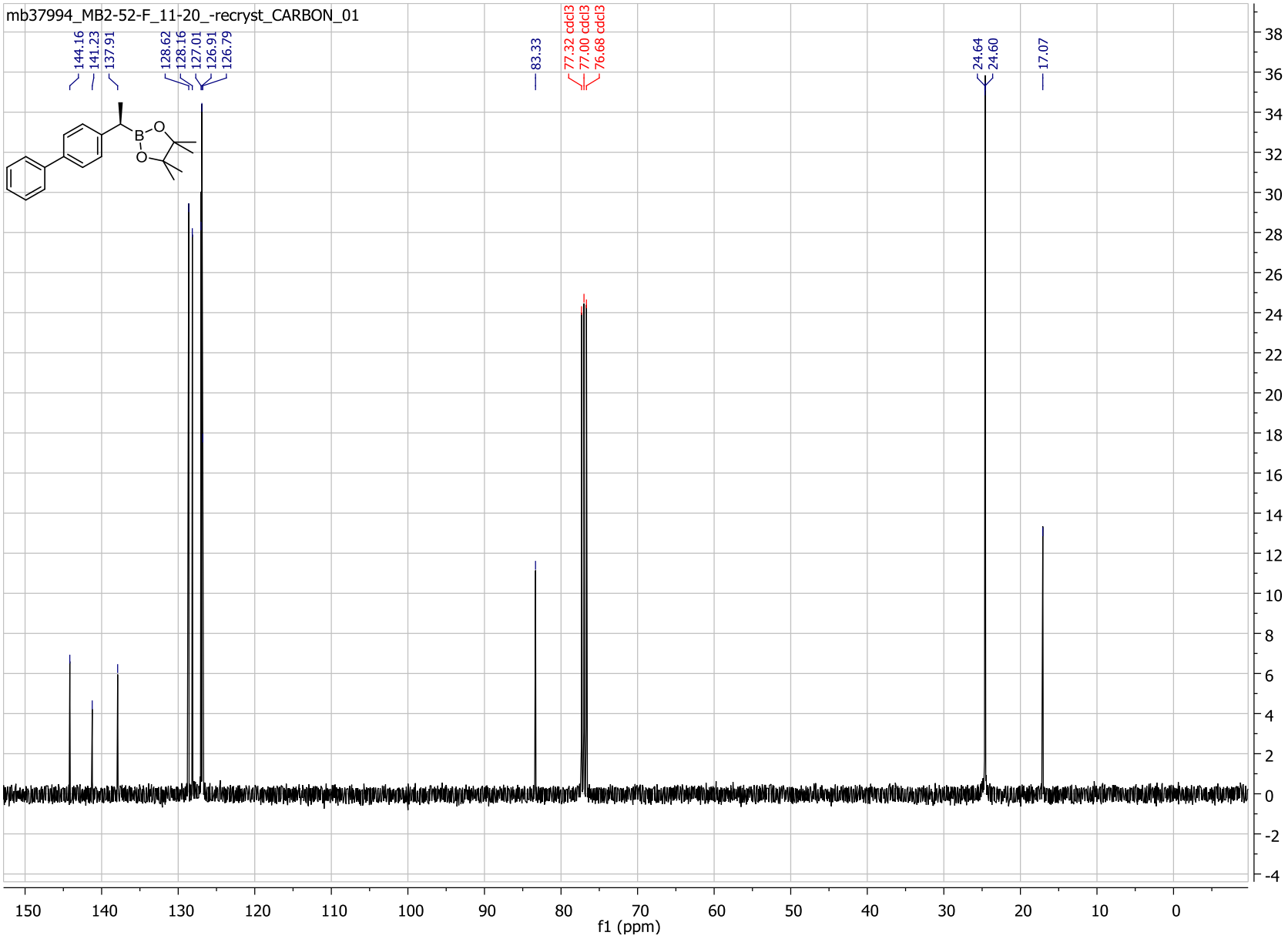
mb37994_MB2-52-F_11-20_-recryst_CARBON_01
144.16
141.23
137.91
128.62
128.16
127.01
126.91
126.79
83.33
77.32 cdcl3
77.00 cdcl3
76.68 cdcl3
24.64
24.60
17.07
f1 (ppm)

(*R*)-(1-Phenylethyl)boronic acid pinacol ester, (*R*)-16

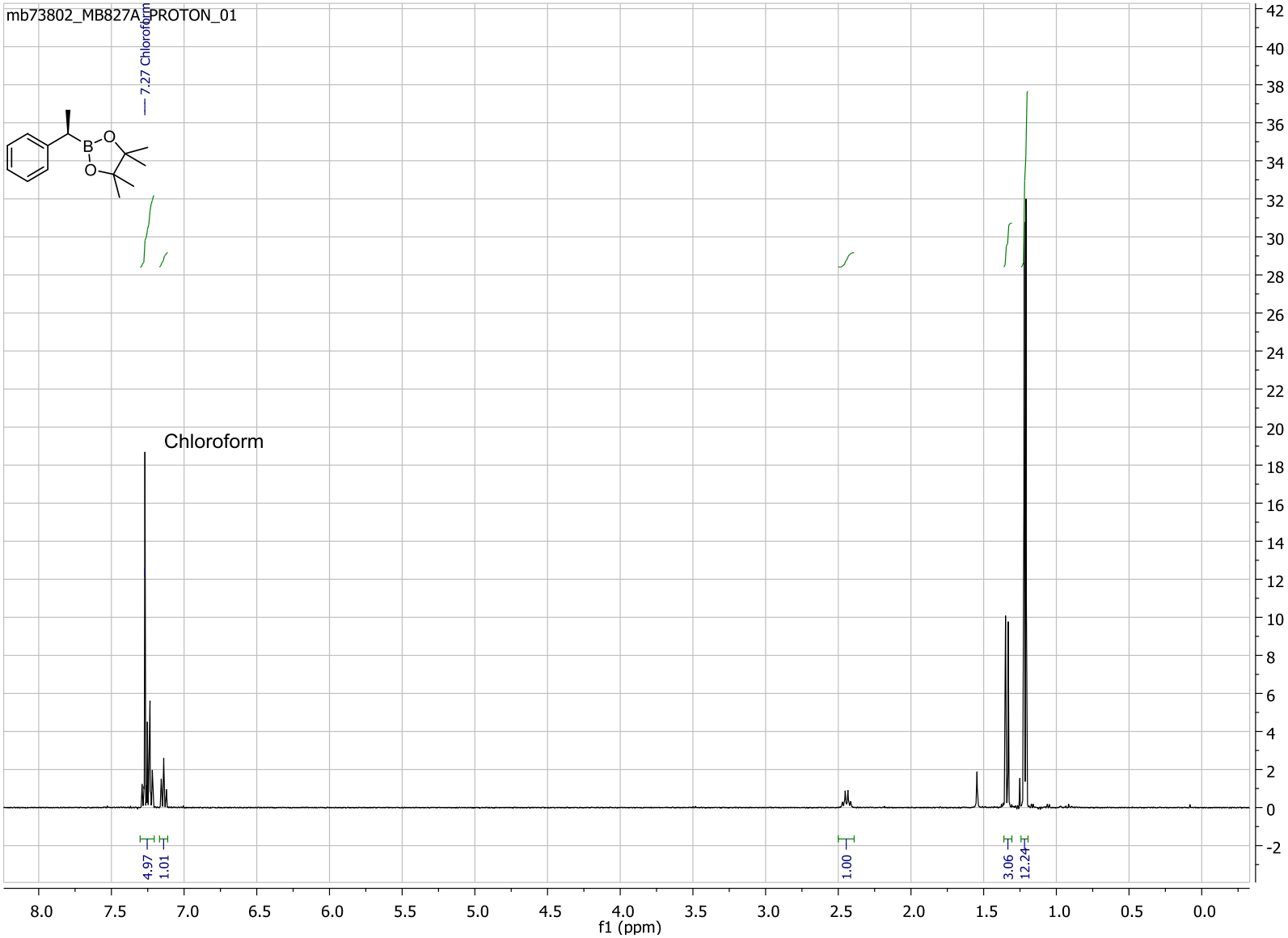

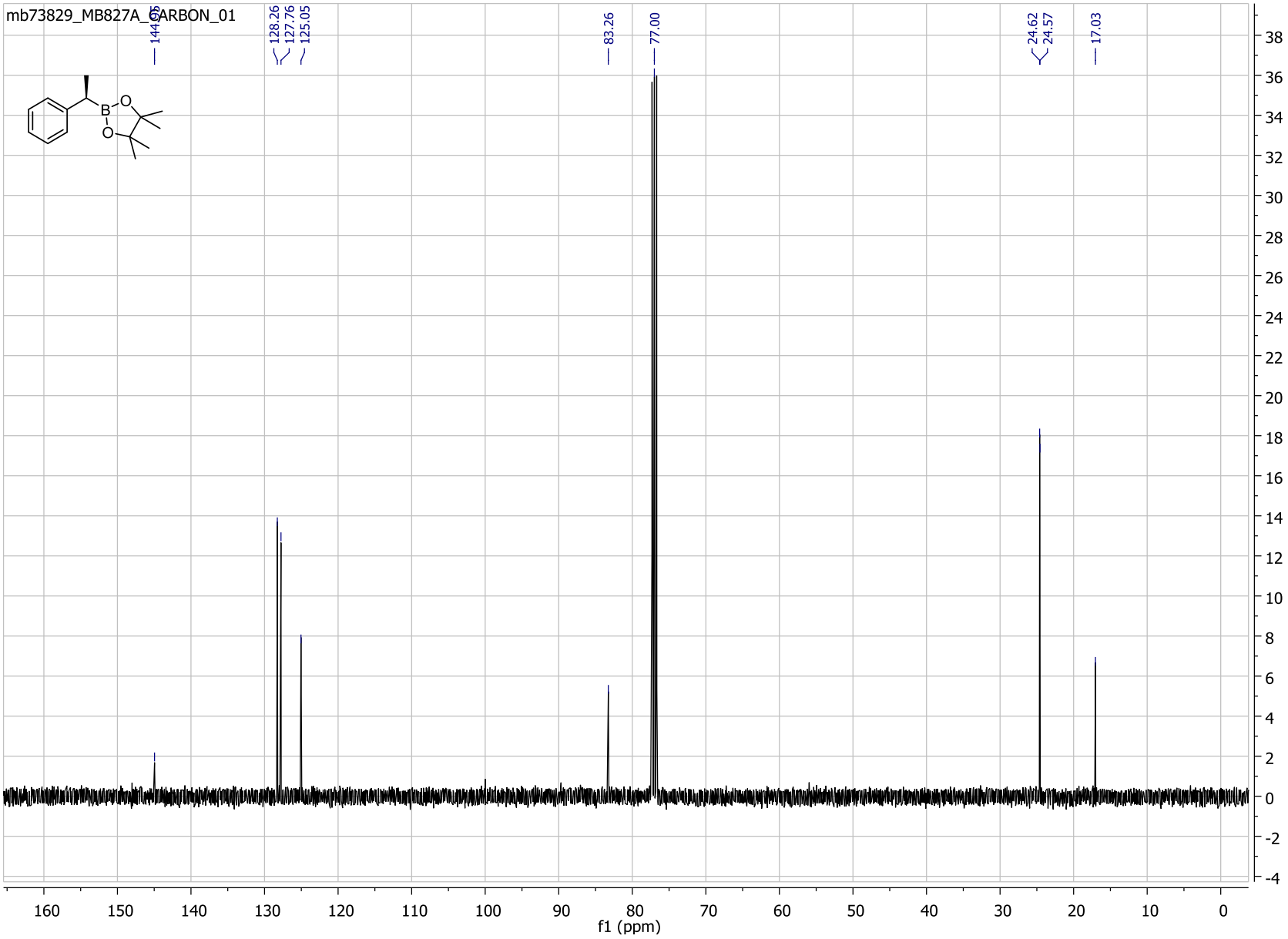
mb73829_MB827A_CARBON_01
144.05
128.26
127.76
125.05
83.26
77.00
24.62
24.57
17.03
f1 (ppm)

2-((2*R*,3*S*,4*S*,5*S*,6*S*,7*S*,8*S*,9*S*,10*S*,11*S*)-11-([1,1'-biphenyl]-4-yl)-3,4,5,6,7,8,9,10-octamethyldodecan-2-yl)-4,4,5,5-tetramethyl-1,3,2-dioxaborolane, 11

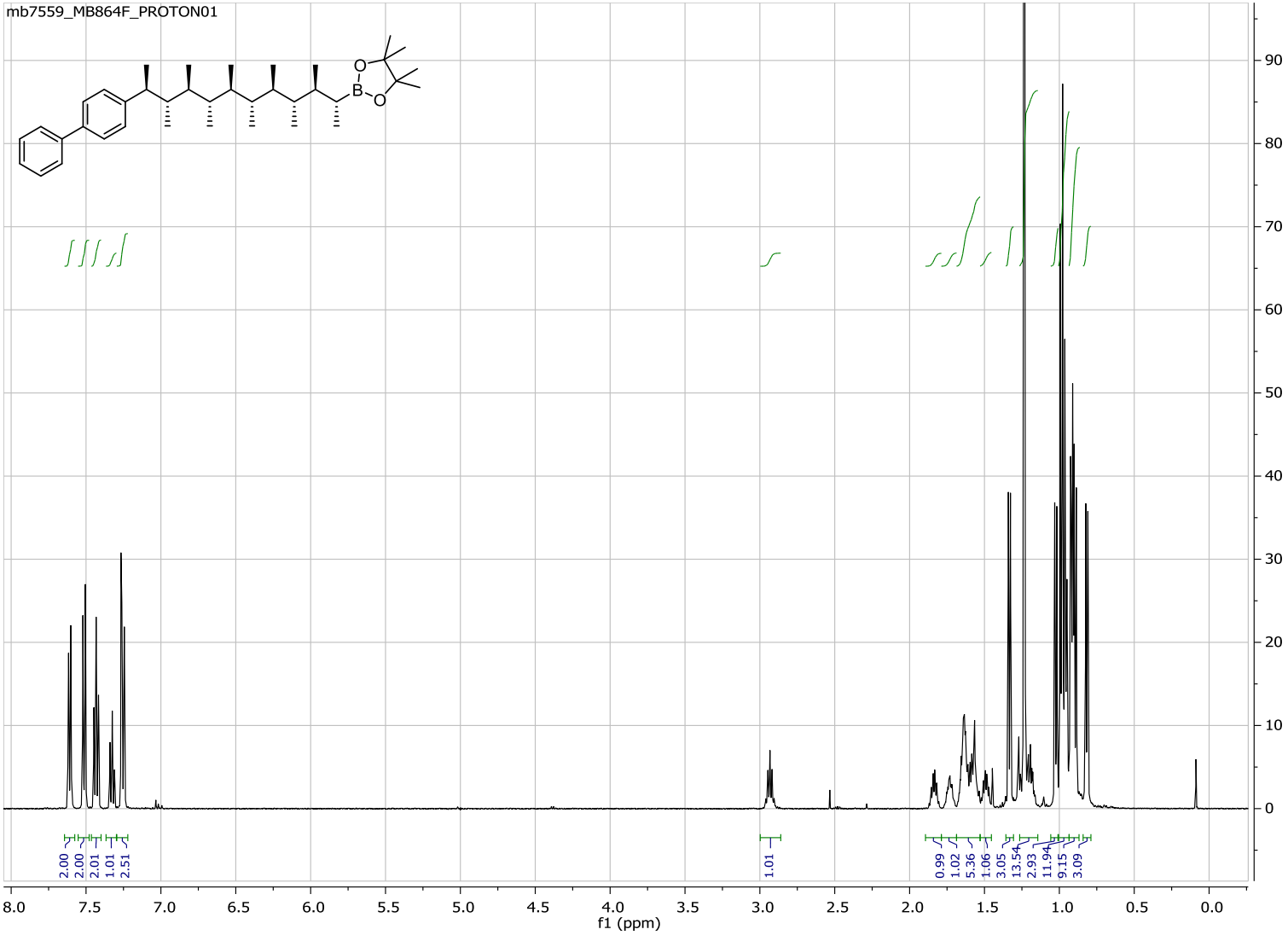

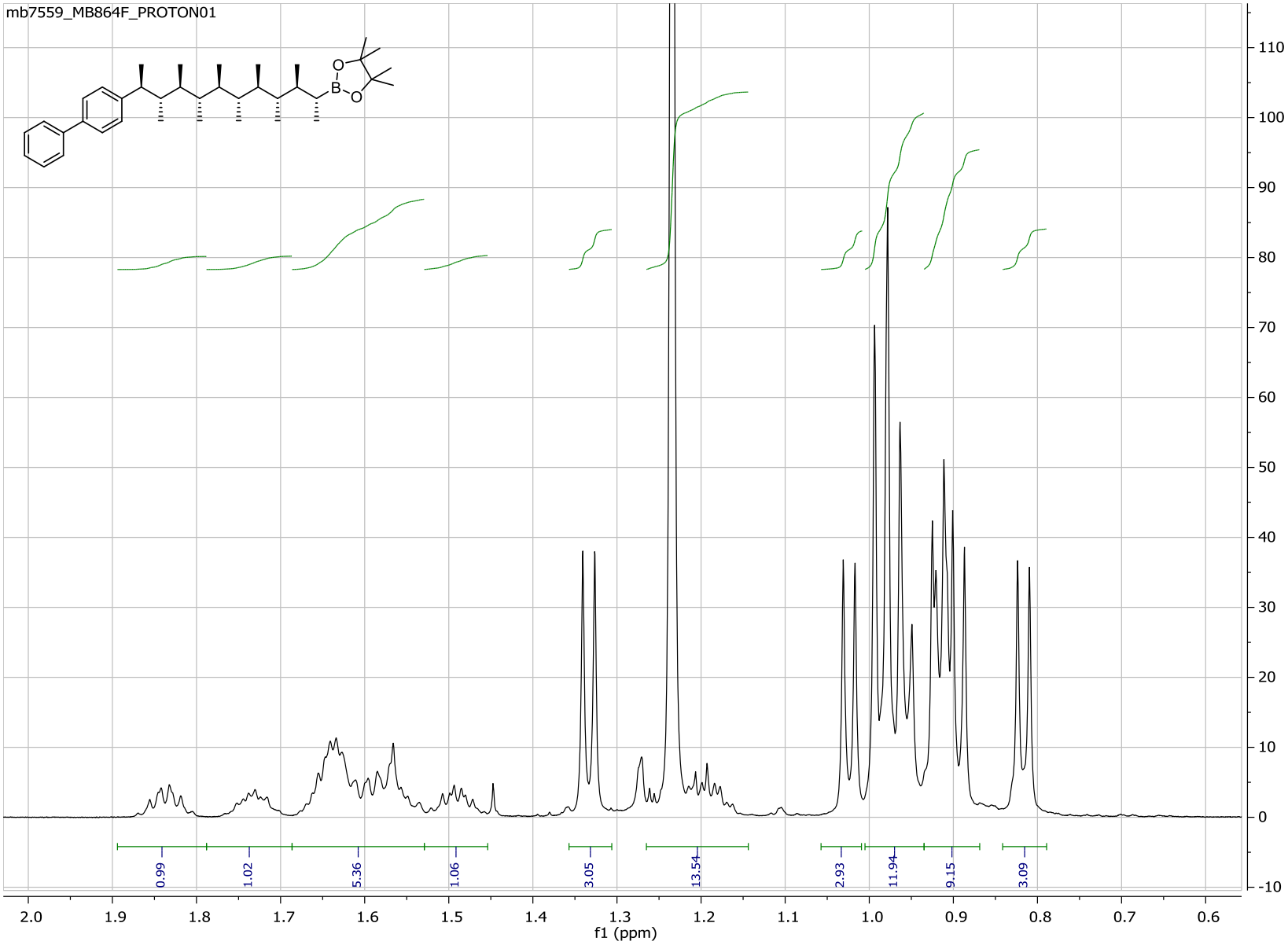
mb7559_MB864F_PROTON01
O
B
O
110
100
90
80
70
60
50
40
30
20
10
0
-10
0.99
1.02
5.36
1.06
3.05
13.54
2.93
11.94
9.15
3.09
2.0
1.9
1.8
1.7
1.6
1.5
1.4
1.3
1.2
1.1
1.0
0.9
0.8
0.7
0.6
f1 (ppm)

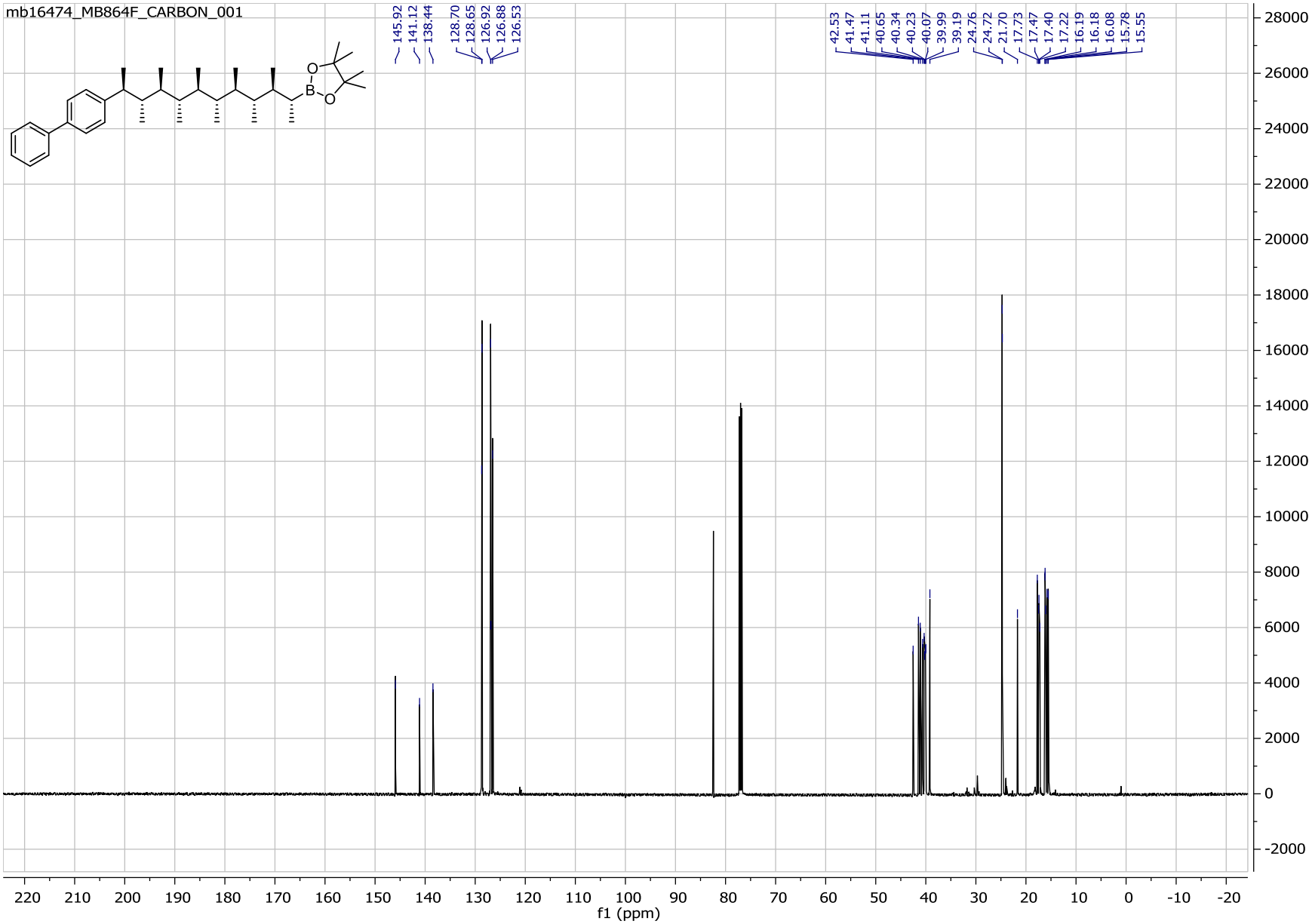
mb16474_MB864F_CARBON_001
145.92
141.12
138.44
128.70
128.65
126.92
126.88
126.53
42.53
41.47
41.11
40.65
40.34
40.23
40.07
39.99
39.19
24.76
24.72
21.70
17.73
17.47
17.40
17.22
16.19
16.18
16.08
15.78
15.55
O
B
O
28000
26000
24000
22000
20000
18000
16000
14000
12000
10000
8000
6000
4000
2000
0
-2000
220
210
200
190
180
170
160
150
140
130
120
110
100
90
80
70
60
50
40
30
20
10
0
-10
-20
f1 (ppm)

4,4,5,5-tetramethyl-2-((2*S*,3*S*,4*S*,5*R*,6*R*,7*S*,8*S*,9*R*,10*R*,11*S*)-3,4,5,6,7,8,9,10-octamethyl-11-phenyldodecan-2-yl)-1,3,2-dioxaborolane, 17

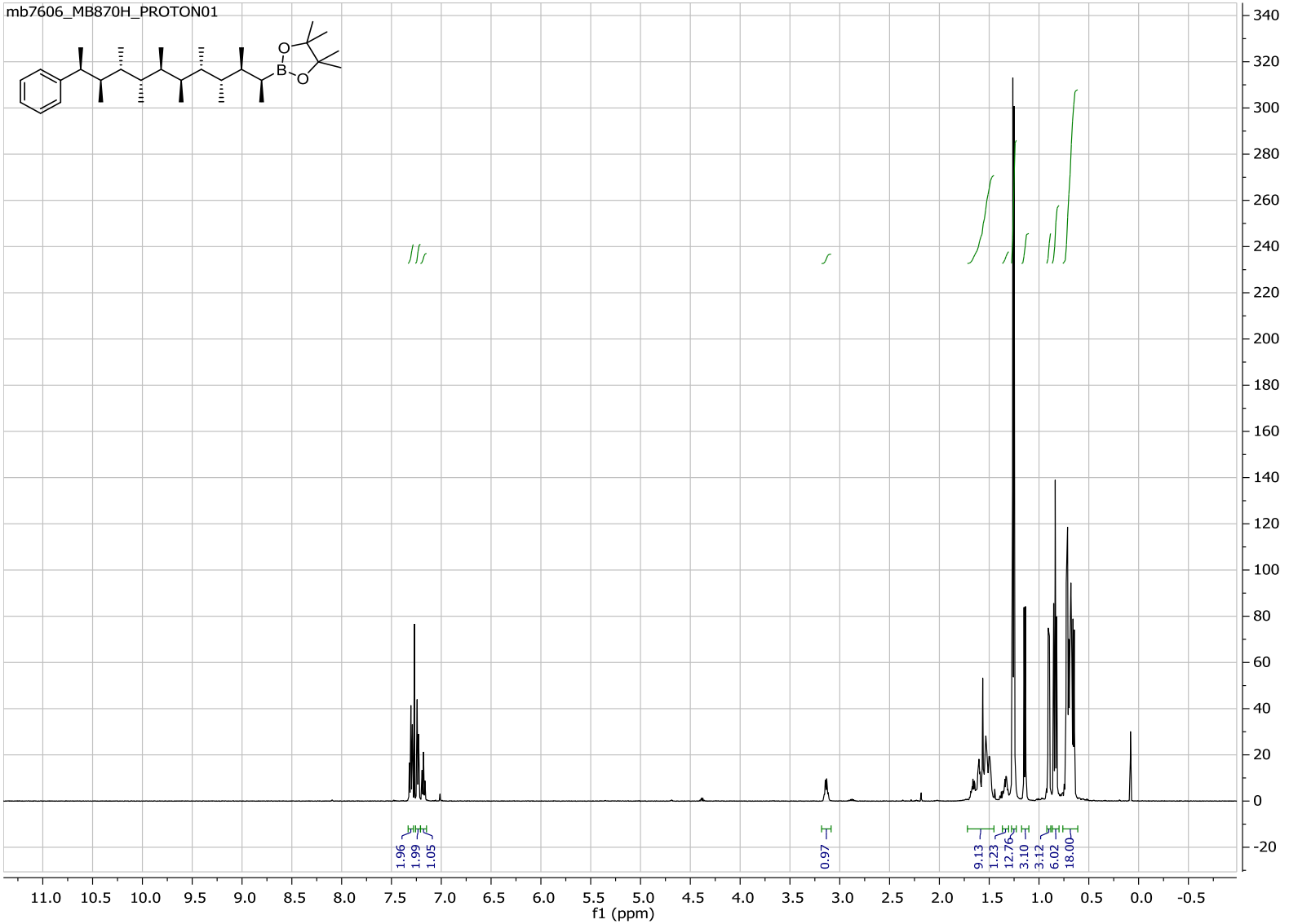

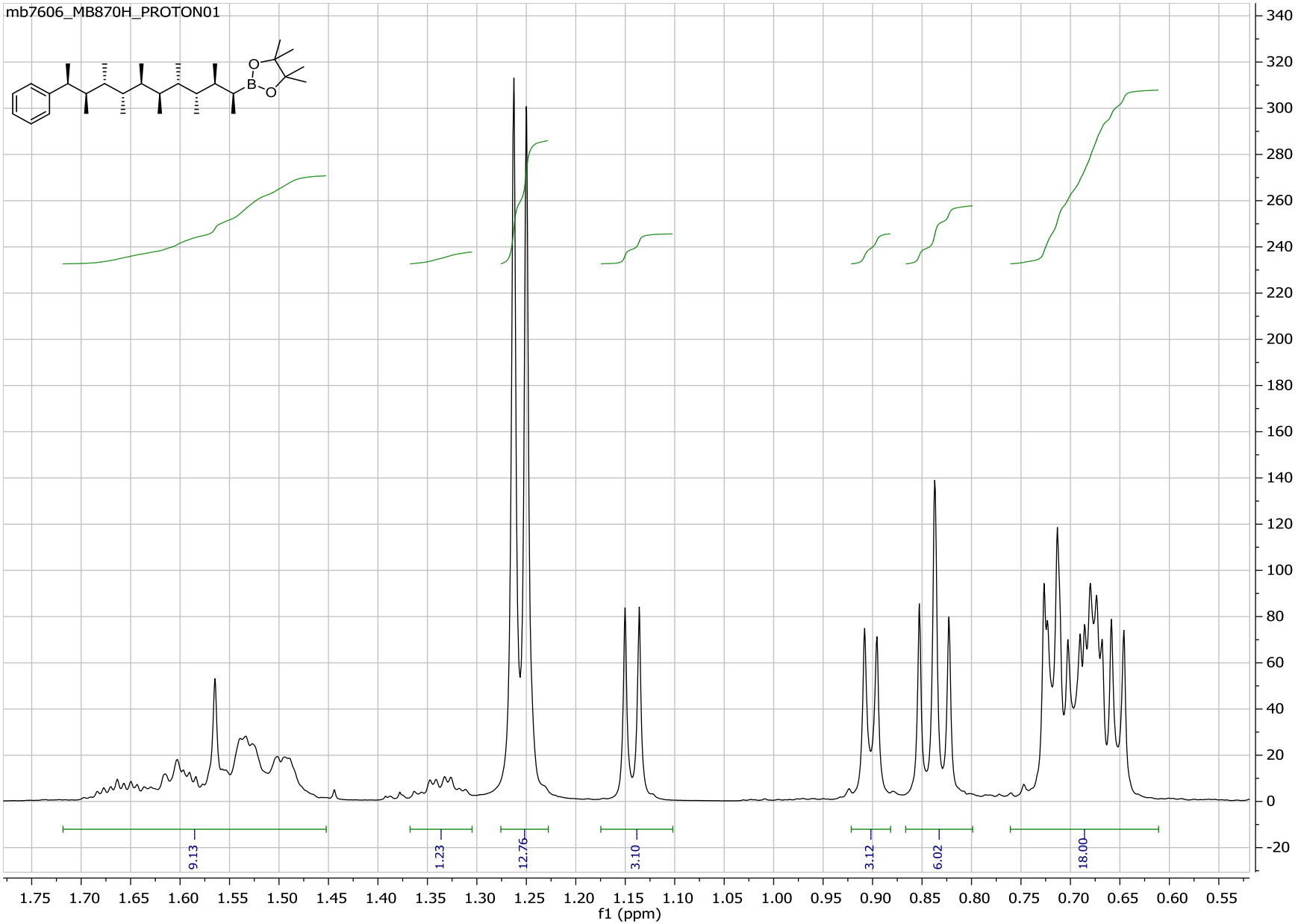
mb7606_MB870H_PROTON01
O
B
O
340
320
300
280
260
240
220
200
180
160
140
120
100
80
60
40
20
0
-20
9.13
1.23
12.76
3.10
3.12
6.02
18.00
1.75 1.70 1.65 1.60 1.55 1.50 1.45 1.40 1.35 1.30 1.25 1.20 1.15 1.10 1.05 1.00 0.95 0.90 0.85 0.80 0.75 0.70 0.65 0.60 0.55
f1 (ppm)

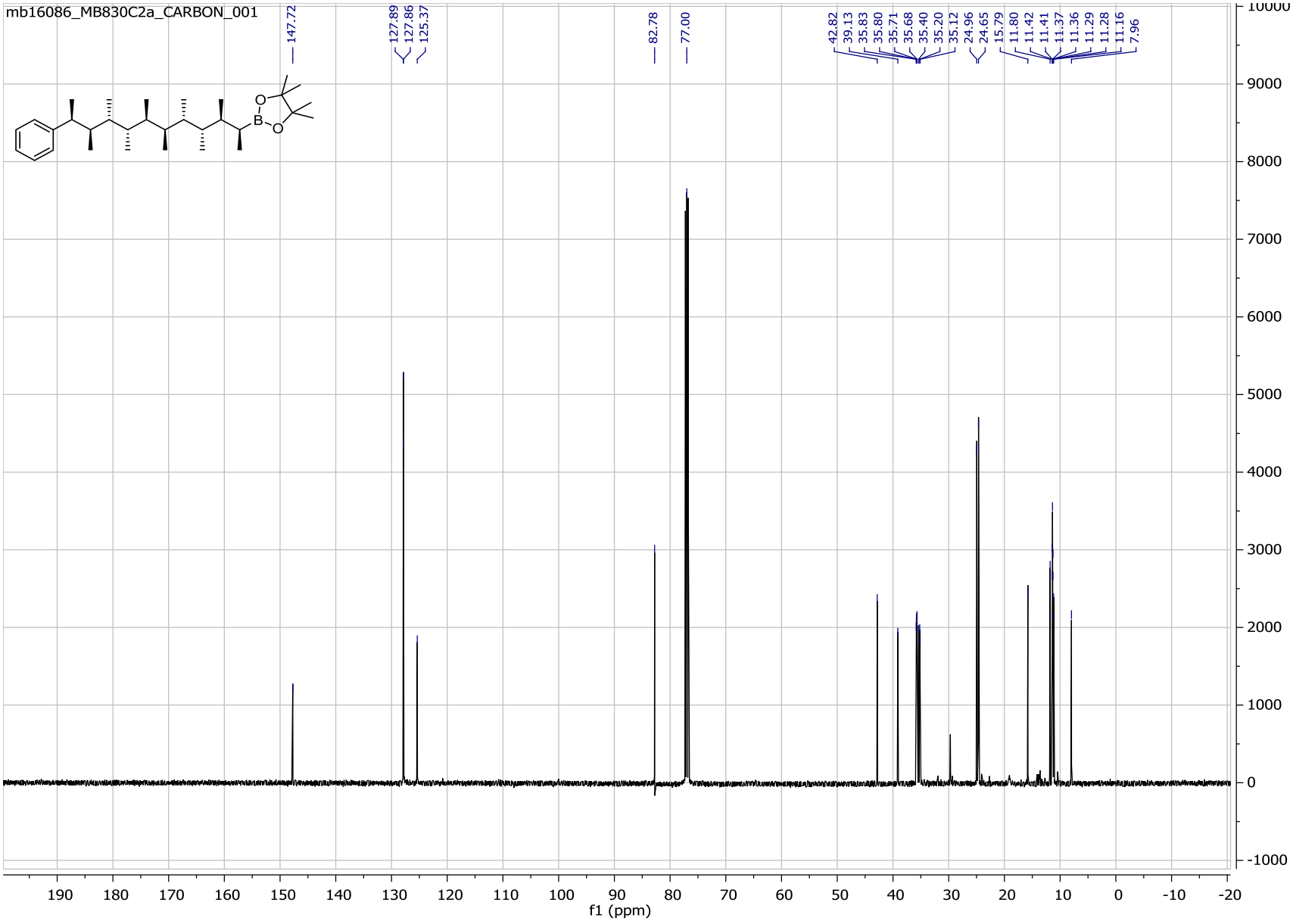
mb16086_MB830C2a_CARBON_001
147.72
127.89
127.86
125.37
82.78
77.00
42.82
39.13
35.83
35.80
35.71
35.68
35.40
35.20
35.12
24.96
24.65
15.79
11.80
11.42
11.41
11.37
11.36
11.29
11.28
11.16
7.96
O
B
O
10000
9000
8000
7000
6000
5000
4000
3000
2000
1000
0
-1000
190
180
170
160
150
140
130
120
110
100
90
80
70
60
50
40
30
20
10
0
-10
-20
f1 (ppm)

2-((2*S*,3*S*,4*R*,5*S*,6*R*,7*S*,8*R*,9*S*,10*R*,11*S*)-11-([1,1'-biphenyl]-4-yl)-3,4,5,6,7,8,9,10-octamethyldodecan-2-yl)-4,4,5,5-tetramethyl-1,3,2-dioxaborolane, 13

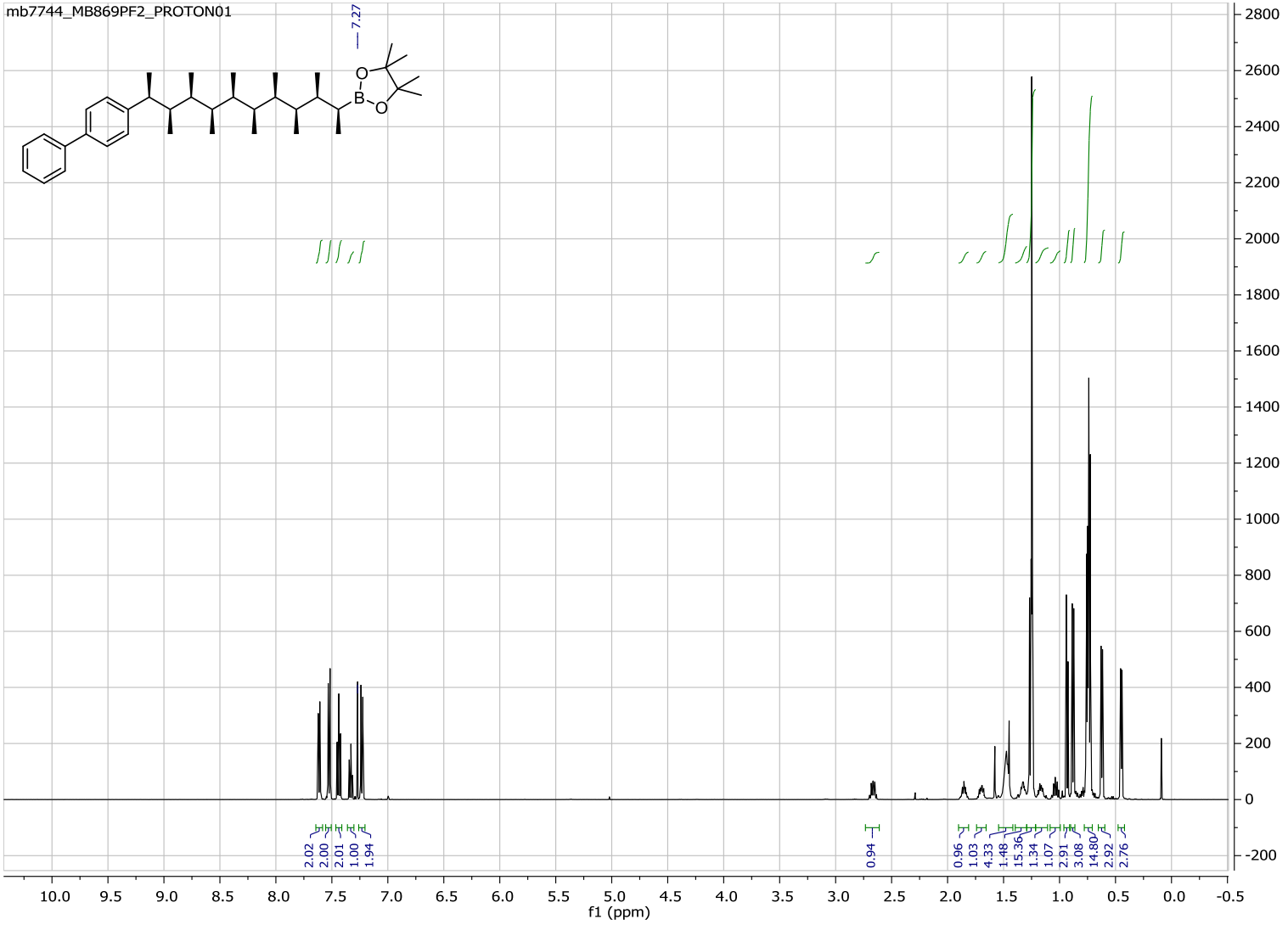

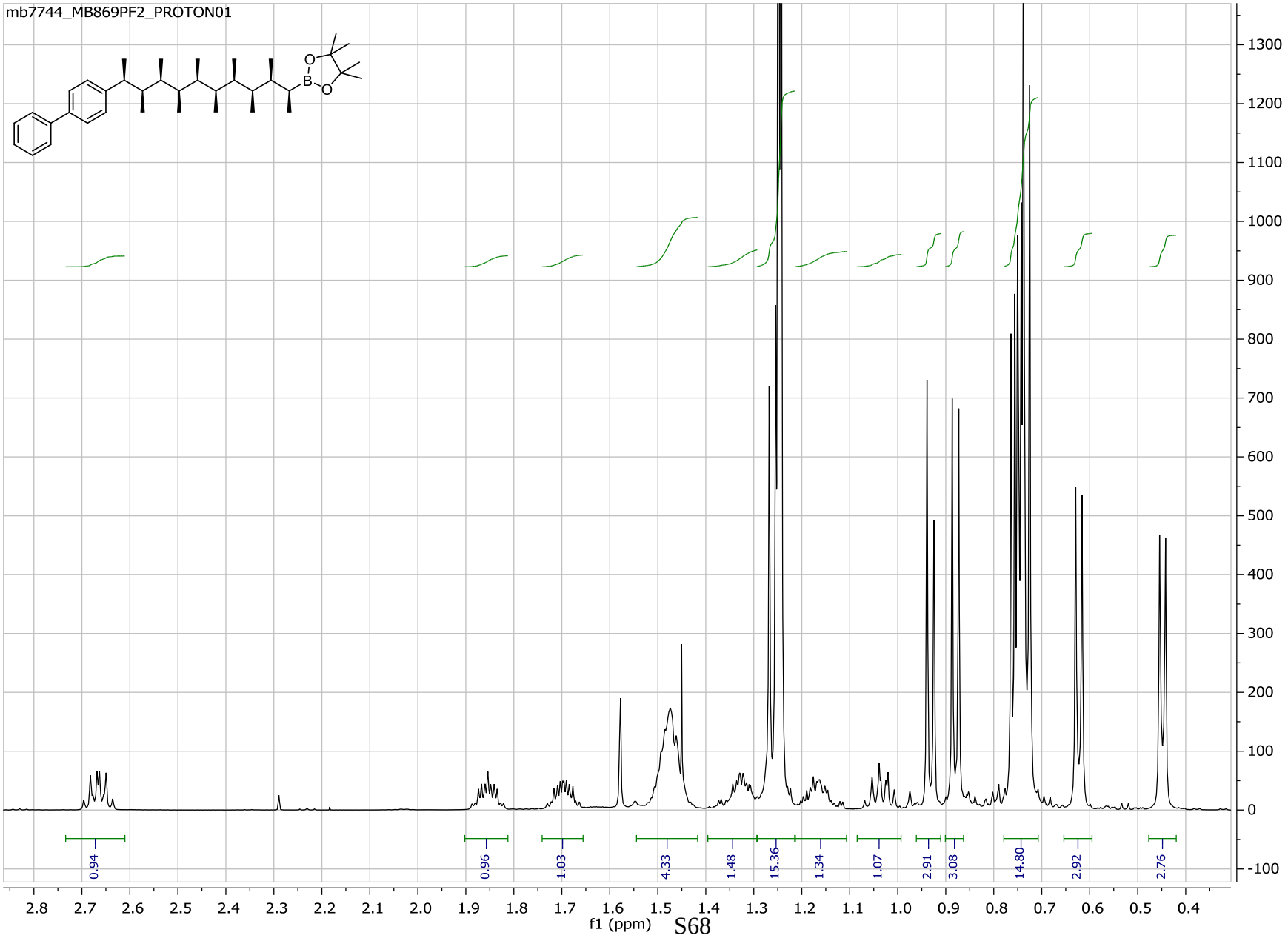
mb7744_MB869PF2_PROTON01
O
B
O
1300
1200
1100
1000
900
800
700
600
500
400
300
200
100
0
-100
0.94
0.96
1.03
4.33
1.48
15.36
1.34
1.07
2.91
3.08
14.80
2.92
2.76
2.8
2.7
2.6
2.5
2.4
2.3
2.2
2.1
2.0
1.9
1.8
1.7
1.6
1.5
1.4
1.3
1.2
1.1
1.0
0.9
0.8
0.7
0.6
0.5
0.4
f1 (ppm)

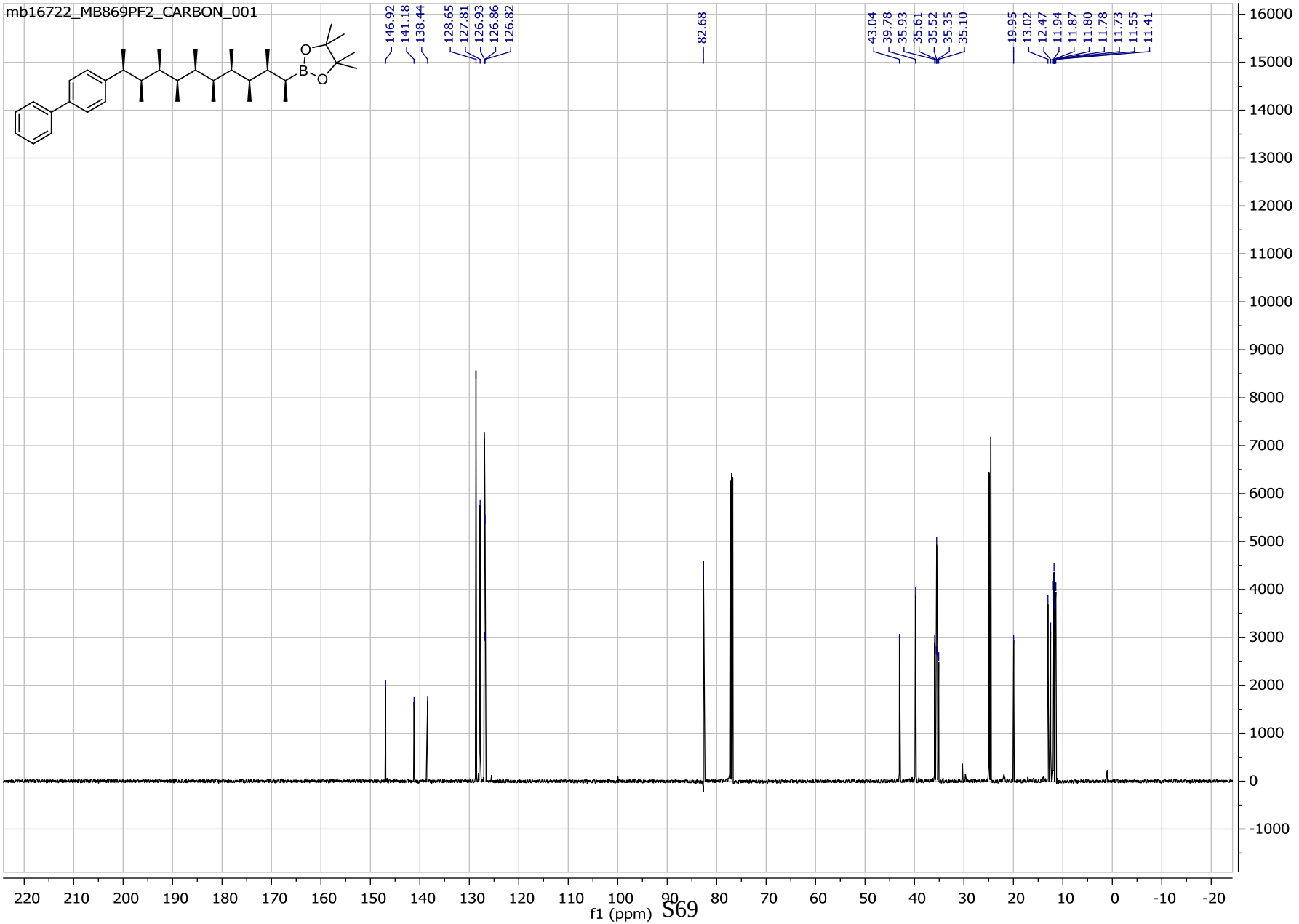
mb16722_MB869PF2_CARBON_001
146.92
141.18
138.44
128.65
127.81
126.93
126.86
126.82
82.68
43.04
39.78
35.93
35.61
35.52
35.35
35.10
19.95
13.02
12.47
11.94
11.87
11.80
11.78
11.73
11.55
11.41
O
B
O
16000
15000
14000
13000
12000
11000
10000
9000
8000
7000
6000
5000
4000
3000
2000
1000
0
-1000
220
210
200
190
180
170
160
150
140
130
120
110
100
90
80
70
60
50
40
30
20
10
0
-10
-20
f1 (ppm)

(2*R*,3*R*,4*R*,5*R*,6*R*,7*R*,8*S*,9*S*,10*S*,11*S*)-11-([1,1'-biphenyl]-4-yl)-3,4,5,6,7,8,9,10-octamethyldodecan-2-ol, 22

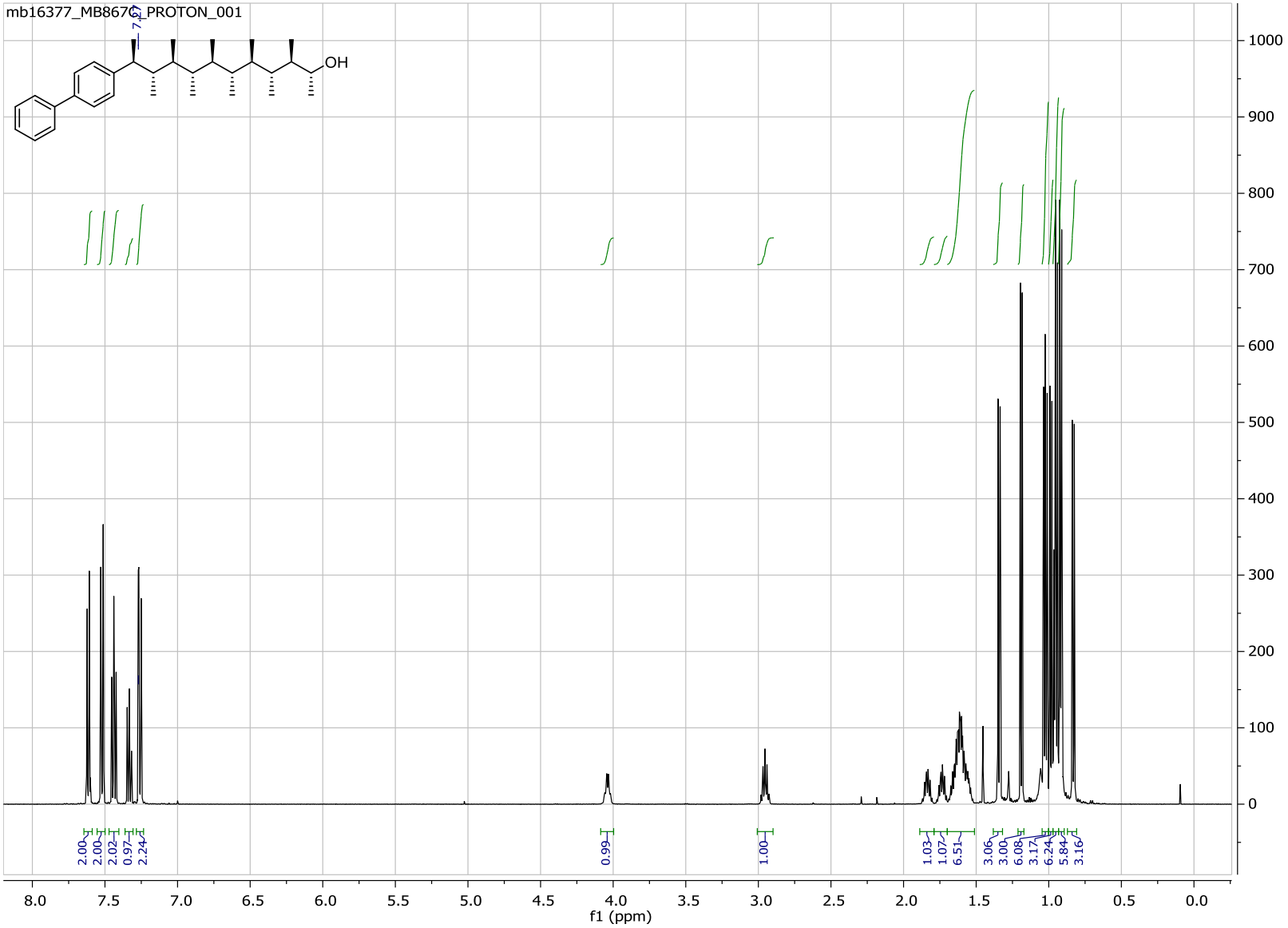

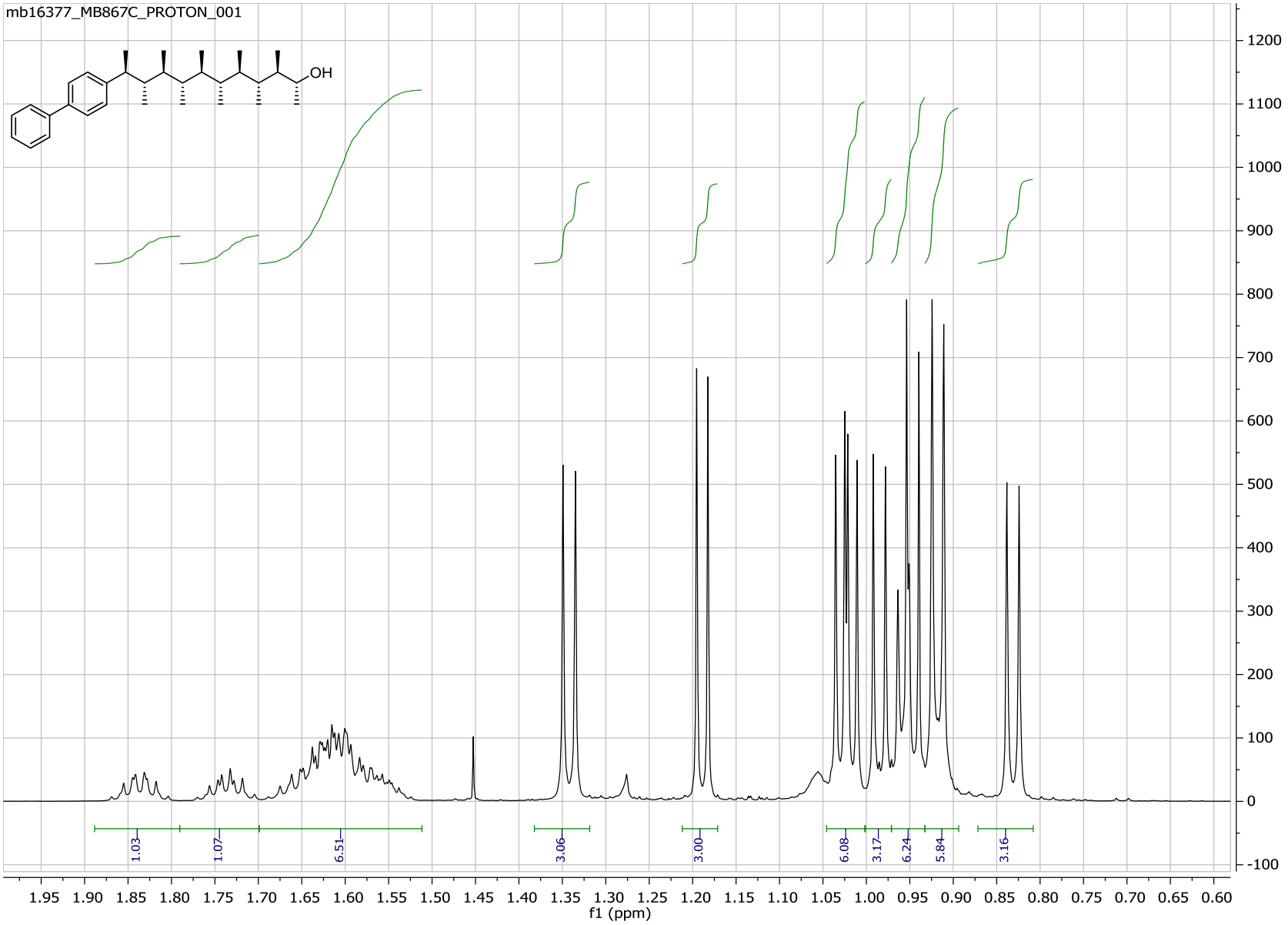
mb16377_MB867C_PROTON_001
OH
1.03
1.07
6.51
3.06
3.00
6.08
3.17
6.24
5.84
3.16
f1 (ppm)

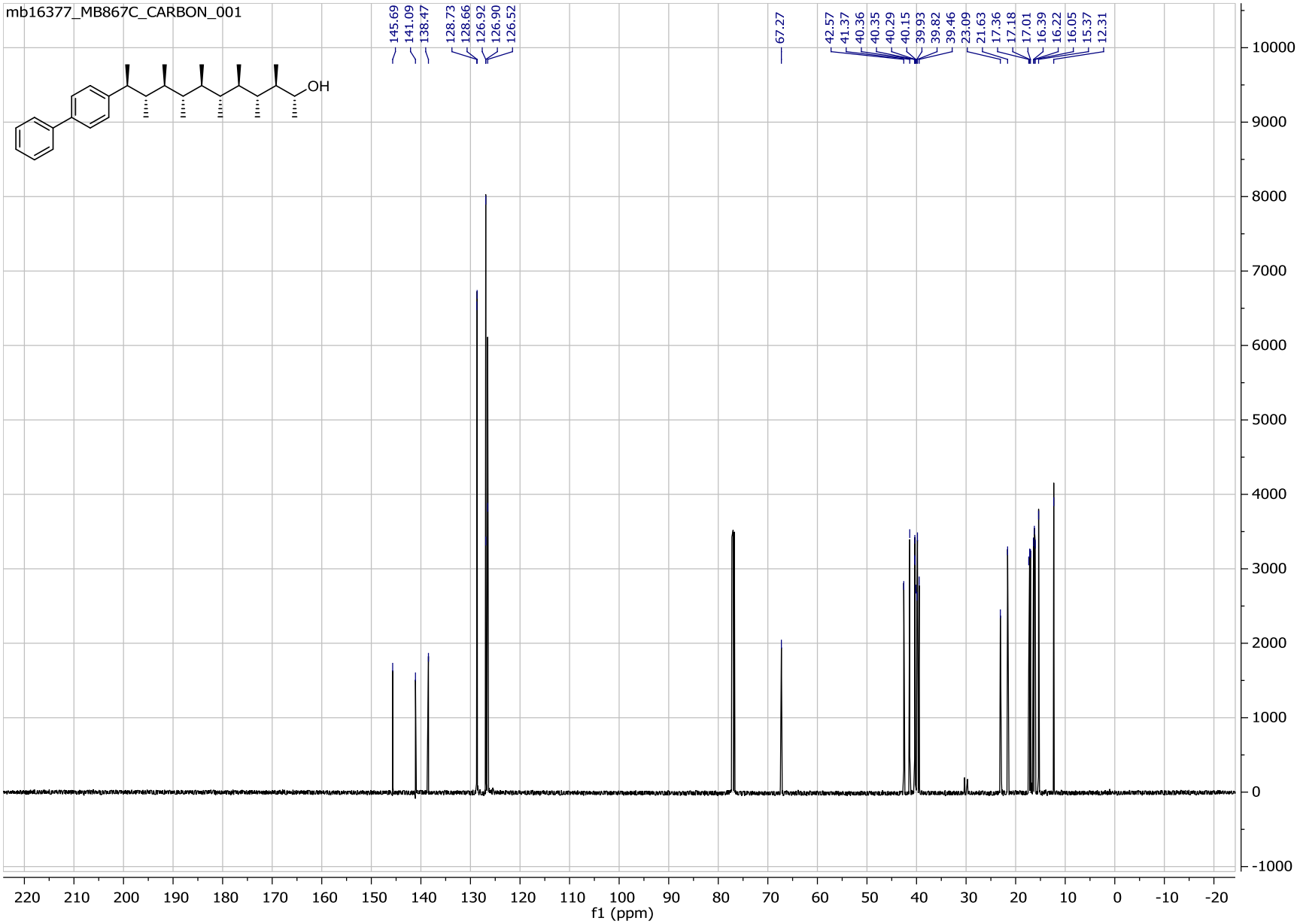
mb16377_MB867C_CARBON_001
OH
145.69
141.09
138.47
128.73
128.66
126.92
126.90
126.52
67.27
42.57
41.37
40.36
40.35
40.29
40.15
39.93
39.82
39.46
23.09
21.63
17.36
17.18
17.01
16.39
16.22
16.05
15.37
12.31
f1 (ppm)

((2*S*,3*R*,4*R*,5*S*,6*R*,7*S*,8*S*,9*R*,10*R*,11*S*)-11-(methoxymethoxy)-3,4,5,6,7,8,9,10-octamethyldodecan-2-yl)benzene, 18

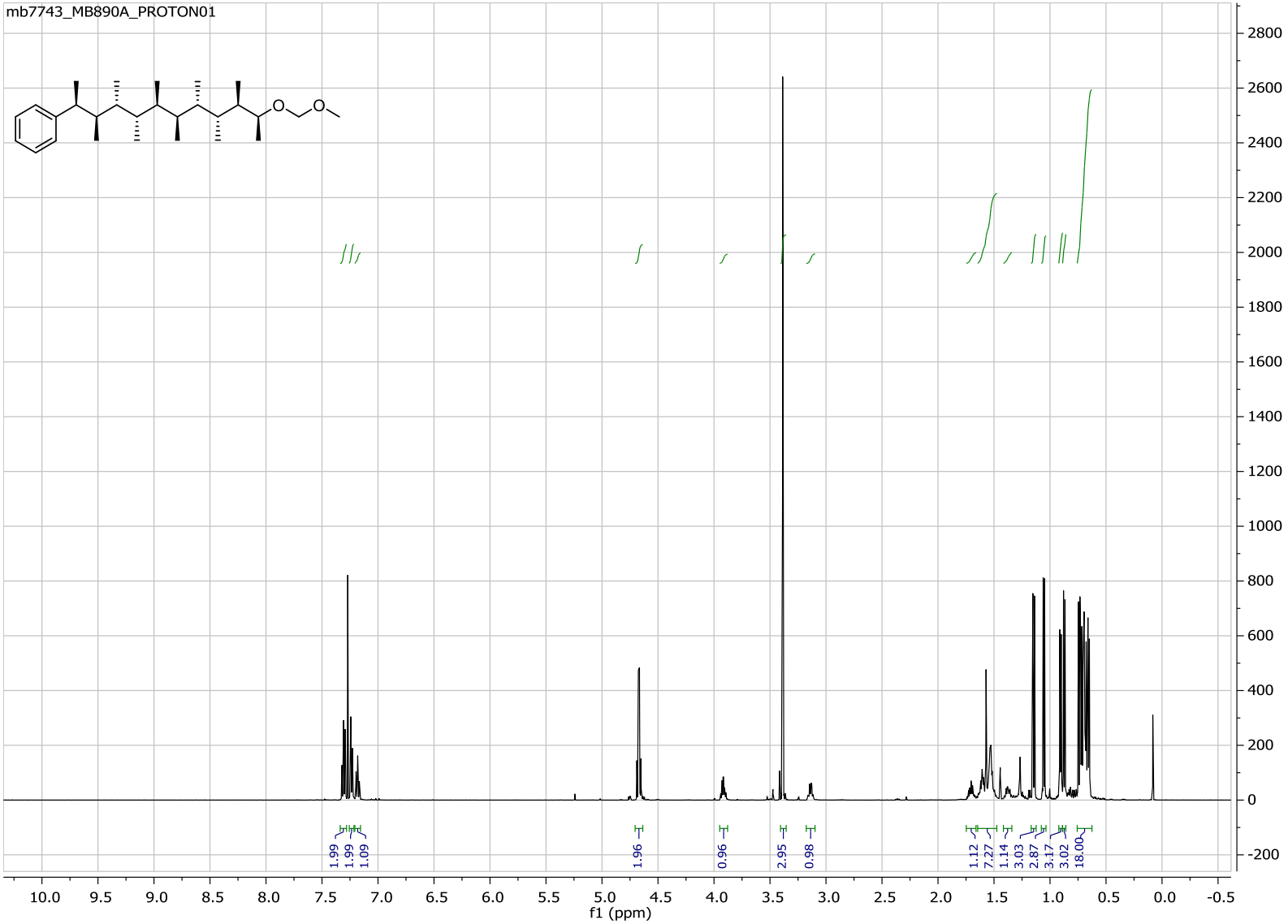

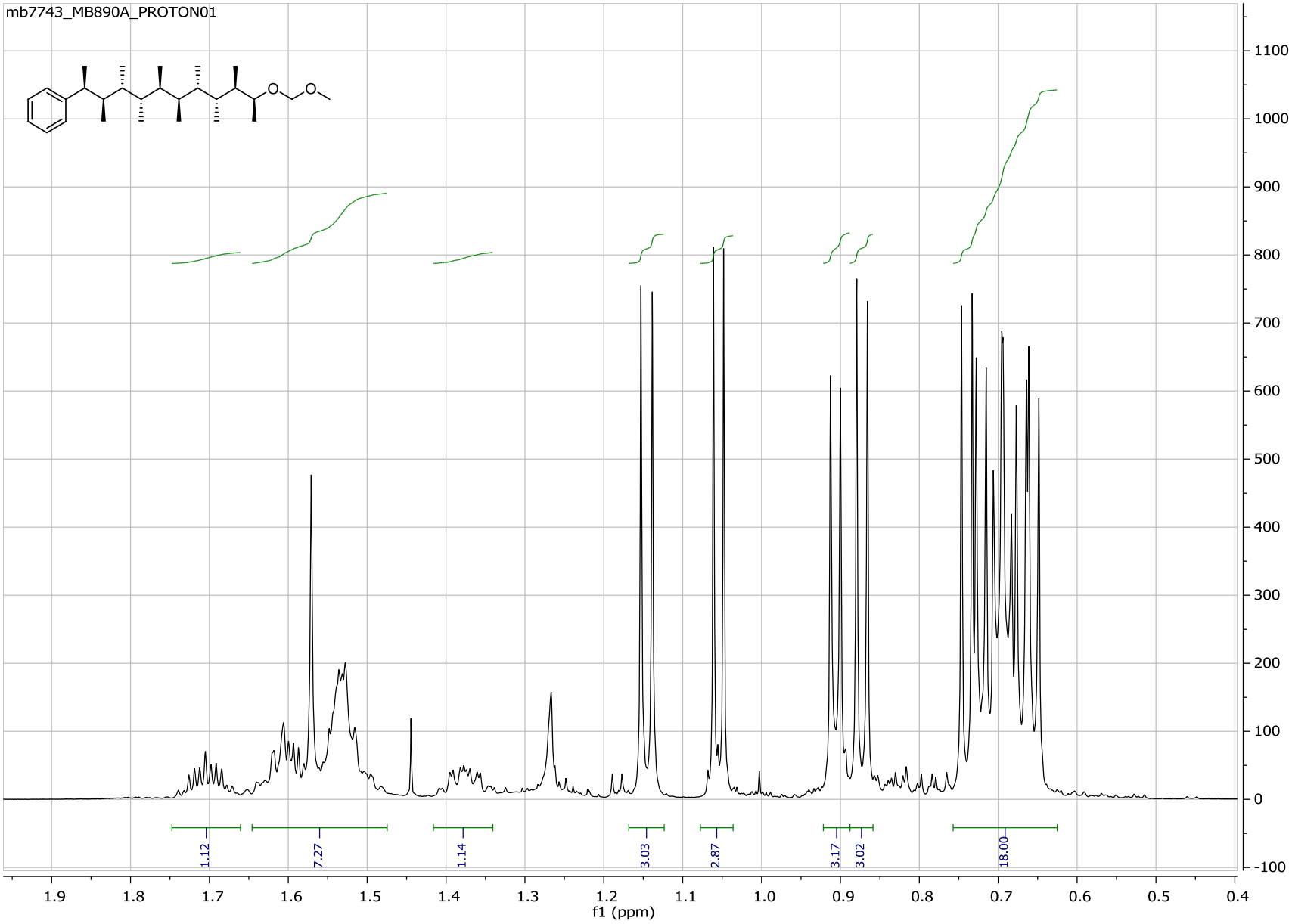
mb7743_MB890A_PROTON01
1100
1000
900
800
700
600
500
400
300
200
100
0
-100
1.12
7.27
1.14
3.03
2.87
3.17
3.02
18.00
1.9
1.8
1.7
1.6
1.5
1.4
1.3
1.2
1.1
1.0
0.9
0.8
0.7
0.6
0.5
0.4
f1 (ppm)

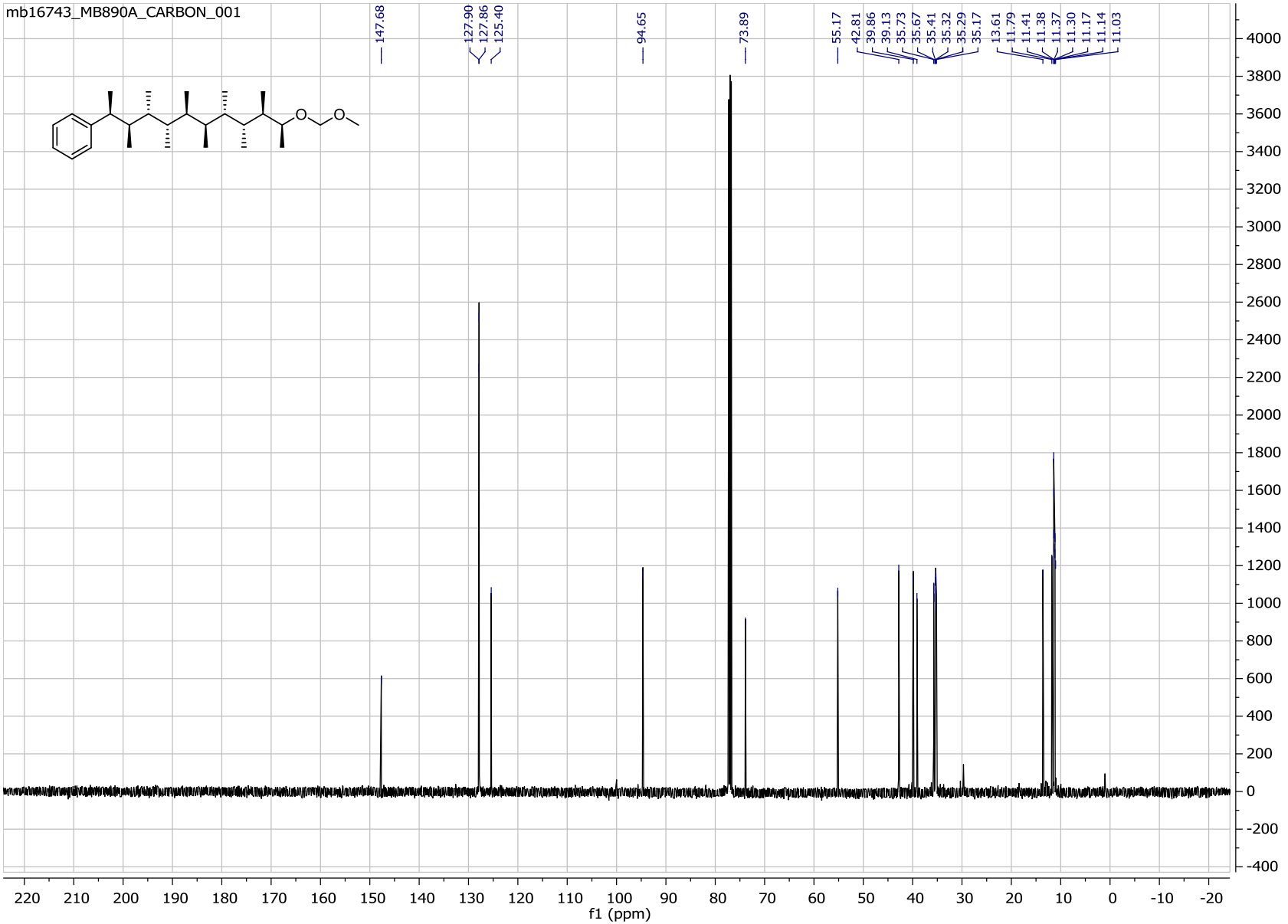
mb16743_MB890A_CARBON_001
147.68
127.90
127.86
125.40
94.65
73.89
55.17
42.81
39.86
39.13
35.73
35.67
35.41
35.32
35.29
35.17
13.61
11.79
11.41
11.38
11.37
11.30
11.17
11.14
11.03
O
O
4000
3800
3600
3400
3200
3000
2800
2600
2400
2200
2000
1800
1600
1400
1200
1000
800
600
400
200
0
-200
-400
220
210
200
190
180
170
160
150
140
130
120
110
100
90
80
70
60
50
40
30
20
10
0
-10
-20
f1 (ppm)

(2*S*,3*R*,4*S*,5*R*,6*S*,7*R*,8*R*,9*S*,10*R*,11*S*)-11-([1,1'-biphenyl]-4-yl)-3,4,5,6,7,8,9,10-octamethyldodecan-2-ol, 14

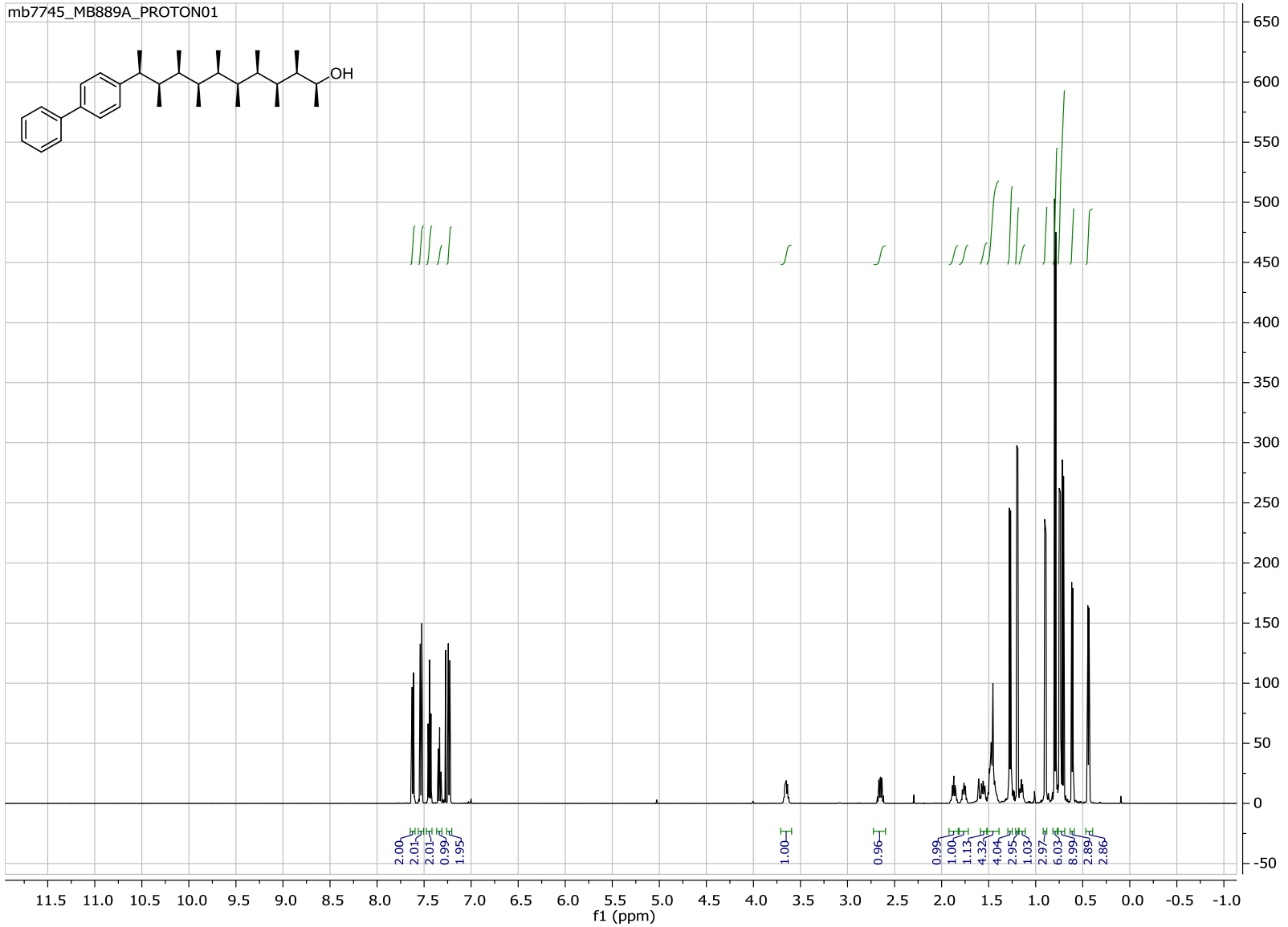

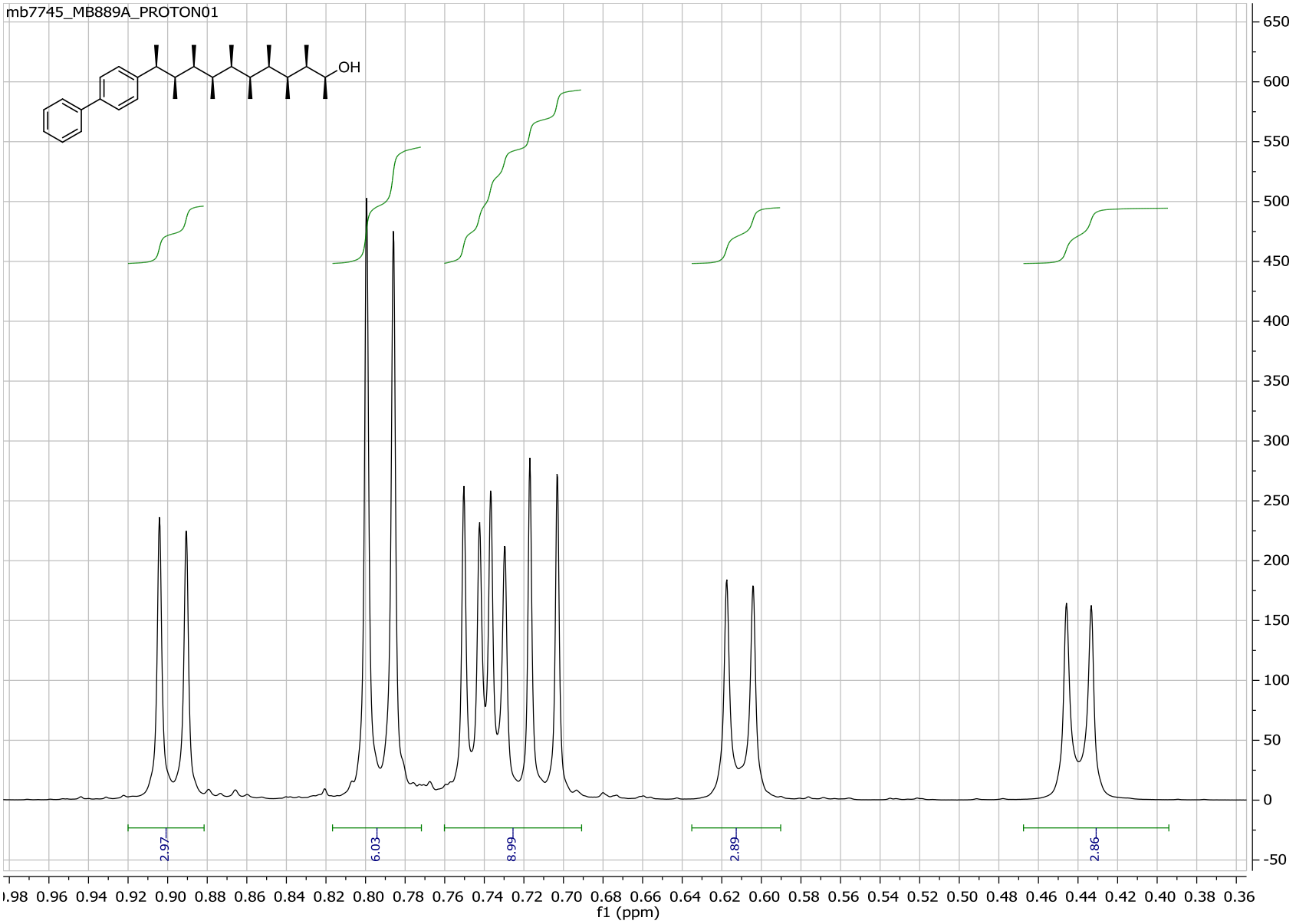
mb7745_MB889A_PROTON01
OH
650
600
550
500
450
400
350
300
250
200
150
100
50
0
-50
2.97
6.03
8.99
2.89
2.86
.98 0.96 0.94 0.92 0.90 0.88 0.86 0.84 0.82 0.80 0.78 0.76 0.74 0.72 0.70 0.68 0.66 0.64 0.62 0.60 0.58 0.56 0.54 0.52 0.50 0.48 0.46 0.44 0.42 0.40 0.38 0.36
f1 (ppm)

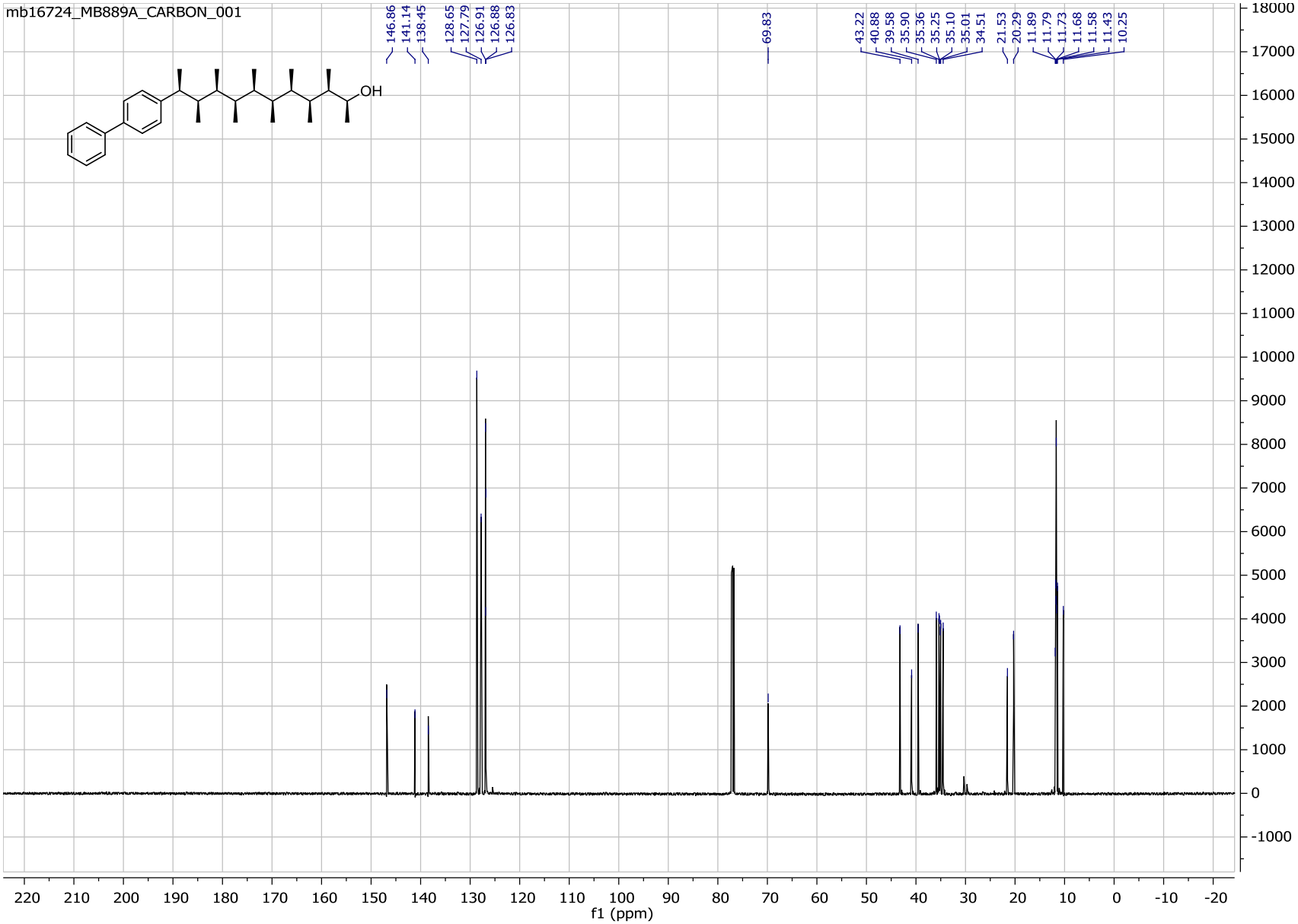
mb16724_MB889A_CARBON_001
OH
146.86
141.14
138.45
128.65
127.79
126.91
126.88
126.83
69.83
43.22
40.88
39.58
35.90
35.36
35.25
35.10
35.01
34.51
21.53
20.29
11.89
11.79
11.73
11.68
11.58
11.43
10.25
f1 (ppm)

(2*R*,3*R*,4*R*,5*R*,6*R*,7*R*,8*S*,9*S*,10*S*,11*S*)-11-([1,1'-biphenyl]-4-yl)-3,4,5,6,7,8,9,10-octamethyldodecan-2-yl 4-nitrobenzoate, 12

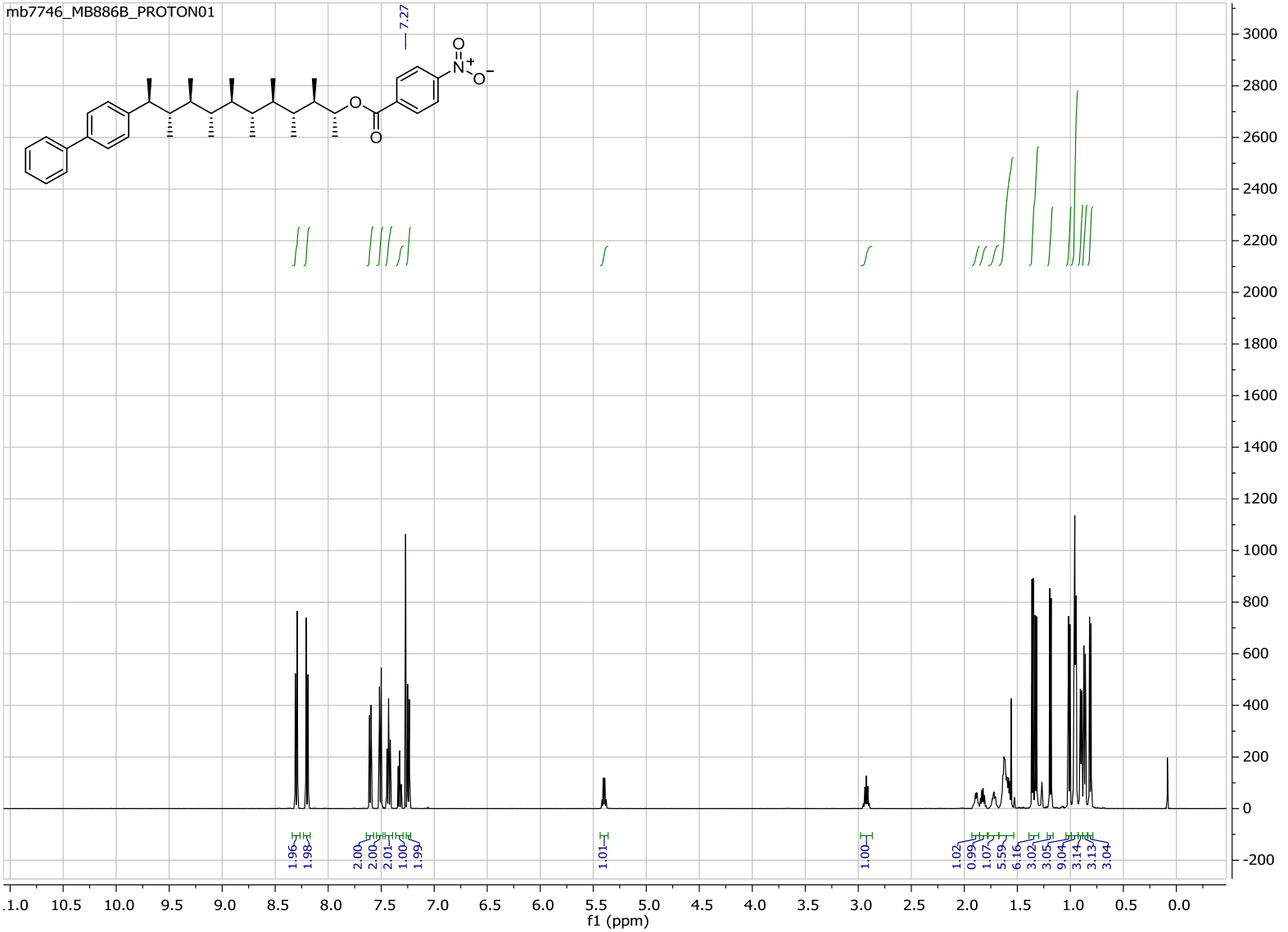

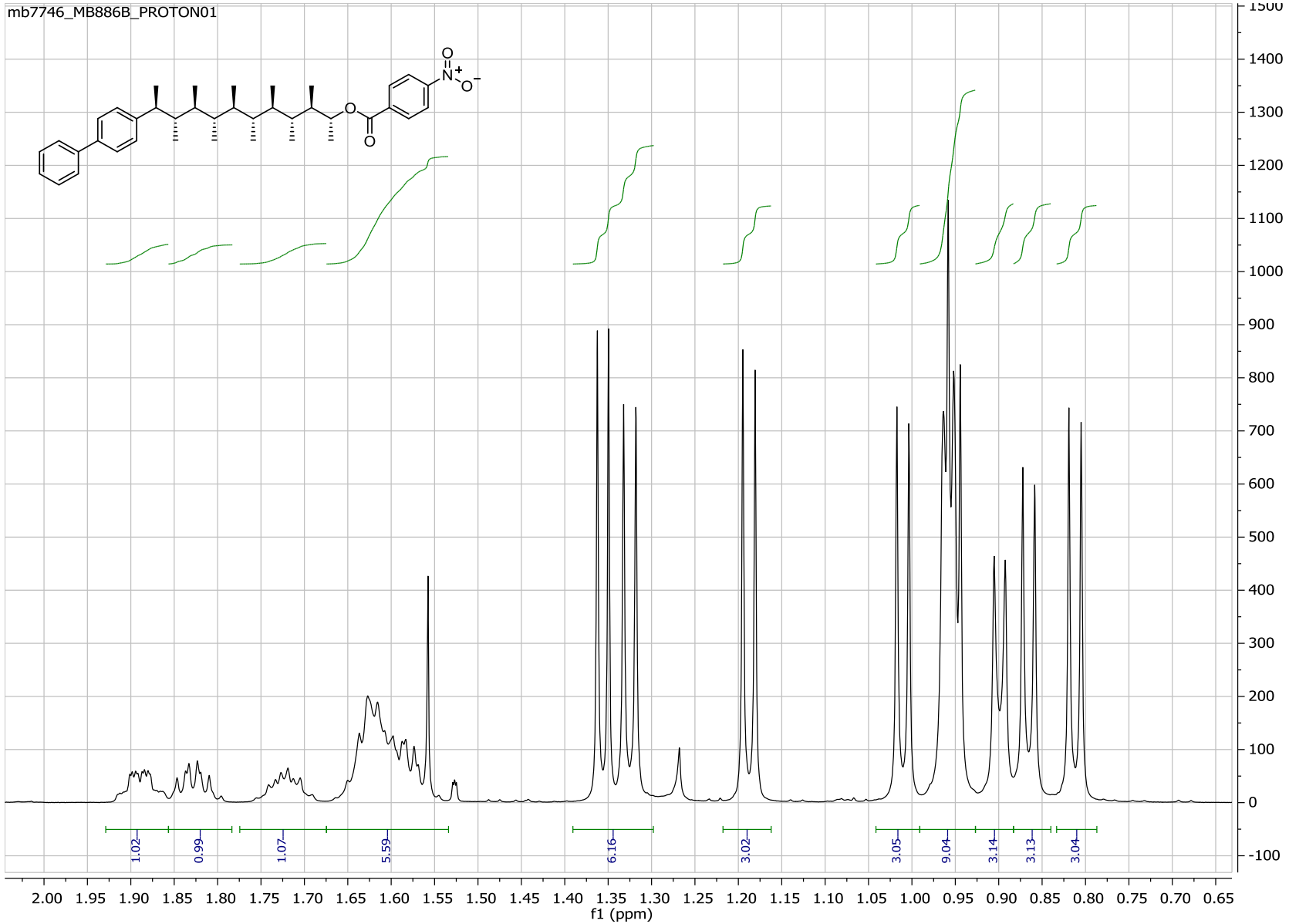
mb7746_MB886B_PROTON01
1.02
0.99
1.07
5.59
6.16
3.02
3.05
9.04
3.14
3.13
3.04
f1 (ppm)

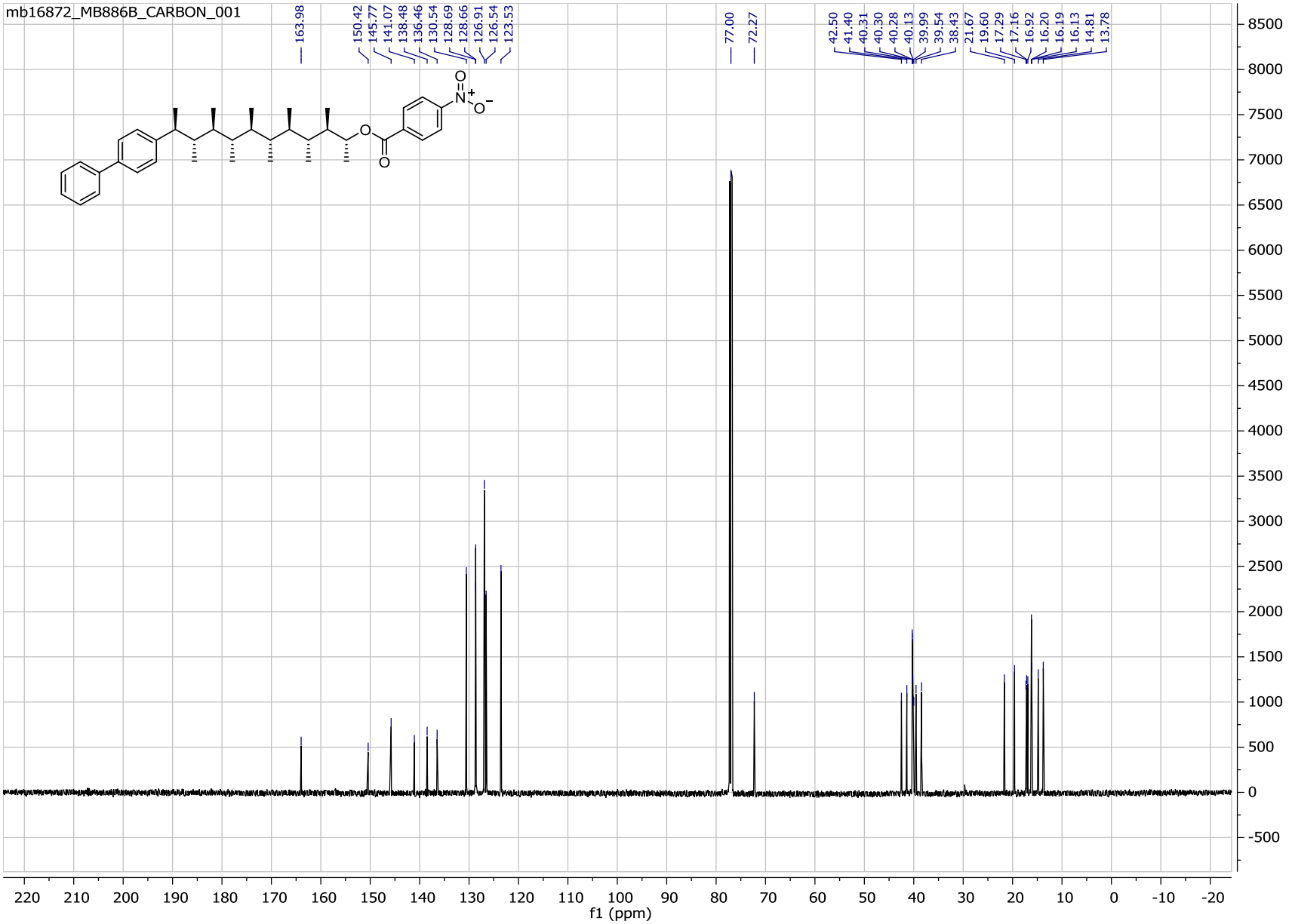
mb16872_MB886B_CARBON_001
163.98
150.42
145.77
141.07
138.48
136.46
130.54
128.69
128.66
126.91
126.54
123.53
77.00
72.27
42.50
41.40
40.31
40.30
40.28
40.13
39.99
39.54
38.43
21.67
19.60
17.29
17.16
16.92
16.20
16.19
16.13
14.81
13.78
f1 (ppm)

(2*S*,3*R*,4*S*,5*R*,6*S*,7*R*,8*R*,9*S*,10*R*,11*S*)-11-([1,1'-biphenyl]-4-yl)-3,4,5,6,7,8,9,10-octamethyldodecan-2-yl 4-nitrobenzoate, 15

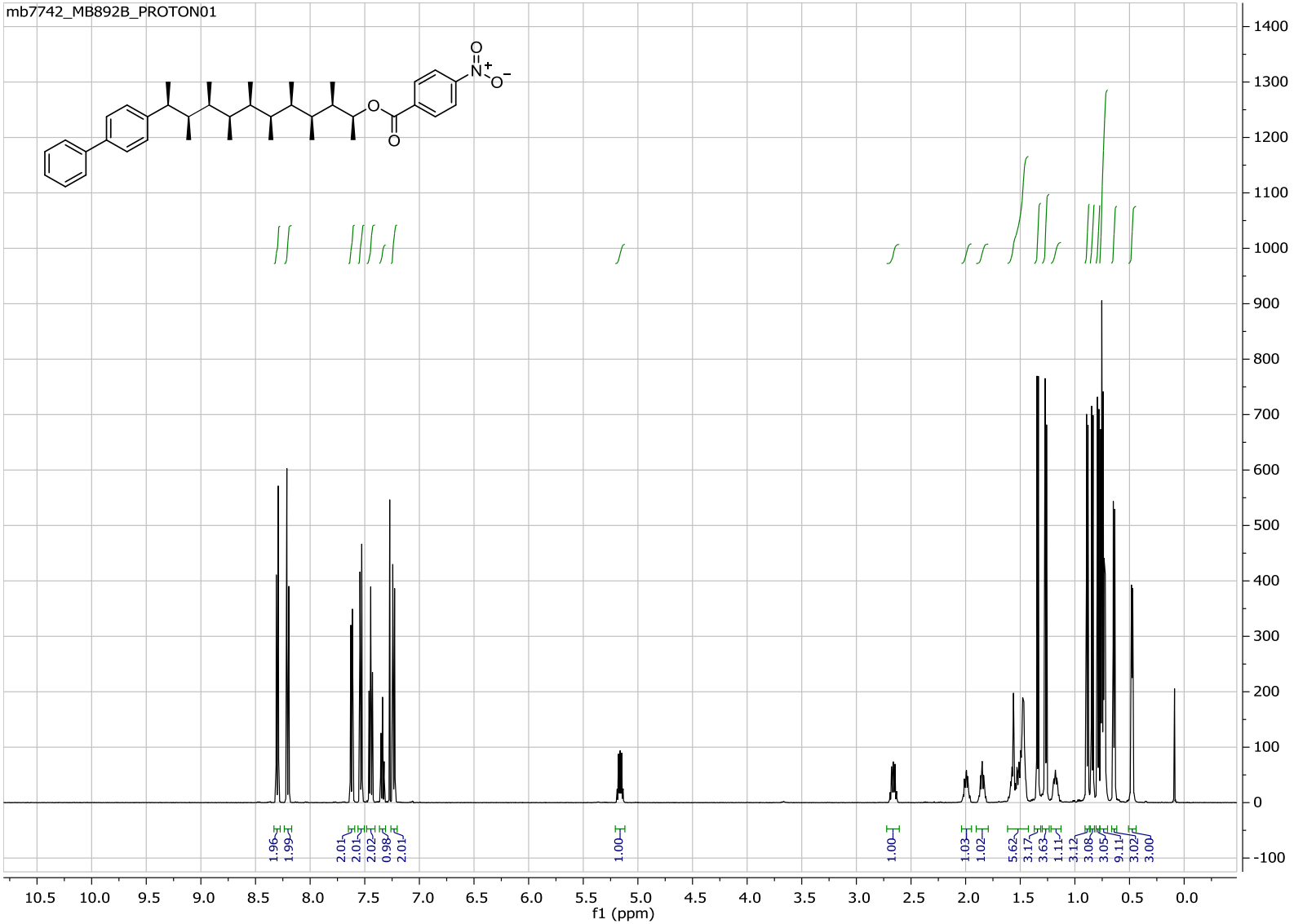

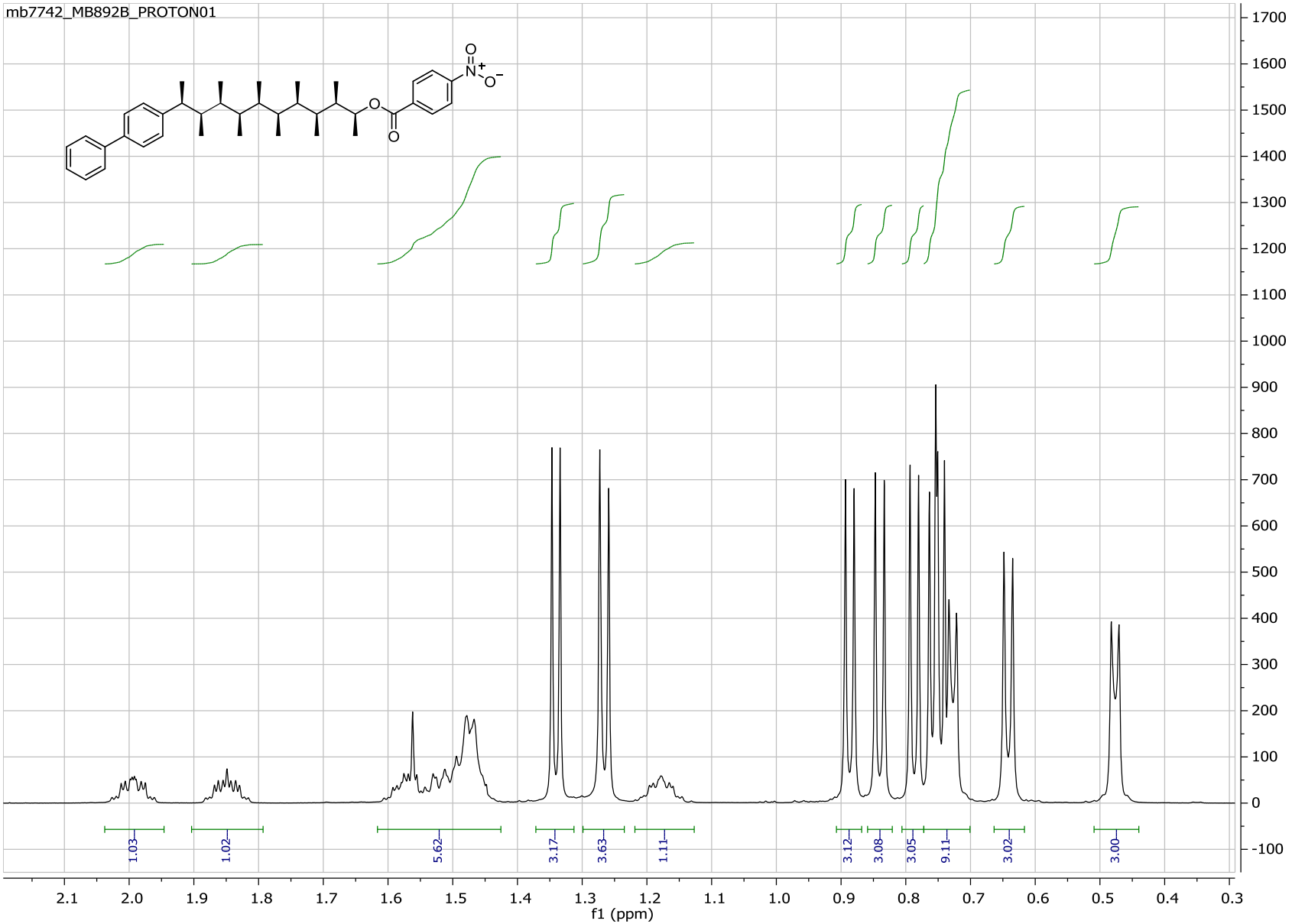
mb7742_MB892B_PROTON01
1.03
1.02
5.62
3.17
3.63
1.11
3.12
3.08
3.05
9.11
3.02
3.00
f1 (ppm)

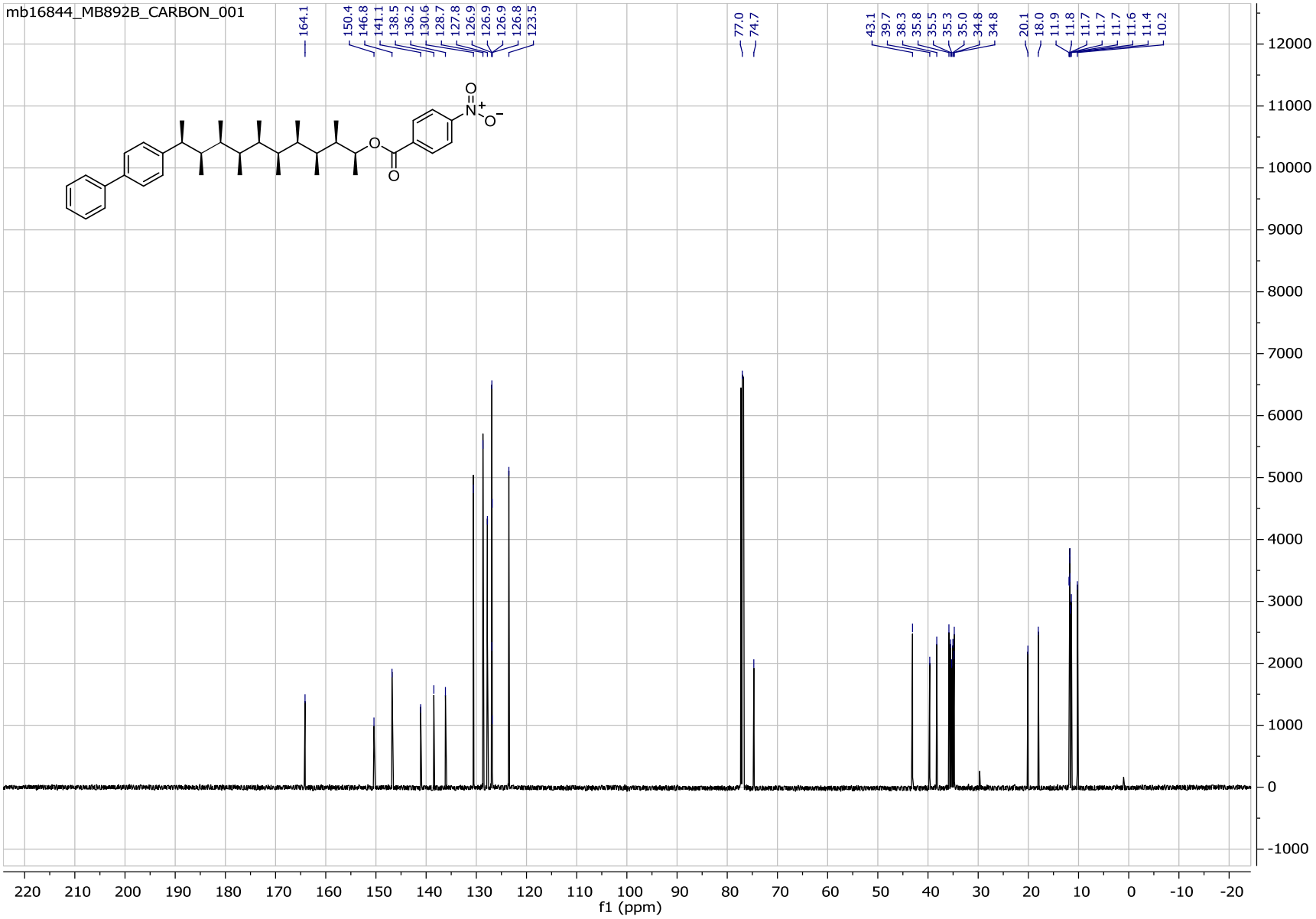
mb16844_MB892B_CARBON_001
164.1
150.4
146.8
141.1
138.5
136.2
130.6
128.7
127.8
126.9
126.9
126.9
126.8
123.5
77.0
74.7
43.1
39.7
38.3
35.8
35.5
35.3
35.0
34.8
34.8
20.1
18.0
11.9
11.8
11.7
11.7
11.7
11.6
11.4
10.2
O
N+
O-
O
O
12000
11000
10000
9000
8000
7000
6000
5000
4000
3000
2000
1000
0
-1000
220
210
200
190
180
170
160
150
140
130
120
110
100
90
80
70
60
50
40
30
20
10
0
-10
-20
f1 (ppm)

Apiezon high vacuum grease

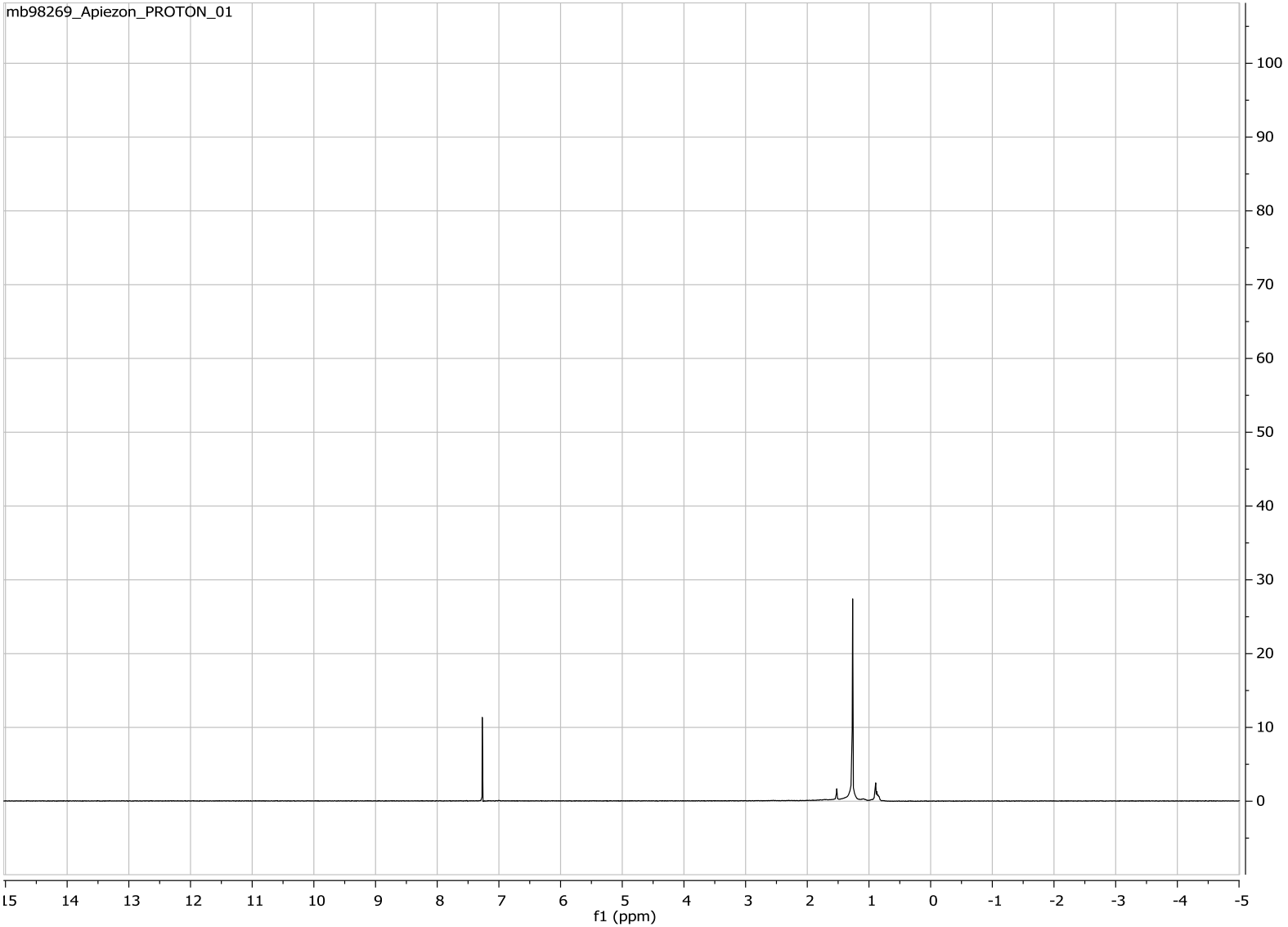

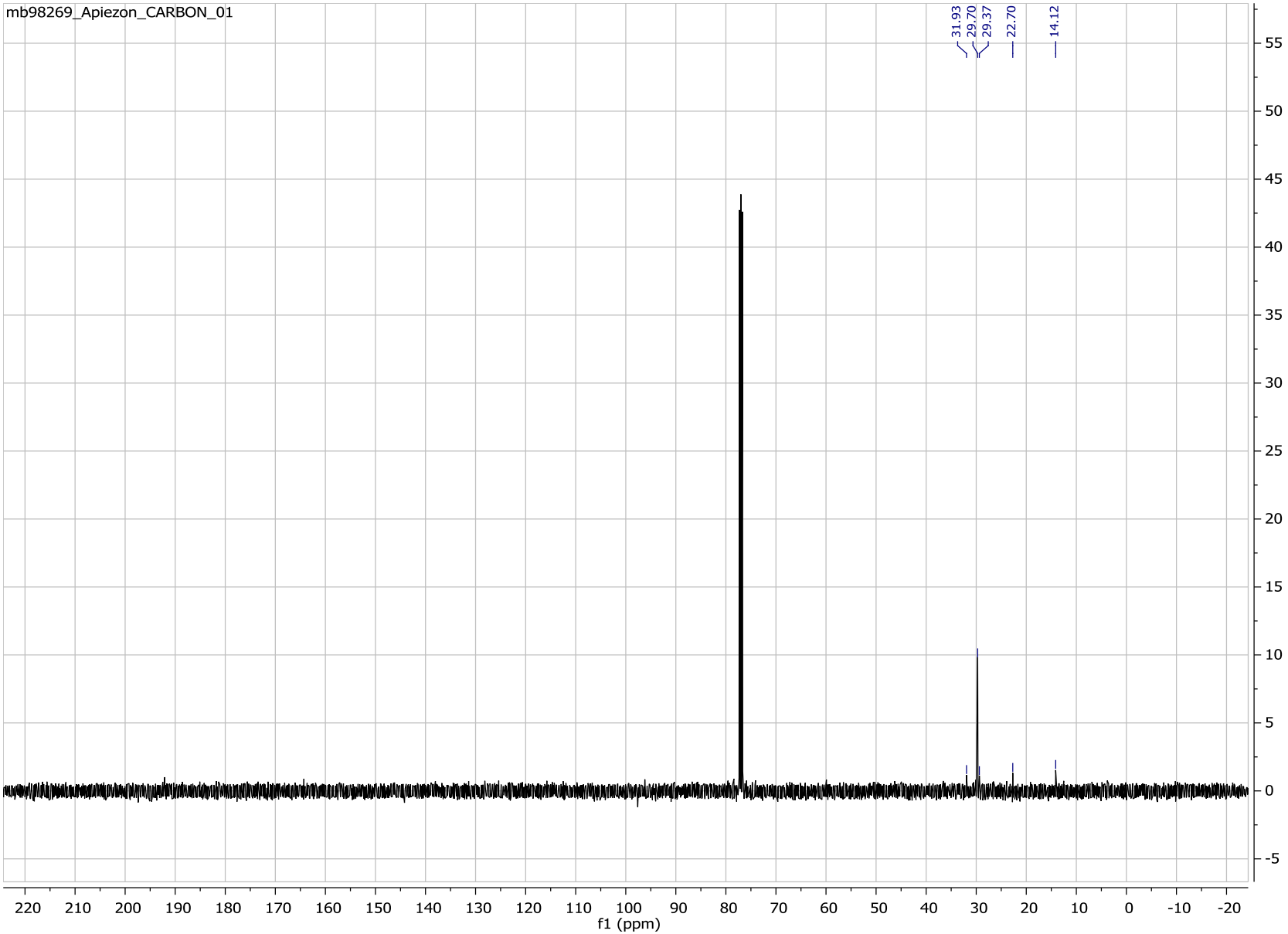
mb98269_Apiezon_CARBON_01
31.93
29.70
29.37
22.70
14.12
55
50
45
40
35
30
25
20
15
10
5
0
-5
220
210
200
190
180
170
160
150
140
130
120
110
100
90
80
70
60
50
40
30
20
10
0
-10
-20
f1 (ppm)